THE ADHESIVE WEAR OF MODERN AND TRADITIONAL ENGINEERING COATINGS

by

ROBERT LYNDON THOMAS

Master of Philosophy

THE UNIVERSITY OF ASTON IN BIRMINGHAM

June 1988

THE UNIVERSITY OF ASTON IN BIRMINGHAM

THE ADHESIVE WEAR OF MODERN AND TRADITIONAL ENGINEERING COATINGS

ROBERT LYNDON THOMAS

MASTER OF PHILOSOPHY

JUNE 1988

SUMMARY

The adhesive wear and frictional characteristics of modern and traditional engineering coatings have been investigated under conditions of constant load and sliding speed. The wear tests were carried out under dry sliding contact using the standard pin-on-disc wear testing equipment.

The engineering coatings investigated were electroless nickel PTFE composite, conventional electroless nickel, hard chromium, tin/nickel, tin/cobalt and titanium nitride.

The coatings were tested against Sursulf treated low alloy steel BS970 708M40 (EN 19) and BS970 534A99 (EN 31) discs. The Sursulf treated steel was originally chosen for the disc material because this process is used in-house at Jaguar Cars in the production of automotive crankshafts. Sursulf treatment was chosen as an alternative to the high cyanide Tuftriding process that was originally used for the above applications. Therefore it was considered beneficial to examine new applications involving a number of tribological counterface coatings.

The original nine wear tests involved only Sursulf treated discs and pins coated with electroless nickel PTFE composite. It was then decided to duplicate all subsequent wear tests using a standard steel disc. The disc chosen was BS970 534A99 (EN 31) hardened and tempered to obtain maximum hardness.

The coating that exhibited the best wear properties was titanium nitride (CVD) on D2 pin material, when tested against Sursulf treated BS970 709M40 "T" condition discs, or BS970 534A99 discs; although titanium nitride incurred catastrophic adhesive wear when deposited on BS970 605M36 "T" pin material.

When the more traditional engineering coatings were investigated, the lowest wear rates were achieved by hard chromium when tested against BS970, 534A99 discs.

Keywords: Adhesive wear; Pin-on-disc; Sursulf; Titanium Nitride; Hard Chromium

ACKNOWLEDGEMENTS

I would like to thank my employer, Jaguar Cars plc, for enabling me to carry out my research by providing financial and technical support, and allowing me to spend the necessary time at Aston University. I would also like to thank my Head of Department, Mr. R. W. Smith and my Supervisor, Mr. M. J. Stiles, together with the members of the Laboratory at Radford, for their co-operation and invaluable assistance.

Dr. J. K. Dennis has had the difficult job of being my supervisor and receives my thanks for his help and guidance throughout the research and production of this thesis.

Acknowledgements go to the companies who have provided me with wear resistant engineering coatings, with particular thanks going to Mr. B. Greaves from P.M.D. Chemicals Ltd., Coventry, who not only provided their standard Nistan solution, but also produced a cobalt/tin plating solution especially for my work.

Mr. Kam Sagoo, a fellow research student, has given me considerable assistance during the experimental stage, and also with technical facilities at Aston University. I would like to take this opportunity to give him my thanks and to wish him well in his future career.

Last, but not least, my thanks and admiration go to my wife, Lesley, who has had the mammoth task of deciphering my notes, correcting my spelling and grammar and producing the presentable typewritten thesis, at the same time as producing our wonderful son, Richard.

CONTENTS

		Page
	SUMMARY	2
	ACKNOWLEDGEMENTS	3
	CONTENTS	4
	LIST OF FIGURES, TABLES, PHOTOGRAPHS	6
1.0	INTRODUCTION	11
2.0	LITERATURE REVIEW	19
2.1	Basic Wear Theory	19
2.2	The Sursulf Process	30
2.2.1	Basic Principles	32
2.2.2	Composition and Metallography of the Layer	34
2.2.3	The Layer Properties	35
3.0	EXPERIMENTAL TECHNIQUES	38
3.1	Specimen Preparation	38
3.2	Disc Materials and Heat Treatment	38
3.2.1	BS970, 708A37 (EN19)	38
3.2.2	BS970, 534A99 (EN31)	39
3.3	Pin Materials	40
3.4	Wear Testing	49
3.5	Setting up Procedure for Wear Testing	49
3.6	Setting up Transducers and Recorders	50
3.7	The Wear Test	50
3.8	Surface Roughness Measurements	53
3.9	Micro Hardness Measurements	54
4.0	PIN COATINGS	56
4.1	Electroless Nickel and Electroless Nickel/PTFE	56
4.2	Hard Chromium	64
4.3	Titanium Nitride	67
4.4	Tin-Nickel	74
4.5	Tin-Cobalt	78

Page
5.0 RESULTS 82
5.1 The Sursulf Layer 82
5.2 Coating Thickness and Microhardness of Surface Coatings 84
5.3 Weight Loss and Wear Rates of Coatings 92
5.3.1 Wear Test Results 99
5.4 Coefficients of Friction 104
5.5 Surface Roughness 134
5.6 Photomicroscopy 140
5.6.1 Electroless Nickel/PTFE 141
5.6.2 Electroless Nickel 143
5.6.3 Hard Chromium 145
5.6.4 Tin/Nickel 146
5.6.5 Tin/Cobalt 147
5.6.6 Titanium Nitride (CVD) 148

6.0 DISCUSSION 151

7.0 CONCLUSIONS 162

SUGGESTIONS FOR FURTHER WORK 164

REFERENCES 165

LIST OF FIGURES, TABLES, PHOTOGRAPHS

		Page
Fig. 1	Isothermal transformation BS970 708A37	43
Fig. 2	Jominy Hardenability BS970 708A37	44
Fig. 3	Isothermal transformation BS970 534A99	45
Fig. 4	Jominy Hardenability BS970 534A99	46
Fig. 5	Isothermal transformation BS970 605A36	47
Fig. 6	Jominy Hardenability BS970 605A36	48
Photograph 1	Wear Testing Equipment	51
Fig. 7	Pin on Disc Wear Testing Equipment	52
Table 1	Operating Conditions of Chromium Plating Baths to give the Hardest Electrodeposits	66
Fig. 8	Ion Plating Equipment (PVD)	69
Fig. 9	CVD Furnace	70
Table 2	Comparison of Titanium Nitride Coatings by CVD and PVD	71
Table 3	Comparison of Titanium Nitride Coatings by CVD and PVD	72
Table 4	Comparison of Titanium Nitride Coatings by CVD and PVD	73
Table 5	Hardness Plot across Diffusion Zone	82
Fig. 10	Hardness Vs Depth across Sursulf Layer	83
Table 6	Electroless Nickel PTFE As plated	87
Table 7	Electroless Nickel PTFE (Heat treated at 300°C for 4 hours)	87
Table 8	Electroless Nickel As plated	88
Table 9	Electroless Nickel Heat treated at 400°C for 1 hour	88
Table 10	Hard Chromium	89
Table 11	Electrodeposited Tin/Nickel	89
Table 12	Electrodeposited Tin/Cobalt	90
Table 13	Titanium Nitride CVD (Pin material 605A36)	90
Table 14	Titanium Nitride CVD (Pin material D2)	91
Table 15	Titanium Nitride PVD (Pin material D2)	91
Table 16	Electroless Nickel PTFE As plated	94
Table 17	Electroless Nickel PTFE Heat treated	94
Table 18	Electroless Nickel As plated	95
Table 19	Electroless Nickel Heat treated	95
Table 20	Hard Chromium	96
Table 21	Electrodeposited Tin/Nickel	96

		Page
Table 22	Electrodeposited Tin/Cobalt	97
Table 23	Titanium Nitride CVD (Pin material 605A36)	97
Table 24	Titanium Nitride CVD (Pin material D2)	98
Table 25	Titanium Nitride PVD (Pin material D2)	98
Table 26	Electroless Nickel PTFE As plated	99
Table 27	Electroless Nickel PTFE Heat treated	100
Table 28	Electroless Nickel As plated	100
Table 29	Electroless Nickel Heat treated	101
Table 30	Hard Chromium	101
Table 31	Electrodeposited Tin/Nickel	102
Table 32	Electrodeposited Tin/Cobalt	102
Table 33	Titanium Nitride CVD (Pin material 605A36)	103
Table 34	Titanium Nitride PVD (Pin material D2)	103
Table 35	Electroless Nickel PTFE As plated/Sursulf Treated Discs	105
Table 36	Change in Coefficient of Friction with Time for Pins 55-57	105
Fig.11	Change in Coefficient of Friction with Time	106
Table 37	Electroless Nickel PTFE (Heat treated)/ Sursulf Treated Disc	107
Table 38	Change in Coefficient of Friction with Time for Pins 58-60	107
Fig. 12	Change in Coefficient of Friction with Time	108
Table 39	Electroless Nickel PTFE As plated/534A99 (EN31) Discs	109
Table 40	Change in Coefficient of Friction with Time for Pins 52-54	109
Fig. 13	Change in Coefficient of Friction with Time	110
Table 41	Electroless Nickel PTFE Heat Treated/534A99 (EN31) Discs	111
Table 42	Change in Coefficient of Friction with Time for Pins 61-63	111
Fig. 14	Change in Coefficient of Friction with Time	112
Table 43	Electroless Nickel (Heat Treated)/Sursulf Treated Discs	113
Table 44	Change in Coefficient of Friction with Time for Pins 31-33	113
Fig. 15	Change in Coefficient of Friction with Time	114
Table 45	Electroless Nickel As plated/Sursulf Treated Discs	115
Table 46	Electroless Nickel As plated/534A99 Discs	115
Table 47	Electroless Nickel Heat Treated/534A99 Discs	115

		Page
Table 48	Hard Chromium/Sursulf Treated Discs	116
Table 49	Hard Chromium/534A99 (EN31) Discs	116
Table 50	Electrodeposited Tin/Nickel/Sursulf Treated Discs	117
Table 51	Change in Coefficient of Friction with Time for Pins 43-45	117
Fig. 16	Change in Coefficient of Friction with Time	118
Table 52	Electrodeposited Tin/Nickel/534A99 (EN31) Discs	119
Table 53	Change in Coefficient of Friction with Time for Pins 40-42	119
Fig. 17	Change in Coefficient of Friction with Time	120
Table 54	Electrodeposited Tin Cobalt/Sursulf Treated Discs	121
Table 55	Change in Coefficient of Friction with Time for Pins 49-51	121
Fig. 18	Change in Coefficient of Friction with Time	122
Table 56	Electrodeposited Tin Cobalt/534A99 (EN31) Discs	123
Table 57	Change in Coefficient of Friction with Time for Pins 46-48	123
Fig. 19	Change in Coefficient of Friction with Time	124
Table 58	Titanium Nitride CVD/Sursulf Treated Discs	125
Table 59	Titanium Nitride CVD/534A99 (EN31) Discs	125
Table 60	Titanium Nitride CVD/Carbide Discs	125
Table 61	Titanium Nitride CVD/Sursulf Treated Discs	126
Table 62	Change in Coefficient of Friction with Time for Pins 37-39	126
Fig. 20	Change in Coefficient of Friction with Time	127
Table 63	Titanium Nitride CVD/534A99 (EN31) Discs	128
Table 64	Change in Coefficient of Friction with Time for Pins 34-36	128
Fig. 21	Change in Coefficient of Friction with Time	129
Table 65	Titanium Nitride PVD/Sursulf Treated Disc	130
Table 66	Change in Coefficient of Friction with Time for Pins 67-69	130
Fig. 22	Change in Coefficient of Friction with Time	131
Table 67	Titanium Nitride PVD/534A99 (EN31) Discs	132
Table 68	Change in Coefficient of Friction with Time for Pins 67-69	132
Fig. 23	Change in Coefficient of Friction with Time	133
Table 69	Electroless Nickel PTFE As plated	135
Table 70	Electroless Nickel PTFE Heat treated	135

Page
Table 71 Electroless Nickel As plated 136
Table 72 Electroless Nickel Heat Treated 136
Table 73 Hard Chromium 137
Table 74 Electrodeposited Tin/Nickel 137
Table 75 Electrodeposited Tin/Cobalt 138
Table 76 Titanium Nitride CVD 138
Table 77 Titanium Nitride CVD 139
Table 78 Titanium Nitride PVD 139
Photomicrograph 1
Transverse section of unworn Electroless Nickel/PTFE 141
Photomicrograph 2
Transverse section of worn Electroless Nickel/PTFE 141
Photomicrograph 3
As photomicrograph 2, x 5000 magnification 142
Photomicrograph 4
Surface of unworn Electroless Nickel/PTFE 142
Photomicrograph 5
Surface of worn Electroless Nickel/PTFE 143
Photomicrograph 6
Surface of unworn Electroless Nickel 143
Photomicrograph 7
Surface of worn Electroless Nickel 144
Photomicrograph 8
Surface and edge of worn Electroless Nickel 144
Photomicrograph 9
Surface of unworn Hard Chromium deposit 145
Photomicrograph 10
Surface of worn Hard Chromium deposit 145
Photomicrograph 11
Surface of unworn Electrodeposited Tin/Nickel 146
Photomicrograph 12
Surface of worn Electrodeposited Tin/Nickel 146
Photomicrograph 13
Surface of unworn Electrodeposited Tin/Cobalt 147
Photomicrograph 14
Surface of worn Electrodeposited Tin/Cobalt 147
Photomicrograph 15
As photomicrograph 14, x 1000 magnification 148

Page

Photomicrograph 16

Unworn Titanium Nitride Coating 148

Photomicrograph 17

Surface of Titanium Nitride 149

Photomicrograph 18

As photomicrograph 17, x1000 magnification 149

Photomicrograph 19

Surface of Titanium Nitride Coating 150

Photomicrograph 20

"X-ray" map of photomicrograph 19 150

1.0 INTRODUCTION

Eyre[1] points out that wear is rarely catastrophic, but it reduces operating efficiency and increases power losses, oil consumption, and component replacement rates. Wear is not an intrinsic material property, but is characteristic of the engineering system.

A wide variety of conditions cause wear, with many mechanisms contributing to the damage caused. The solution of a particular problem requires precise identification of the nature of the problem, and care must be exercised in applying general solutions to individual problems.

In some situations, increasing the hardness will reduce wear: in others the opposite may be true. Changing the operating conditions may give greater improvements than changing the material or its condition.

Increasing emphasis is being given to tailoring surfaces to match operating conditions; expensive bulk materials can sometimes be replaced by cheaper substrates with a suitably treated surface. It should be noted that this may also modify other material properties, including corrosion and fatigue resistance.

Wear, however, is rarely the result of a single mechanism. There are situations where one type changes to another, or where two or more mechanisms operate together: it is possible, for example, for the debris produced by adhesive wear to cause abrasive wear.

Wear encountered in industrial situations can be broadly classified as follows[1]:

Abrasive	50%
Adhesive	15%
Erosion	8%
Fretting	8%
Chemical	5%

Abrasive or cutting type of wear takes place whenever hard, foreign particles, such as metal grit, metallic oxides, dust and grit from the environment are present between the rubbing surfaces. These particles first penetrate the metal and then tear off metallic particles. Depending upon severity, abrasive wear may be of the gouging or scratching form. Abrasive wear is the most common type encountered in engineering practice and it is the highest single cause of wear in many machine applications.

Adhesive wear occurs when surfaces slide against each other and the pressure between the contacting asperities is high enough to cause local plastic deformation and adhesion. Adhesion is favoured by clean surfaces, non-oxidising conditions, and by chemical and structural similarities between the sliding couple. Adhesion occurs between a few separate asperities which increase in size as motion continues. Eventually, the junctions rupture at their weakest point, usually resulting in metal transfer from one surface to another.

Erosive wear is that due to impact of particles. A popular example of erosion by solid particles is sand blasting. The process is a combination of deformation and cutting, the deformation resulting from the normal component of the impact.

Fluid erosion results from the repeated impact of drops of fluid and shows itself in the form of roughening of the surface under impact and pitting.

In industrial practice, the most common type of erosion is cavitation erosion. Cavitation erosion is caused by high relative motion between the metal and liquid. At such motions, the local pressure on the liquid is reduced, the liquid's temperature reaches the boiling point, and small cavities of vapour are formed. When the pressure returns to normal, implosion occurs and the cavity collapses. This produces high impact forces on the metal, causing work-hardening, fatigue and the formation of cavitation pits. The action is purely mechanical, but often it exists in the presence of galvanic corrosion.

Fretting or frettage corrosion is characterised by minute reciprocating motions between wearing surfaces held together by normal forces. The normal force pressing the surfaces together has to be large enough and the amplitude of the relative sliding motion small enough (< 50 μm) to significantly restrict the flow of wear debris away from the point of origin. Damage may vary from discolouration of the mating surface, to the wearing away of 1.5 mm of material. The mating surfaces may show the formation of a great deal of corroded material or merely a heavily galled appearance with little oxide.

The minute reciprocating motion between the mating surfaces breaks down any natural protective film carried by the surface, causing the metal to adhere and break away at each oscillation. The debris may be converted into an abrasive oxide which causes severe damage.

Seldom is one type of wear found in isolation and this is particularly true of chemical wear. Corrosion wear is a form of chemical wear which results from the interaction of the environment with sliding surfaces, followed by the rubbing off of the products of reaction. Initially the chemical attack will be rapid, usually as a film is formed on the surface, the rate of reaction slows down and may cease completely. If, however, the products do not adhere or the film is porous, the chemical reaction proceeds independent of any sliding and the process is one of pure corrosion.

When the film is removed by the sliding of the mating surfaces, the original surface is again bared and chemical attack continues. However, if the film is wear resistant the basic surface may be protected. This protection may not last long if the film is brittle and starts to break away. Should the film continue to build up, it may itself start to wear when a certain thickness is exceeded. Then, how much of the layer is removed will depend on its own wear properties.

Some films formed as a result of chemical reaction give low wear rates. Examples are the films formed by oil additives, e.g. metallic chlorides, sulphides and phosphates.

Galvanic corrosion is a form of chemical wear involving damage to a surface caused by a flow of current in a liquid, from one metallic surface to another. The galvanic cells may operate either at the surface of the metal, or between dissimilar metals in electrical contact or between areas of unequal electrolyte concentration. This includes a galvanic action as it relates to corrosion in and around crevices and pitting. Electrons are produced at the anode by the reaction,

$$M \longrightarrow M^{2+} + Ze$$

The fundamental cathodic process is the consumption of electrons, but this may be achieved in a number of ways depending on the environment. A common cathodic reaction is the hydrogen evolution reaction in acidic solutions:

$$2H^{+} + 2e \longrightarrow H_2$$

The aim of the research was to examine the adhesive wear and frictional characteristics of modern and traditional engineering coatings. The coatings were tested against Sursulf treated low alloy steel BS 970 708M40 (EN 19) and BS 970 534A99 (EN 31) discs under dry unlubricated conditions. Each coating system was evaluated using the pin on disc wear testing apparatus, optical and scanning electron microscopy and microhardness measurements.

The Sursulf treated steel was originally chosen for the disc material because this process is used in-house at Jaguar in the production of automotive crankshafts. Sursulf treatment was chosen as an alternative to the high cyanide Tuftriding process that was originally used for the above applications.

The wear characteristics of the Sursulf layer have been examined by Hydromechanique et Frottement (the French company that developed the Sursulf process), using both standard wear testing equipment and simulated testing of actual components.

However, it would appear that there has been no research into the wear characteristics of Sursulf treated steel under dry unlubricated conditions. Therefore it was considered beneficial to examine new applications involving a number of tribological counterface coatings.

The original nine wear tests involved only Sursulf treated discs and pins coated with electroless nickel PTFE composite. It was then decided to duplicate all subsequent wear tests using a standard steel disc. The disc chosen was BS 970 534A99 (EN 31) hardened and tempered to obtain maximum hardness.

The electroless nickel PTFE wear tests were repeated using both Sursulf treated and 534A99 discs. For comparison purposes conventional electroless nickel coated pins, both in the as-plated and heat treated condition, were tested. Electroless nickel in the heat treated condition is often used as a substitute for hard chromium. Electroless nickel deposits with 9% phosphorus should increase in hardness to a maximum of about 1000HV 100g after heat treatment at 400°C for one hour. Therefore conventional hard chromium was used for comparison with heat treated electroless nickel.

Electrodeposited tin nickel has a microhardness similar to that of electroless nickel in the as-plated condition. Electrodeposited tin cobalt is marginally harder but this alloy was found to be predominantly cobalt. X-Ray microanalysis confirmed the deposit to be 94% cobalt whereas electrodeposited tin nickel was found to be 28% nickel.

A number of AISI D2 pins were coated with titanium nitride and wear tested against Sursulf treated and 534A99 discs. Titanium nitride coatings are a recent development in the field of wear resistant coatings.

The extreme hardness of the titanium nitride coating, approximately 2000HV, renders it ideal for the coating of tool steels and carbide inserts used for metal cutting operations. Two different coating methods were evaluated. Chemical vapour deposition (CVD) is a thermochemical process which produces what is essentially a duplex coating of approximately 20 μm thick of titanium carbide and titanium nitride. Pins that were coated by chemical vapour deposition require vacuum heat treatment after processing to transform the substrate material. Physical vapour deposition (PVD) is an ion plating process and is applied to the finished pins and requires no further processing. The titanium nitride coatings produced by physical vapour deposition are in essence a single thin coating 1-2.5 μm thick.

During this study of adhesive wear, an attempt was made to remove the wear debris by brushing the wear track. A number of different types of brush were used, none of which was completely successful in the removal of wear debris. So it is probable that some of the results were not strictly under conditions of adhesive wear.

One of the main problems with the pin on disc type of wear tester is the "running in" period. During this time, frictional heating effects cause the pin to expand slightly, however, this expansion counteracts any contraction due to wearing as measured on the displacement transducer. Therefore, the only successful method to establish a wear rate of coatings under these conditions was to weigh the pins before and after testing.

2.0 LITERATURE REVIEW

2.1 Basic Wear Theory

It is over thirty years since Archard[2] made an attempt to express wear rate; he based his concept on that of Holm's equation $W = ZP/pm$, where pm is the flow pressure, Z is the number of atoms removed per atomic encounter and P is the load. This was modified to obtain an expression for the removal of wear particles, instead of the removal of atoms: $W = KP/3a$,

W	is the wear rate
K	is the probability of forming a wear particle at the junction between the surfaces
a	is the circular contact radius of the asperity

Using a pin on ring type of wear machine, Archard measured the wear rates under various loads rubbing 60/40 brass pins and stellite pins on tool steel rings.

In order to prove his theoretical equation with actual wear rates, he measured wear rates of a number of similar and dissimilar metals, and concluded that:-

(1) Wear rate is proportional to load.

(2) Wear rate is independent of apparent contact area.

(3) Wear rate is independent of the speed of sliding, providing K and pm remain constant.

(4) The theoretical wear rate is independent of the model used to represent the surfaces.

Attempts have been made to establish some values for K. Bhansali[3] attempted to find K using a model based on fatigue and indicated that K is the reciprocal of the number of stress cycles required to form a wear particle. Using this model the wear of nickel and cobalt alloys was studied under various conditions of load, speed, sliding distance and surface finish. Conclusions were made that a linear relationship exists between the wear volume and the load, and that there is an abrupt change in the wear rate during the transition from mild to severe wear in the case of cobalt alloys. This was explained by the formation of glassy type spinel oxides forming on the surfaces of both cobalt and nickel during wear; but in the case of cobalt, the layers are not thick enough and the insulating properties are insufficient to withstand thermal softening of the substrate.

Thermal softening of the substrate can explain this phenomenon, but it is also possible that the lubricating properties and the breakdown of these different layers can account for this effect. Bhansali also concludes that alloys containing carbide reach a value at which wear rate is independent of sliding distance, which is believed to be caused by the matrix being worn down to expose carbide, after which no further wear occurs. Bhansali discovered that a slightly higher wear rate occurs on finer surfaces than rougher, and concluded that this was due to the fact that wear debris can become trapped in the grooves of the rougher surface, thus reducing asperity contact.

Finally, Bhansali recommended that Archard's equation should not be used to extrapolate load or material hardness, due to the fact that insufficient variables such as speed have not been used in the equation to predict such properties.

Rabinowinz[4] also attempted to find K for Archard's equation on a model based on shear strength. Rabinowinz' analysis was based on the premise that the strengths of the two sliding surfaces and on the adhesive bond between them varies because of statistical fluctuations in strength values, and that adhesive wear occurs when an unusually low value of strength of one of the surfaces is combined with an unusually high value for the interfacial strength. Rabinowinz points out that a wear coefficient value has been computed for unlubricated identical metals and then values of the wear coefficient have been obtained for combinations of lower shear strengths, as indicated by a lower friction coefficient. In all cases the calculated K values agree well with those that have been measured in practice. This is surprising because the computation covers such a wide range of K values, whereas the assumed model makes only a limited number of assumptions. Rabinowinz questioned the reasonableness of the five estimated parameters.

(1) It was assumed that when shear occurs away from a junction, thus forming a wear particle, the area that must be sheared is twice as large as when shear occurs at the junction. Rabinowinz states this is precisely correct when spherical wear particles are being formed and seems reasonable for other assumed particle shapes.

(2) The shear strength τ_s of a solid has been assumed to be normally distributed with a standard deviation of $0.2\tau_s$. Rabinowinz considers this to be the most questionable assumption, in that the plastic strength properties of a metal, as examined by a hardness test, generally vary by only a few percent about their mean, rather than the 20% postulated. However, it must be remembered first that the size of the junction is much smaller than that of the hardness indentation, so that the statistical scatter in strength values will be larger for the material in the vicinity of a junction, and second that in forming a wear particle interest is in the weakest of all possible paths through the solid in the vicinity of the junction, and thus there can be some kind of extreme value which will tend to fluctuate more than will a parameter based on an average value.

(3) For the interface strength τ_o, it was assumed that the standard deviation is $0.5\tau_o$. The interface, which contains possible oxides and contaminates, will have a greater scatter than will a region inside one of the solids. In work carried out on the statistical scatter of friction coefficient values, typical standard deviations in friction values about the mean friction coefficient $\bar{f}$ have been found to be $0.2\bar{f}$. In these tests a number of junctions were present whose effects were combined. For an individual junction, a standard deviation of 50% of the average shear strength seemed reasonable.

(4) For the case of identical metals sliding together, it was assumed that the mean strength of the interface τ is $0.8\tau_s$. Based on the fact that the interface should be somewhat weaker than the bulk material but not too much weaker. (The general assumption in the adhesion theory of friction is that the shear strength of the interface is equal to the bulk strength of the softer material.)

(5) It was assumed that for unlubricated identical hard metal pairs a friction coefficient value of 0.8 was considered appropriate.

Clemow and Daniell[5] investigated the influence of microstructure on the adhesive wear of a Co-Cr-Mo alloy and found that the difference in wear behaviour between three microstructural conditions of Co-Cr-Mo are independent of hardness of material and presence of carbide. (This is contrary to Bhansali findings.) However, this is due to a variation in the effective chromium content at the sliding surfaces which influences the type of oxide produced and therefore the load necessary to cause a transition in wear from mild to severe. Bhansali also indicated that oxide layers effect the wear transition.

In a paper by Moore[6] working on ferritic steels, it was indicated that bulk hardness is not a direct measure of the resistance to wear but is related to microstructure, determined by composition and heat treatment. Moore points out that there is a close similarity between these relationships and those established between flow stress, hardness and microstructure. For pearlitic steels containing over 10% by volume pearlite, wear resistance and bulk hardness are linear functions of the pearlitic volume. For martensitic steels the wear resistance and bulk hardness are linear functions of the square root of the carbon weight percent. For non-pearlitic cementite/ferrite and spheroidised cementite steels, the wear resistance is thought to be a function of the particle size and mean ferrite path.

Moore's work was carried out under abrasive wear conditions, and if considering the loss of an abrasive particle from, for example, a dispersion hardened spheriodal cementite steel, the role of the cementite particle may alter wear rates considerably more than those for adhesive type wear.

Lipson[7] indicates three types of wear theory for adhesive wear; namely, adhesion theory, interlocking theory and quanta theory.

Adhesion Theory

This assumes that the load W between two bodies in sliding contact is divided among a number of asperities whose total area "A" equals W/p, where p is the yield pressure of the softer material. If there is good adhesion between the two surfaces at the asperities, that are thought of as forming a single body, then the frictional force is found by multiplying the adhered area by the shear strength of the two bodies, F = As. This results in f = F/W = S/p, indicating that the coefficient of friction is independent of load. However, the quantities s and p cannot be identified with the bulk shear strength and hardness of the material.

This introduces a major difficulty in quantitative evaluation. Plastic flow takes place, accompanied by local heating and high local pressures, forming welded junctions between the two surfaces. The strength of these junctions determines the "seizure" strength. Thus the force required to shear a particular adhered junction in the presence of a normal load is not the same as that required when the load is absent, as in a conventional shearing test.

It was found that when strong adhesion occurs at the regions of real contact between metal surfaces, the force to shear the junctions was very close to the product of the cross-sectional area of the junctions and the bulk strength of the material. This frictional force is about 80% of the tangental force necessary to shear the weld. The remaining 20% is required to "plough" the harder asperities into the softer ones. From the above it would suggest that the wear rate for a given material should increase linearly with increasing load, which it does for mild and severe forms of wear, but it does not relate to the marked transition from mild to severe and severe back to mild form of wear as observed by Welsh[8].

Interlocking Theory

This theory is based on plastic deformation in crystalline bodies. Asperities are thought to be deformed plastically by abrupt movement, which usually takes place along several sets of crystallographic planes, causing roughening of the interfaces of contacting high spots. This tends to form a matched interlocking pattern during plastic deformation. The interlocking effect contributes substantially to the resistance to tangental motion. Thus if a pair of asperities is strongly interlocked, a fracture tends to occur at the weakest section inside one of the asperities rather than at the interface.

Quanta Theory

This theory of wear considers the following hypothesis for the formulations of models predicting mechanical wear processes.

1. The rubbing materials receive energy in quanta, all of which are of the same sizes.

2. The quanta of energy are added to the rubbing surfaces at domains that are randomly spaced over their surface.

3. The quanta are added at moments which are randomly spaced in time.

4. The quantized energy which is added at the surface diffuses continuously into the material at a known rate.

5. Sufficient energy in any one piece of the material causes that piece to detach itself in the form of a wear particle.

Lipson states that of the three theories the adhesion theory is most widely accepted, since it explains satisfactorily most of the actual phenomena of wear. However, many investigators report wear by "ploughing" which is consistent with the plastic deformation theory. Lipson also reports that work carried out by Halliday supports this theory. Thus, it seems that plastic deformation plays a part in wear which might be the basis for a combined explanation of wear by adhesion and plastic deformation.

The quanta theory represents an effort to formulate laws for wear comparing analytical conclusions with practical observations. Lipson also reports that Davies made the assumption that the energy wholly decays in the asperity, but there is the possibility that energy might leak to neighbouring surfaces or interior domains, perhaps becoming part of the same wear particle. Furthermore, energy might not be received in equal quanta. Also different shapes of wear particles might deviate considerably from the normal distribution curve.

Welsh[8] in 1965 investigated the wear behaviour of steels under dry conditions. He discovered two transitions in the wear behaviour with increasing load. At light loads, severe wear is inhibited by the combined effects of strain hardening and oxidation. The wear debris at these light loads is finely divided and highly oxidised. At loads immediately above this severe adhesive wear occurs with coarse metallic debris as the lubricating oxide breaks down and contact points soften. At loads above this mild wear is re-established essentially the same as that under light load conditions. The wear rates differ to two orders of magnitude.

This mild wear condition is said to be the consequence of a change of phase, i.e. martensitic hardening induced by frictional heating and increased oxidation due to higher temperatures.

Quinn[9] states that there are three laws of tribology.

(1) $F_{kin} \propto W$ (the load applied normal to the direction of sliding)

(2) $w \propto W$, provided the nature of the surfaces does not change

(3) F_{kin} and w are independent of the "apparent area of contact"

F_{kin} is defined as the force of friction whilst sliding, w is the wear rate and W is the load. The wear rate is normally defined as the volume of surface removed per unit sliding distance.

The author points out that the laws of friction have been given much theoretical attention and had universal validity, however, this was not so for wear. From the many investigations of wear under different conditions a confused picture had arisen. Wear rates had been shown to increase substantially in some instances, without any increase in the frictional force.

This appears to disagree with laws (1) and (2) above, however, Quinn suggests that the factors of proportionality in laws (1) and (2) are not necessarily related to the same operating parameters.

However, Archard[10] in his article in the New Scientist 1959, explains this apparent anomaly by stating that all contacts between asperities contribute to friction, but only a small proportion contribute to wear. So for most contacts, friction is dominated by the behaviour of the undamaged contacts and is practically independent of what happen to the small number of encounters contributing to the wear. If, however, there is an increase in the number of encounters which cause wear, e.g. increase in applied load, then the wear rate will increase, but this will not affect the friction significantly.

Quinn suggests that severe wear occurs by the removal of lumps plastically deformed during contact, but during mild wear such a drastic process cannot occur, although it is likely that parts of heavily oxidised surfaces are removed by some elastic fatigue mechanism. Archard[2] indicates that theoretically, for elastic lump removal as that indicated by Quinn during mild wear, the wear rate is proportional to $W^{4/5}$ (Load) and for plastic lump removal as that indicated for severe wear then the wear rate is directly proportional to the load. However, later work by Archard and Hirst[11] found that the wear rate in both mild and severe forms of wear are directly proportional to load. Quinn explained this by stating that the real area of elastic contact is probably more complete from a geometric viewpoint than that proposed by Archard's hemispherical surface contact.

2.2 The Sursulf Process

During this study of adhesive wear, BS970 708 A37 (EN 19) steel discs were Sursulf treated. This is a salt bath process involving the diffusion of nitrogen and carbon into the surface of the steel.

Gregory[15] points out that the most common way of preventing adhesion is to interpose a third element between the two surfaces so that they may be prevented from touching while in relative motion. This third element, or lubricant, may be oil or grease, graphite or molybdenum disulphide, or gas under pressure. Where the applied load causes breakdown of this lubricant film or the environment is hostile to it, for example in the presence of solvents or at high operating temperatures, other methods of preventing adhesion and the resulting wear must be sought. In many cases, metallic surfaces can be converted with suitable chemical reagents, into compounds having quite different properties and changing the chemical composition at the surface of one or both mating parts, and substantially reduce the risk of mutual welding of the asperities, even when operating without conventional lubrication.

Conventional molten salt baths based on cyanide compounds have been used for many years for nitrocarburising ferrous components. However, since the late 1960s, concern about the overall environmental aspects of heat treatment with cyanide based salts has been increasing. Consequently, there has been intense interest in the development of cyanide-free nitrocarburising treatments as technically and economically viable alternatives to the cyanide-based processes.

The Sursulf process is a non-toxic salt bath process which has been developed by a French company, Hydromécanique et Frottement. Since the salt is cyanide-free it does not give rise to toxic effluents and is virtually free from sludge formation. It is also claimed to be often cheaper to operate and more effective in the fight against scuffing, wear and fatigue than other sulphur-bearing and sulphur-free processes.

The Sursulf process, as with other ferritic nitrocarburising processes, is a thermochemical treatment which involves the diffusional addition of both nitrogen and carbon to the surface of ferrous materials at a temperature completely within the ferrite phase field. This process, as with the Sulfinuz treatment also involves the diffusional addition of sulphur.[12,13,15]

The primary object of this type of treatment is usually to improve the anti-scuffing characteristics of ferrous engineering components by producing a compound layer on the surface, which has good tribological properties. In addition, the fatigue characteristics of the material can be improved considerably, particularly when nitrogen is retained in solid solution in the 'diffusion zone' beneath the compound layer. This is normally achieved by quenching into oil or water from the treatment temperature.[13]

The Sursulf process differs from other sulphur bearing nitrocarburising treatments, in that a cyanide free salt is used, making the process non-toxic. The main advantage of this factor is that the detoxification of effluents and quench waters is a lot simpler[15].

This process was developed by the Tribology and Hydromechanics Centre in France and marketed as an alternative to both the Tufftride and Sulfinuz treatments[12].

2.2.1 Basic Principles

According to Bell[13], conventional nitrocarburising methods use baths based on cyanide, cyanate and carbonate salts of potassium and sodium. These processes are largely controlled by two reactions - an oxidation reaction and a catalytic reaction - the kinetics of which are shown below:

(A) $4NaCN + 2O_2 \rightarrow 4NaCNO$

This reaction can proceed by natural oxidation of the cyanide bath eventually leading to the desired cyanate content. However, this reaction is controllable to some extent, by introducing dry air into the bath.

The catalytic reaction involves the breaking down of sodium cyanate in the presence of the steel components which are being treated, thus supplying carbon and nitrogen to the surface.

(B) $4NaCNO \longrightarrow Na_2CO_3 + 2NaCN + CO + 2N$

In the case of the Sursulf Process[14], the bath is based on cyanate and carbonate salts of lithium, sodium and potassium. As with the conventional processes, cyanate is the source of the necessary nitrogen, the cyanate decomposing as per formula (B).

Sulphur is also added, as potassium sulphide, in very small amounts so that it does not cause excessive porosity in the surface layers of treated parts. It has a threefold action in that:

(a) It produces sulphur compounds in these surface layers which, being lubricants, help to increase scuffing and wear resistance[14,16,17].

(b) It accelerates the nitriding operation[14].

(c) In the oxidised form it is able to neutralise any traces of cyanide formed during the operation of the bath. The main source being reaction (B). The reaction which occurs is of the type indicated in reaction (C)[14,16].

(C) $SO_3^{2-} + 3CN^- \longrightarrow 3CNO^- + S^{2-}$

The principle of this process, according to Gregory[14], is that the carbonate produced, instead of being allowed to build up as a wasteful product of the reaction, is constantly recycled by conversion back to cyanate by means of a special regenerator. The regenerator is based on a compound in the amides-amines group and is introduced into the bath as a daily addition. The Sursulf Licencees Manual[19] gives the following reaction:

(D) $\text{CR2(regenerator)} + xCO_3^{2-} \rightarrow yCNO^- + NH_3 + zCO_2$

The regenerator reacts with the carbonate forming cyanate, ammonia and carbon dioxide.

2.2.2 Composition and Metallography of the Layer

Components treated in a Sursulf bath exhibit a similar microstructure to those produced by other nitrocarburising treatments[12-19]. The treatment produces a white 'compound layer' with a certain amount of porosity at the immediate surface, and a 'diffusion zone' beneath this layer.

Compound layers formed by other conventional nitrocarburising methods consist of a variety of carbon and nitrogen based phases[12,13]. The predominant one being the epsilon carbonitride phase. However, an X-ray diffraction investigation by Gregory[14], of the compound layer produced by the Sursulf process has shown it to consist of iron sulphide (FeS) and epsilon iron nitride (Fe_3N). No iron carbides have been detected.

The porous zone of the compound layer contains salt from the bath and sulphur compounds in a fine dispersion[19]. The total thickness of the compound layer and the depth to which it is porous depends on the bath composition (particularly sulphur and cyanate content) and treatment time.

Beneath the compound layer is a nitrogen 'diffusion zone' in which the concentration of nitrogen decreases with distance from the surface [18,19]. The appearance of this zone is dependent on the cooling rate from the treatment temperature. A water or oil quench results in the nitrogen being held in solid solution. Whereas a slow cool results in the precipitation of iron nitride (Fe_4N) needles within the grains.

2.2.3 The Layer Properties

The Sursulf layer is claimed to improve scuffing (adhesive wear), abrasive wear and fatigue[12-15,18]. Whilst the improved wear resistance is generally attributed to the formation of the compound layer, the diffusion zone is accepted as being responsible for promoting a high fatigue resistance in a component.

Sursulf treatment, like other nitrocarburising processes, converts ferrous metal surfaces into non-metallic nitrides and sulphides, and so reduces metal to metal contact, thus reducing adhesive wear.

The abrasive wear is also improved. Since abrasion is basically a cutting operation, abrasion resistance is increased if hardness is increased.

As stated earlier, the extreme region of the compound layer is porous. This is an advantage when oil lubrication is being used, since the pores act as minute reservoirs to carry oil into contact areas[14].

Another factor is that sulphur compounds (which act as lubricants) are also present in the porous region[16].

As already explained, the diffusion zone beneath the compound layer contains nitrogen, either in solid solution or as needles of Fe_4N [12,13,14]. Although the anti-friction properties of this diffusion zone are much less than those of the compound layer, it shows about the same resistance to wear as, for example, a carburised and quenched component. However, the diffusion zone is of much greater value in promoting a high resistance to fatigue, especially where treated parts are water quenched so as to retain the maximum amount of nitrogen in solution and thus attain maximum surface compressive stress.

There are a very large number of applications for Sursulf treatment (this would also apply to other similar patented ferritic nitrocarburising processes) and include:-

(1) Automotive Industry - Crankshafts, universal joints, cylinder liners, camshafts, spline shafts, stub axles, tappets, distributor pinions, valve guides, oil pump plungers, tappet adjusters, tachometer gears, passenger seat slides, change speed forks, connecting rods.

(2) Hydraulic machine conponents - Valves, sleeves crankshafts, pistons, pump bodies, bearings, gears and piston seals, distributor plates, universal joints, guides and guide rods, gear type pumps.

(3) Machine tool components - Lead screws, bending machine tools, drilling spindles, lead screw nuts, clutch plates, indexing gears, boring bars, slideways, spline shafts, worms and worm wheels, spindle bearings, cams, racks, operating forks.

(4) Diecasting Industry - Bolsters, ejector pins, plungers, moving cores, sleeves.

(5) Forging and extrusion industry - Drop hammer slides, forging press slides, extrusion dies for aluminium alloys.

(6) Textile Industry - Spinning spindles, loom spindles, stenter clips, winding machine spindles, loom gears.

(7) Domestic appliances - Sewing machine parts, lawn mower parts, typewriter parts, vacuum cleaner parts, cash register parts.

(8) Railways - Hydraulic buffers, brake pins, valve guides for locomotives, dampers, bogie pins, valve spindles.

3.0 EXPERIMENTAL TECHNIQUES

A number of 708A37 (EN19) and 534A99 (EN31) discs were used for wear testing.

3.1 Specimen Preparation

The discs were machined, heat treated and then ground flat on each face. The 6mm diameter 50mm long pins were manufactured from 4 metre lengths of wire. The pins were rough machined to 50.5mm then ground flat on each end for subsequent coatings. The pins and the discs were then de-magnetised in order to avoid the possibility of ferritic debris adhering to the surface.

3.2 Disc Materials and Heat Treatment

3.2.1 BS970, 708A37 (EN19)

(a) Composition*

Element	Result	Specification
Carbon	0.401	0.35 - 0.40%
Manganese	0.811	0.70 - 1.00%
Nickel	0.031	
Chromium	1.04	0.90 - 1.20%
Molybdenum	0.198	0.15 - 0.25%
Silicon	0.203	0.10 - 0.35%
Sulphur	0.015	0.04% max.
Phosphorus	0.0172	0.04% max.

(b) Heat Treatment

The discs were hardened in oil from a temperature of 860°C, after soaking for 1 hour, and tempered at 600°C for 2 hours to give "T" condition hardness.

Hardness	Specification
298	248 - 302 Hb

Isothermal and hardenability data is given in Figures (1) and (2) for 708A37 (EN19) steel of typical cast analysis.

These discs were subsequently Sursulf treated after final grinding for 90 minutes at 570°C. After treatment, they were lightly lapped to remove the porous layer which is always present after this treatment.

3.2.2 BS970, 534A99 (EN31)

(a) Composition*

Element	Result	Specification
Carbon	0.997	0.95 - 1.10%
Manganese	0.613	0.40 - 0.70%
Nickel	0.151	
Chromium	1.38	1.20 - 1.60%
Molybdenum	0.029	
Silicon	0.198	0.10 - 0.35%
Sulphur	0.024	0.04% max.
Phosphorus	0.028	0.04% max.

(b) Heat Treatment

The discs were hardened in oil from a temperature of 820°C after soaking for 1 hour and tempered at 150°C for 1 hour to give a hardness 840 - 860°C.

Isothermal and hardenability data is given in Figures (3) and (4) for 534A99 (EN 31) steel of typical cast analysis.

* The analysis of the discs was carried out using a Unicam E970 polyvac direct reading spectrophotometer.

3.3 Pin Materials

The material used to manufacture the pins was BS970 605M36 T (EN16T) for the majority of the coatings examined. For titanium nitride coatings AISI D2 steel was used.

(a) BS970 605M36T (EN16T) Steel: 605A36 (EN16) is a medium carbon manganese-molybdenum steel suitable for tensile ranges 700-850 (R), 775-925 (S), 850-1000 (T), 925-1075 (U) and 1000-1150 N mm^{-2}, according to the limiting ruling section of the part. For any composition of steel the limiting ruling section is the largest diameter in which certain specified mechanical properties are achieved after a specified heat treatment.

The steel was supplied in the hardened and tempered and finally bright drawn condition. Mechanical testing gave the following results.

	Result	Specification
Tensile Strength Rm	1009	850-1000 Nmm^{-2}
Yield Stress	796	680 Nmm^{-2} min
Elongation*	16.6	13% min
Hardness**	302	248-302 HB

* % min. on $5.65\sqrt{SO}$ Gauge length

** Converted from Vickers Hardness

Chemical composition range for 605A36 (EN16)

Carbon	0.32 - 0.4%
Manganese	1.3 - 1.7%
Molybdenum	0.22 - 0.32%
Silicon	0.1 - 0.35%
Sulphur	0.04% max.
Phosphorus	0.04% max.

Isothermal and hardenability data is given in Figures (5) and (6) for 605A36 (EN16) of typical cast analysis.

(b) AISI D2 Steel: D2 steel is a nondeforming high chromium tool steel suitable for long life press tools, blanking dies, thread rolling dies, build up tools etc., where resistance to abrasion is essential and long tool life imperative.

Chemical composition of D2 Steel

Carbon	1.5%
Molybdenum	1.0%
Chromium	12.0%
Silicon	0.35%
Manganese	0.35%

The D2 tool steel pins were rough machined to 7mm dia. then heated slowly to 850°C and soaked at this temperature for 30 minutes. The temperature was increased to 970°C and the pins were allowed to soak for a further 15 minutes. The pins were removed from the furnace and hardened by cooling in an air blast from the hardening temperature. Tempering was carried out immediately after quenching at 200°C for 1 hour. The pins were abrasive grit blasted to remove the heat treatment scale and centreless ground to 6mm dia. The recorded hardness of the pins after hardening and centreless grinding was 59.9 - 61.7 Rockwell "C" scale.

QUALITY

En 19

BS970 708A37

Isothermal transformation

AUSTENITIZING CONDITIONS

TEMPERATURE 860°C (1580°F); TIME 30 MIN.

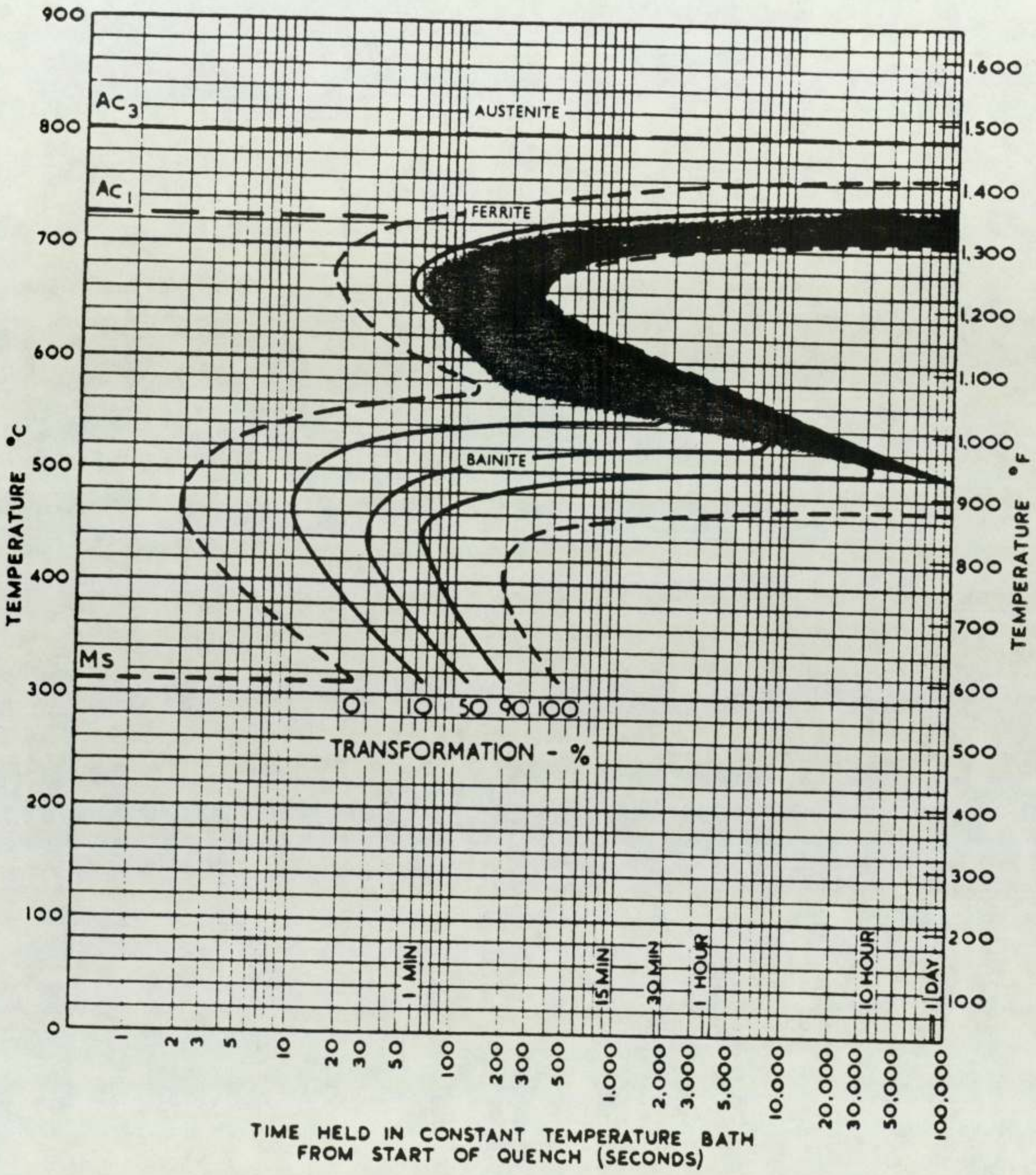

Fig. 1

QUALITY

En 19

Specification range

Carbon	Manganese	Silicon	Sulphur	Phosphorus	Chromium	Molybden
0·35/0·45%	0·50/0·80%	0·10/0·35%	0·050% max.	0·050% max.	0·90/1·50%	0·20/0·40

BS970 708A37

Jominy Hardenability

AUSTENITIZING TEMPERATURE 860°C

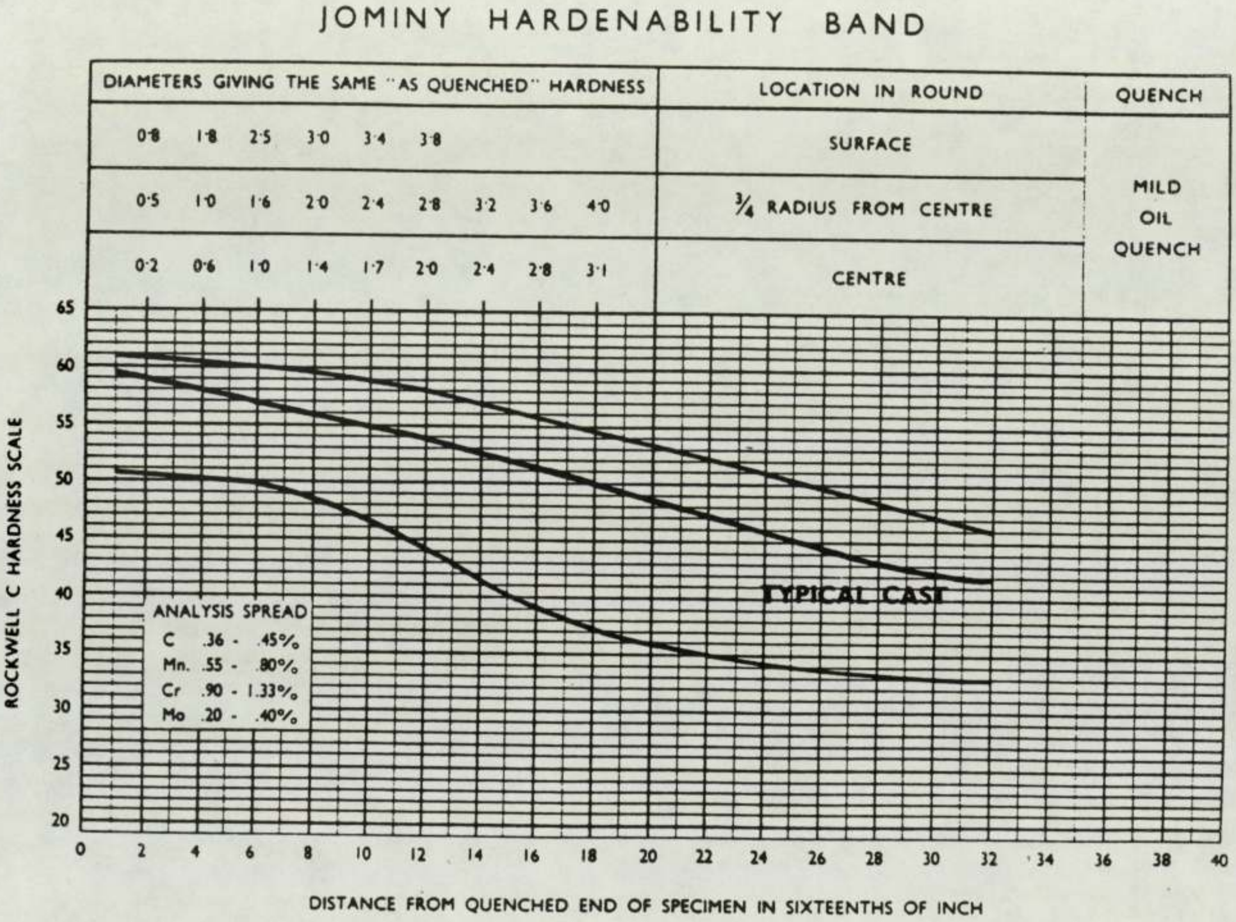

Fig. 2

QUALITY

En 31

BS970 534A99

Isothermal transformation

AUSTENITIZING CONDITIONS
820 C FOR 30 MIN.

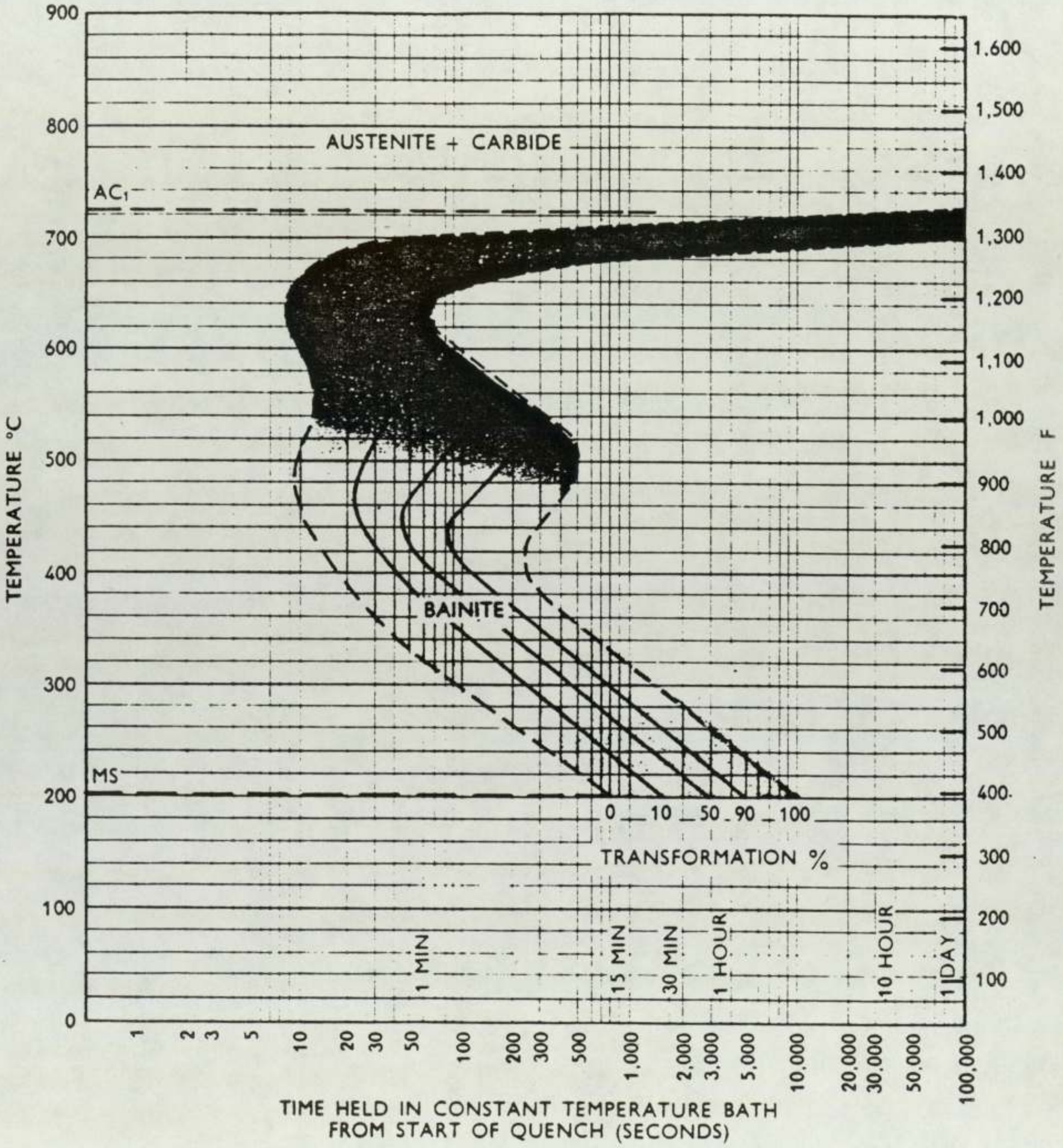

Fig. 3

QUALITY

En 31

Specification range

Carbon	Manganese	Silicon	Sulphur	Phosphorus	Chromium
0·90/1·20%	0·30/0·75%	0·10/0·35%	0·050% max.	0·050% Max.	1·00/1·60

BS970 534A99

Jominy Hardenability

PRE-TREATMENT SPHERODISE ANNEAL 820°C

AUSTENITIZING TEMPERATURE 820°C

JOMINY HARDENABILITY BAND

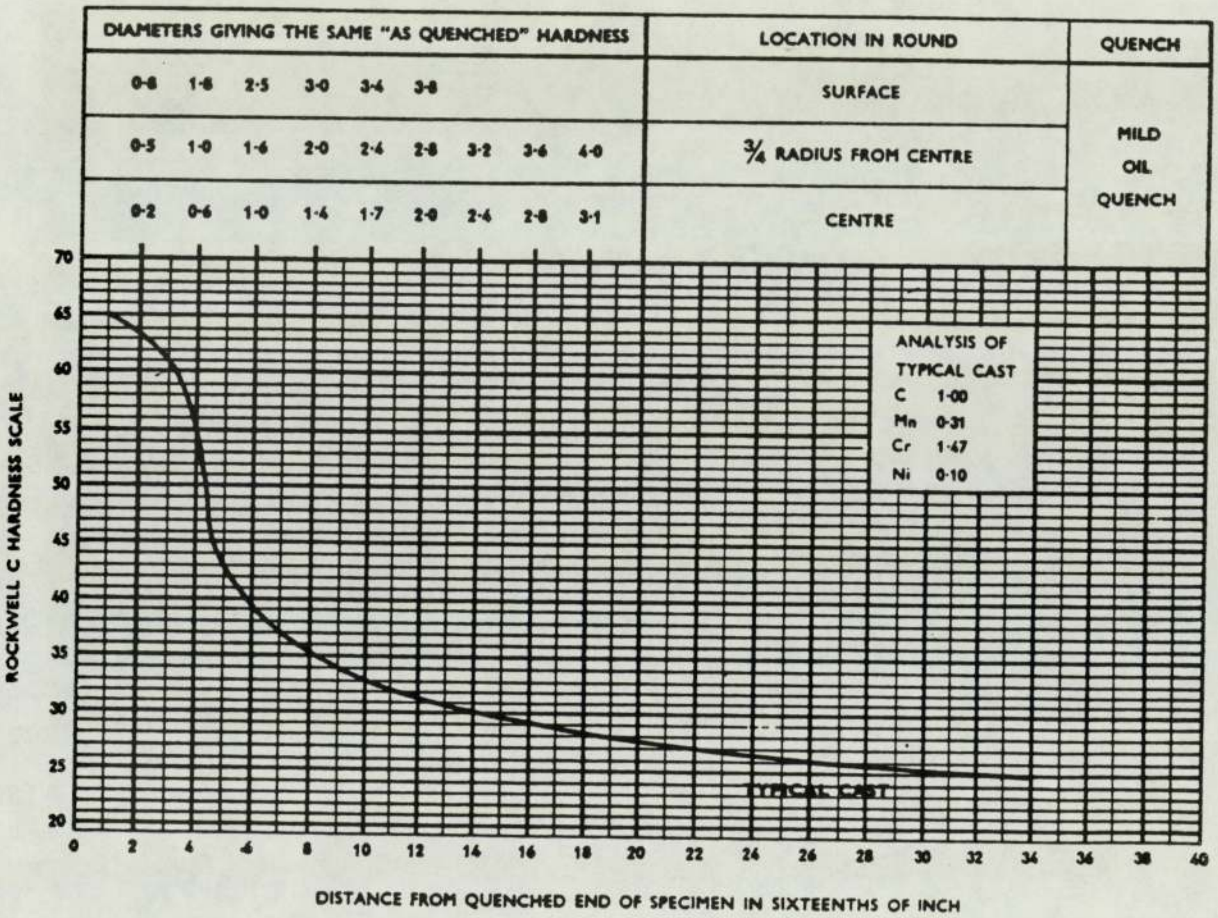

DIAMETERS GIVING THE SAME "AS QUENCHED" HARDNESS	LOCATION IN ROUND	QUENCH
0·8 1·8 2·5 3·0 3·4 3·8	SURFACE	MILD OIL QUENCH
0·5 1·0 1·6 2·0 2·4 2·8 3·2 3·6 4·0	¾ RADIUS FROM CENTRE	
0·2 0·6 1·0 1·4 1·7 2·0 2·4 2·8 3·1	CENTRE	

ANALYSIS OF TYPICAL CAST
C 1·00
Mn 0·31
Cr 1·47
Ni 0·10

Fig. 4

QUALITY

En 16

BS970 605A36

Isothermal transformation

AUSTENITIZING CONDITIONS

TEMPERATURE 845°C (1553°F); TIME 30 MIN.

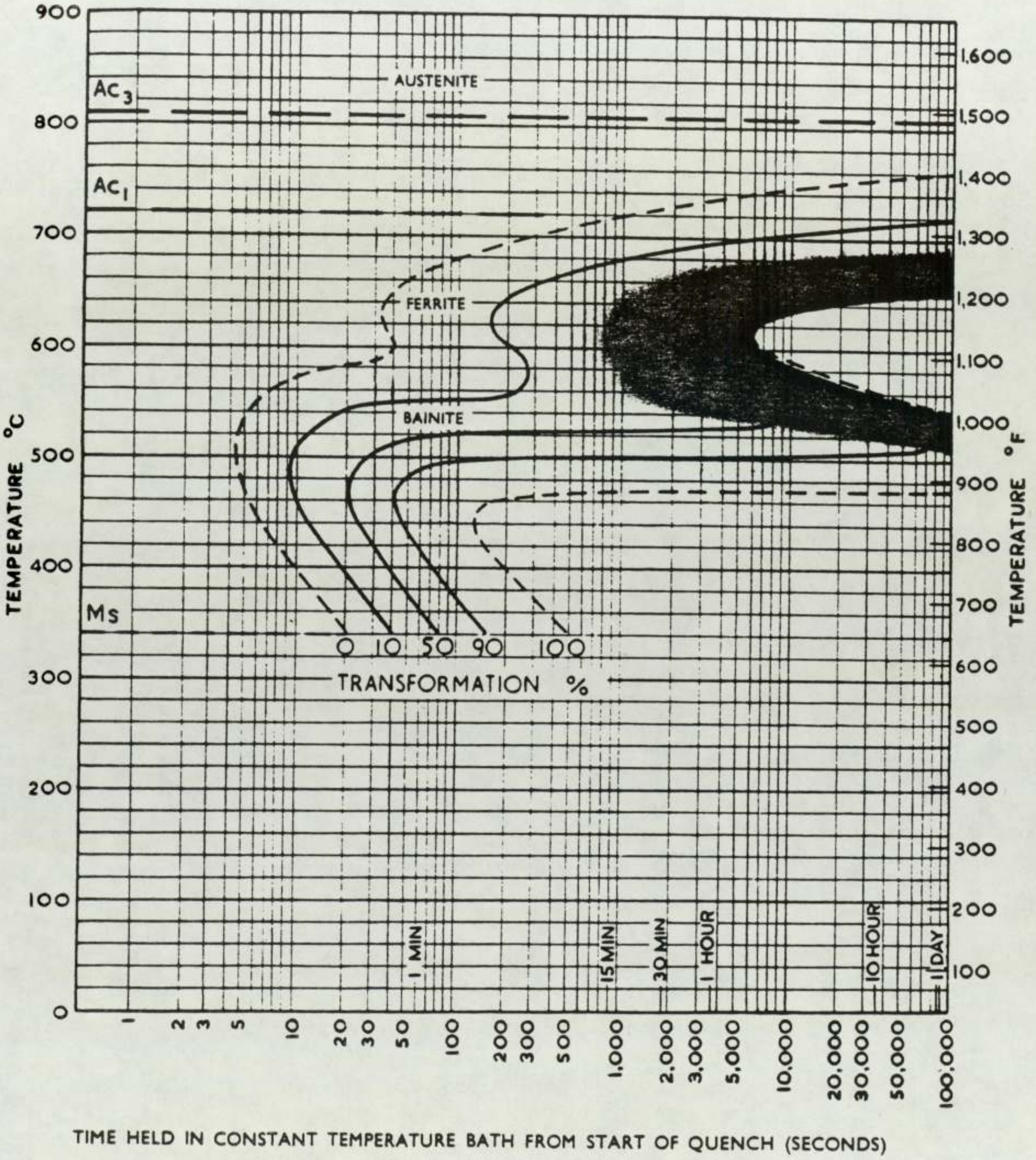

Fig. 5

QUALITY

En 16

Specification range

Carbon	Manganese	Silicon	Sulphur	Phosphorus	Molybdenum
0·30/0·40%	1·30/1·80%	0·10/0·35%	0·050% max.	0·050% max.	0·20/0·35%

BS970 605A36

Jominy Hardenability

AUSTENITIZING TEMPERATURE 840°C

JOMINY HARDENABILITY BAND

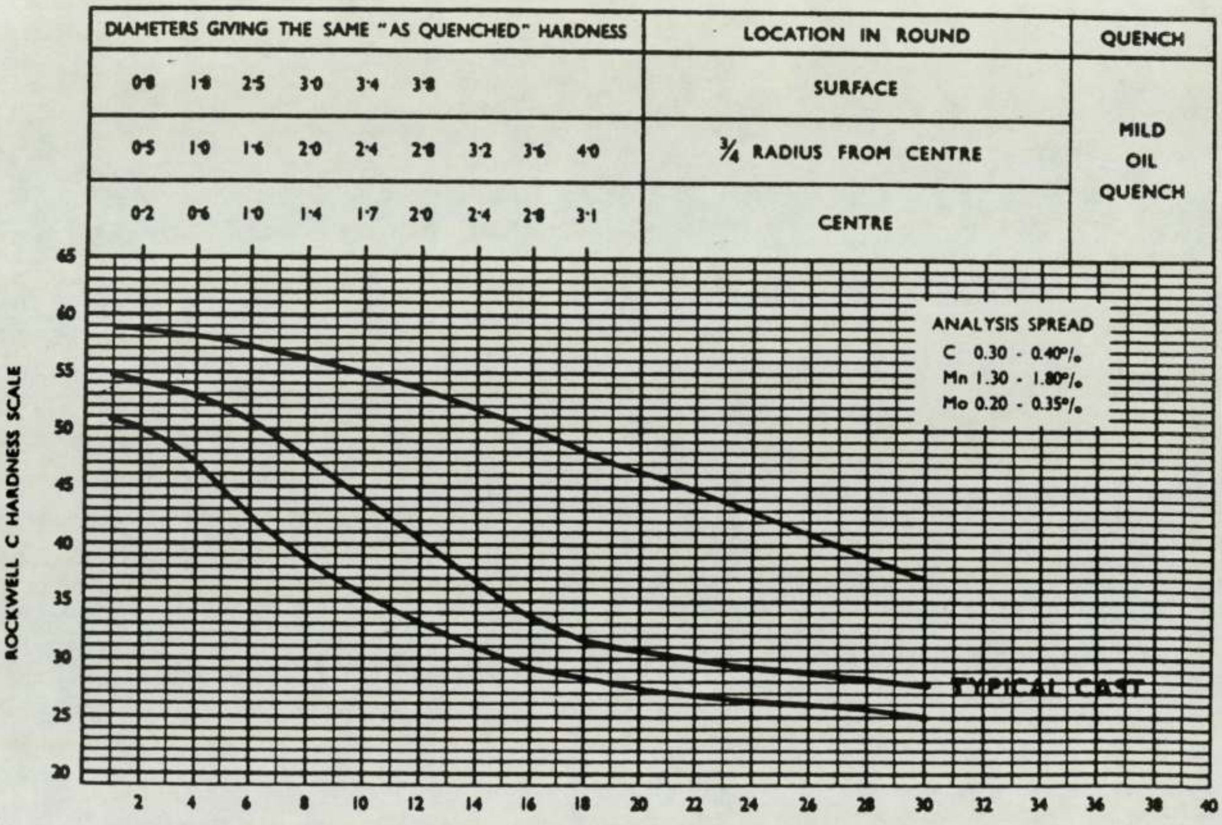

Fig. 6

3.4 Wear Testing

The disc is rotated beneath a loaded pin. The pin is held stationary in the loading arm. The vertical displacement (wear) and torque (side thrust) are measured and recorded on a chart recorder via a transducer set-up. Wear occurs on the disc in the form of a groove or wear track and on the pin, whose area of contact is worn flat.

3.5 Setting up Procedure for Wear Testing

(a) The pins are degreased and then weighed. The length and diameter is measured by a micrometer.

(b) The loading arm can be adjusted by means of four bolts to achieve the desired wear track diameter on the disc.

(c) The disc is degreased, placed on the disc platform of the wear machine and its position secured with the location screw in a hole on the underside of the disc and in the centre by an Allen screw.

(d) The pin is held by a 6mm collet which is pushed into the arm of the wear tester. To ensure the arm and disc are parallel, an accurately machined block is placed between the end of the loading arm and the platform for the stop screw. Therefore, the pin is perpendicular to the disc and thus achieves maximum contact between rubbing surfaces. The collet is then secured onto the arm by the use of a brass nut.

3.6 Setting up Transducers and Recorders

The wear transducer is placed into a hole in the arm attached to the machine over the loading arm. It is adjusted to a position to give a recorder reading of about 10mV after which the transducer is held in position by an Allen screw. The torque transducer is fixed on to the machine and should register midscale on the recorder. The position on the recorder of both transducer readings just needs to be standardised to give a zero setting. The chart speed is 120mm/hour. This value can be changed depending on the sensitivity and expected duration of the test.

3.7 The Wear Test

The speed of the disc is determined from the equation:-

$$\text{Speed} = \frac{\text{r.p.m.} \times \pi \times D}{60}$$

D = Diameter of the wear track in cms.

To set the speed the pin should be clear of the disc, i.e. disc running free. The speed is adjusted with the motor running by altering the machine counter reading.

The r.p.m. value is determined by a linear graph of r.p.m. versus the machine's counter reading. When the speed is set, the motor is turned off and the loading arm lowered until the pin comes in contact with the disc. The stop screw is turned until it is about one millimetre away from the loading arm. This prevents the arm from coming into contact with the disc in the case of severe pin wear rates.

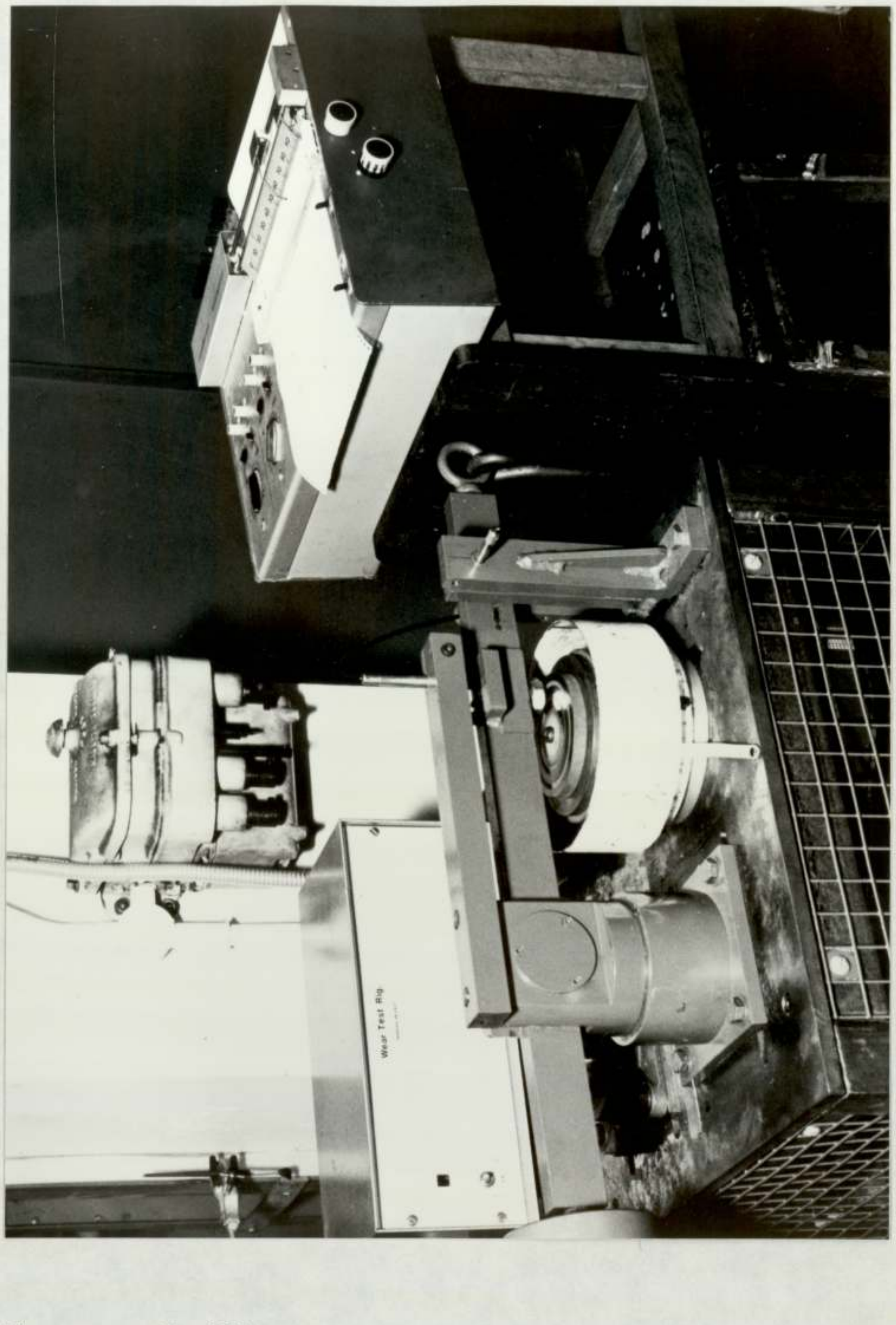

Photograph (1)

Wear Testing Equipment showing Pin on Disc Tester, Transducer Set and Chart Recorder

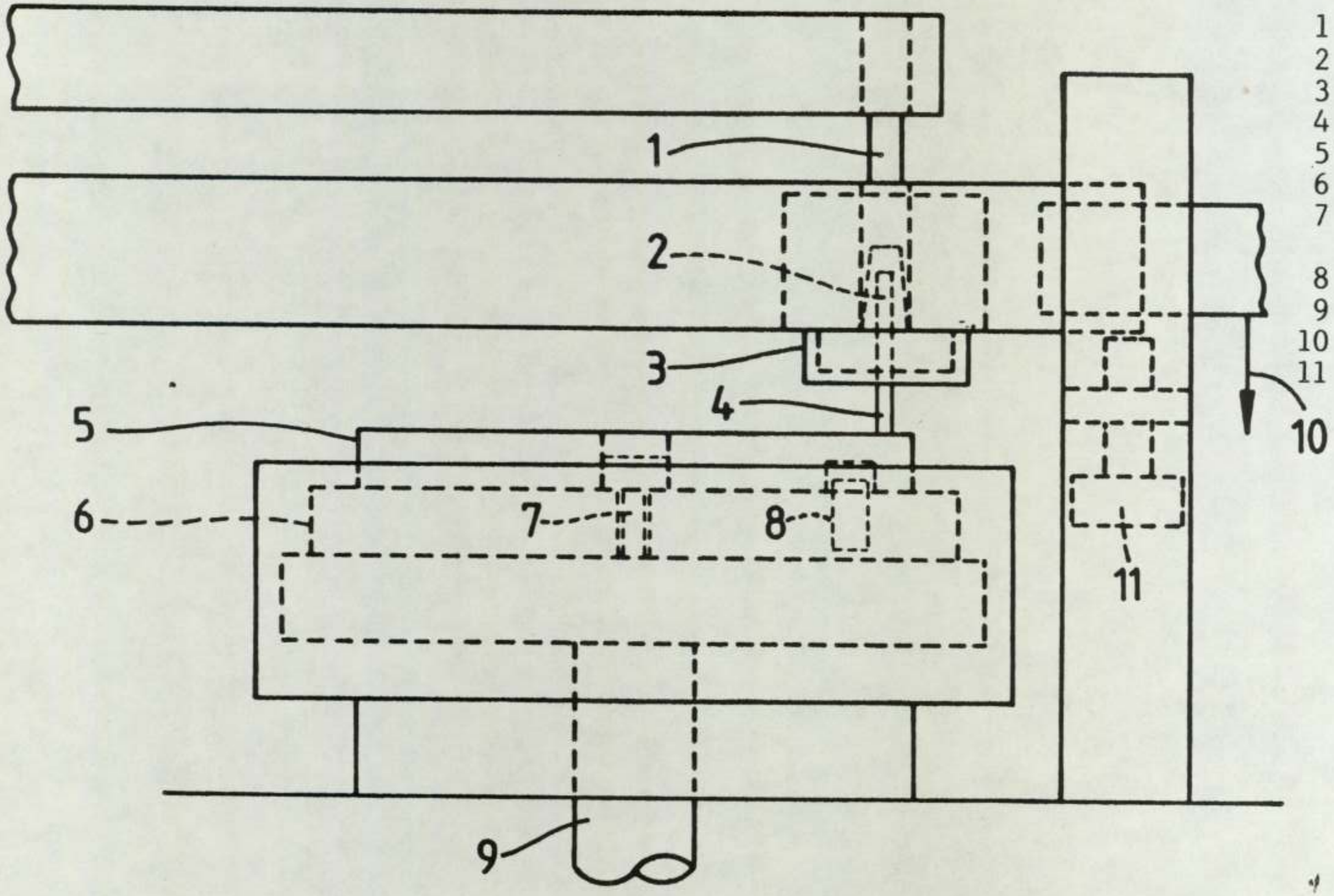

Key

1 - Wear Transducer
2 - Collet
3 - Brass Nut
4 - Pin
5 - Disc
6 - Disc Platform
7 - Allen Screw
(Socket Screw)
8 - Locating Screw
9 - Shaft
10 - Load
11 - Stop Screw

Pin on Disc Wear Testing Equip.

Fig. 7

The machine is started with the torque and wear transducer readings set to zero and the chart recorder switched on. If there is a deflection of more than about 2mV on the wear transducer reading, this indicates that the disc is not flat against the platform. The machine should then be stopped and the disc adjusted.

The wear debris is removed by means of a brush which is attached to a clamp.

During wear testing, the load and the sliding velocity are kept constant at 4Kg. and 100cm/second respectively. Frictional heating effects cause the pin to expand slightly, however, this expansion counteracts any contraction due to wearing as measured on the displacement transducer. The only successful method to establish a wear rate for all coatings examined under these conditions was to weigh the pin before and after testing.

The coefficient of friction was calculated by dividing the measured friction force by the applied load to the pin, i.e. $\mu = F/N$.

3.8 Surface Roughness Measurements

The roughness average, Ra (formerly referred to as the Centre-Line-Average, C.L.A.) was determined for each pin and disc using the Rank Taylor Hobson Talysurf 10 Surface Texture Measuring Instrument.

The standard method of assessing the roughness average is based on traversing a stylus across a surface which follows the surface irregularities.

The pick-up has an optical transducer and the vertical movements of the stylus are sensed photo-electrically. The signal is processed for display either on a recorder or roughness average meter. Roughness average is defined as the arithmetical average of the departures of the profile above and below the reference line throughout the prescribed sampling length. The surface roughness values were assessed as mean results of several sample lengths. The roughness average values recorded for the discs were the mean of four readings taken at 90° to each other around the periphery of the disc, using a special long stroke cut-off of 2.5mm. The roughness average values recorded for each pin was the mean of all the roughness average values taken consecutively across the surface of the pin using a sample cut-off of 0.25mm.

3.9 Micro Hardness Measurements

After wear testing each pin was sectioned and the microhardness measured on a transverse microspecimen. The microhardness testing equipment was the Leitz Miniload 2 microhardness tester using the Knoop diamond indenter.

The Knoop indenter is of pyramidal form having an included longitudinal angle of 172 deg. 30 min. and included transverse angle of 130 deg. 0 min. Under the microscope the Knoop impression appears rhombic in shape, with a long diagonal to short diagonal ratio of 7.11 to 1, thus making it ideal for hardness testing of thin coatings.

The long diagonal is measured and the Knoop hardness number is computed from the following formula:

$$I = \frac{Cp \times F \times 10^3}{L^2}$$

I = Knoop Hardness

Cp = Constant for indenter (1450)

F = Testing force in Newtons (N)

L = Length of longer diagonal in μm

The hardness number, corresponding to a measured length L for a given force, may be determined from tables supplied with the tester.

4.0 PIN COATINGS

4.1 Electroless Nickel and Electroless Nickel/PTFE

Dennis and Such[20] in their book point out that the process termed electroless nickel plating was rediscovered by Brenner and Riddel in 1944.

Brenner and Riddel observed that when electrodepositing nickel from a bath containing sodium hypophosphite, the cathode current efficiency was much greater than 100%, and it was then found that in addition to the nickel being electrodeposited, additional metal was being plated out by means of a chemical reduction reaction which supplied the necessary electrons.

The authors state that one important feature of this hypophosphite reduction of nickel ions is that only certain metals provide the necessary catalytic effect to initiate deposition. Fortunately, all those in Group VIII of the Periodic Table, including nickel, have this property. Therefore, once an initial coating of nickel has been established, the electroless process is self-perpetuating and thus has been better described as auto-catalytic. This differentiates this deposition reaction, which theoretically imposes no limit on the thickness of metal that can be deposited, from those processes which operate only by a displacement reaction leading to thin "immersion" coatings, which are due to the fact that the metal to be coated has a more negative potential than the potential of the metal ions of the coating metal.

The mechanism involved in the hypophosphite reduction has given rise to much speculation, the reduction can be represented by the following equation:

$$Ni^{2+} + (H_2PO_2)^- + H_2O \rightarrow Ni + 2H^+ + H(HPO_3)^- \quad (1)$$

The details of how this reaction occurs have not yet been finalised. Gutzeit[31,32] has suggested that equations (2) and (3) indicate a possible route with the nickel ions being catalytically reduced in equation (3) by means of the active atomic hydrogen which is formed according to equation (2) and adsorbed onto the catalytic surface, with simultaneous formation of othophosphate and hydrogen ions.

$$(H_2PO_2)^- + H_2O \rightarrow H(HPO_3)^- + 2H \text{ (on catalytic surface)} \quad (2)$$

$$Ni^{2+} + 2H\text{(on catalytic surface)} \rightarrow Ni + 2H^+ \quad (3)$$

Whatever the mechanism, the deposits are not pure nickel, but nickel/phosphorus alloy, whose limits of composition are 3 - 15% phosphorus and typical 4 - 10%

Hence, electroless nickel plate normally refers to a nickel/phosphorus which not unexpectedly has very different properties from unalloyed nickel.

Heat treatment of electroless nickel coatings produces a substantial increase in hardness reaching a maximum after 1 hour at 400°C, this is attributed to the precipitation of hard nickel phosphides[21-23].

The wear behaviour of electroless nickel has been studied by Ma and Gawne[23] using the Falex machine, reciprocating pin on flat, Taber Abraser and diamond scratch tester. All tests were performed on 40μm thick electroless nickel coated samples under non-lubricated conditions, with a relative humidity of 50 - 65% and ambient temperature of 15 - 20°C. It was found that the coatings heat treated at 350 - 400°C exhibited the greatest resistance to adhesive and abrasive wear, whereas the as-plated coating gave the highest ductility.

Randin and Hinterman[24] using a ball and disc machine, examined the influence of the phosphorus content of the coating upon unlubricated wear. It was found that maximum wear took place in the as-deposited state for a coating containing 7wt% phosphorus. Increasing the temperature of heat treatment reduced the wear and at treatment temperatures above 400°C the wear decreased as the level of phosphorus increased.

In a more recent publication Ma and Gawne[33] studied the wear behaviour of electroless nickel against itself, plain carbon steel (080M40), austenitic chromium under conditions of dry sliding contact using a Falex machine. The authors state that the rate of wear of electroless nickel coatings is shown to be strongly dependant upon the nature of the counterface material. Electroless nickel in the as-deposited state incurred catastrophic adhesive wear against all the counterfaces tested with the exception of electrodeposited chromium, although significant adhesive wear was observed at the latter counterface. Heat treatment of the electroless nickel coating eliminated catastrophic wear against all counterfaces except stainless steel which consistantly gave rise to the most severe wear.

The lowest wear rates were achieved when both surfaces were heat treated electroless nickel at 600°C. The 400°C heat treated electroless nickel against itself exhibited a higher wear rate but still significantly lower than the other combination of materials.

The severe wear of as-deposited electroless nickel against plain carbon steel is related to adhesive transfer between the two contacting surfaces. Heat treatment produces a marked reduction in the adhesive wear rate. This severe - mild wear transition on heat treatment has been attributed to the formation of nickel phosphides and crystalline nickel, which are expected to exhibit high interfacial free energies and correspondingly less adhesive wear relative to the amorphous nickel in the as-deposited coating.

Ma and Gawne discovered high wear rates of electroless nickel against stainless steel, with the 600°C heat treated coatings proving to be superior to the 400°C heat treated and as-plated electroless nickel coatings.

After wear testing the 400°C heat treated electroless nickel pins against stainless steel blocks, fragments of the electroless nickel coatings were attached to the surface of the stainless steel. This metal transfer on a macro-scale was observed with all the electroless nickel coatings worn against stainless steel with the exception of the 600°C heat treated coating. The effect was similar to that observed with the plain carbon steel counterface and indicates that adhesive wear was the major material-removal mechanism for the electroless nickel-stainless steel couple.

The severe adhesive wear of electroless nickel against stainless steel counterface is attributed primarily to the high degree of mutual solubility between nickel and γ-iron. However, the microstructure of the stainless steel may also promote adhesive transfer. The steel consisted of a solid solution of chromium and nickel in coarse grained f.c.c. iron with carbon in solution and as grain-boundary precipitates of chromium rich carbides. The volume fraction of carbide is small and the steel is essentially single phase.

The presence of second phases, such as carbides, which are less compatible with nickel than is the iron matrix will act to decrease the extent of adhesive transfer by reducing the area fraction of compatible surface and decreasing the cross-section of adhesive junctions. The absence of a substantial amount of second phase in the stainless steel is thus likely to enhance adhesive wear.

The presence of chromium in the stainless steel produces a thin stable oxide film on the surface which is responsible for its corrosion resistance. In principle, the oxide film may act as a barrier layer between the stainless steel and counterface thereby suppressing adhesive wear. However, from the results obtained by Ma and Gawne, higher wear rates of electroless nickel are incurred against stainless steel than against plain carbon steel, which indicates that this mechanism has little influence. The oxide film most likely fractures and delaminates during wear to expose the underlying steel surface.

Catastrophic adhesive wear of electroless nickel did not occur when electrodeposited chromium was used as a counterface. Adhesive transfer of nickel to the chromium counterface was observed but this gave intermediate rather than severe wear. The reason for this reduced adhesive transfer with the chromium counterface was not clear since chromium is soluble in nickel and is a single-phase material. A possible explanation is that the oxide film on chromium is a more effective barrier layer in suppressing adhesive transfer than that on stainless steel. The higher elastic modulus and hardness of chromium compared with stainless steel results in less deflection of the underlying metal, lower stresses in the brittle oxide film and hence less tendency for its fragmentation and removal during wear.

Tulsi[25] points out that electroless nickel has demonstrated that it is a versatile material which is valuable for protecting parts from corrosion and/or wear. The scope of electroless nickel has further been increased by codepositing materials such as silicon carbides, ceramics, diamonds and fluoropolymers. This is achieved by taking advantage of different but often complementary properties of nickel-phosphorus alloy and the particles.

Incorporation of particles into metallic coatings creates an enormous number of possibilities, as the nature of the powder as well as the particle size can be varied. For example, silicon carbide particles are codeposited to increase significantly hardness and wearability of the deposit, whereas polytetrafluoroethylene (PTFE) particles are used to lower coefficient of friction and impart lubricity.

Brown[26] states that the latest development in electroless co-deposits is PTFE. The author points out that the dispersion used in the process is prepared in water with a high polymer concentration and is made stable by mixing it with a blend of cationic and non-ionic fluorocarbon surfactants. The cationic surfactants adhere very strongly to the surface, which enables sufficiently large quantities of them to be added without a significant amount of free surfactant being present in the plating solution. It is postulated that since both surfactants are strongly adsorbed by the PTFE surface, the increase in the dispersion stability in concentrated salt solutions is caused by steric hindrance of the ethylene oxide groups.

The most important factors influencing the incorporation of the PTFE polymer are the concentration, size distribution and the zeta potential (controlled by the ratio of cationic and non-ionic surfactants) of the particles, the type and pH of the electrolyte and the flow velocity of the electrolyte [25, 26].

Brown[26] indicates that because the particles themselves are soft, the bulk hardness of the deposit is low at about 250HV, but the actual nickel/phosphorus matrix has a normal electroless nickel hardness of about 450HV. In addition, the author points out that the initial wear rate of such coatings is similar to electroless nickel coatings, but as the electroless nickel PTFE is transferred to the mating surface, the coefficient of friction falls and the wear rate drops.

The particle size of the PTFE is less than one micron and the amount co-deposited is 25 - 30% by volume.

The main benefits of such a deposit are that it confers release (non-stick), non-galling, dry lubrication, lower coefficient of friction[25,26], bearing improvement, lower uniform and precise torque or tension values and gives good corrosion resistance[25].

The electroless nickel/PTFE composite coated pins were supplied by The Montgomery Plating Company, Coventry. No process data was given for the production of the coatings. The conventional electroless nickel plating was carried out at Aston University using a commercial acid-hypophosphite solution "Nifoss 2000", supplied by W. Canning Materials Limited.

The total volume of the bath for each Nifoss plating operation was two litres and was maintained at a pH of 4.8 - 5.3 and at a temperature of 88°C using a thermostatically controlled water bath. The metal ion and reducing agent concentrations were maintained by appropriate additions of base solution and reducing agent as determined by analysis and maintenance procedure in instruction sheet[27].

4.2 Hard Chromium

Hard chromium deposits are widely used for the provision of hard, abrasion resistant wearing surfaces and for the building up of undersized and worn parts. The value of chromium for such purposes lies in its hardness, resistance to abrasion, passivity of surface, and its "anti-seize" properties when applied to rotating or reciprocating parts.

The technique of heavy deposition differs from those involved in bright chromium plating for decorative effect. The deposits are thicker and are generally applied directly to the basic metal without any precoating of nickel, except under special circumstances, as when building up badly worn or undersized parts, and where the components are subject to highly corrosive conditions in service.

It is generally accepted that a thickness of 0.3 - 0.4mm of chromium is the maximum practical limit for any purpose, whether for salvaging an article or for rendering it abrasion resistant; deposits in excess of this are apt to be brittle. As a general rule, a finished thickness of 0.13mm is ample for most purposes and in many cases thin deposits of 12 - 50µm are sufficient to give protection against wear or prevent seizing of moving parts[28].

Dennis and Such[20] in their book indicate that the baths used for hard chromium plating are very similar in formulation to those used for the deposition of thin decorative chromium, except that the more concentrated solutions are not often employed, and the usual composition range being 150 - 300g/l of CrO_3.

Solutions containing fluoride type ions are frequently utilised because of their greater cathode efficiency. Higher temperatures (over 50^{o}C) and higher current densities, up to 80 A. dm^{-2}, are used than are employed for decorative chromium. Higher temperatures are necessary to prevent burning and the formation of rough deposits at the rapid rate of deposition given by these high current densities.

In order to obtain the maximum hardness, it is necessary to consider both bath temperature and current density (see Table 1). The presence of fluoride type ions enables faster deposition rates to be employed, but greater care may be required in some cases because of their greater etching effects on unplated areas. Since very high current densities are used when depositing thick coatings, it is frequently necessary to have the vat fitted with facilities not only for heating, but also for cooling; the latter being necessary due to the heating effect of the large current passed per unit volume.

The pins were hard chromium plated in a working proprietary hard chromium plating solution supplied by W. Canning Materials Limited, "Hycrome Hard Chromium Solution". This type of solution is catalysed by both sulphate and fluoride type ions, and is recommended for high speed production of hard chromium deposits, and it has a cathode current efficiency of the order of 20%.

<u>Operating Conditions</u>:

Cathode Current Density	40 - 50 A. dm^{-2}
Voltage	5.5 - 7 volts
Temperature	55 - 57^{o}C
Solution Density	1.20 sp.gr 15^{o}C 1.18 sp.gr 54^{o}C

The pins were electroplated after suitable pretreatment for 90 mins., 120 mins. and 150 mins. at approximately 45 A. dm^{-2}. After hard chromium plating the pins were centerless ground back to 6mm diameter and the end ground flat to remove high points due to any chromium build-up at the edges.

Table 1

Operating Conditions of Chromium Plating Baths to give the Hardest Electrodeposits

Current Density A. dm^{-2}	Temperature ^oC	
	250g/l CrO_3 Solution*	400g/l CrO_3 Solution*
22	48 - 50	43 - 45
33	50 - 54	45 - 49
44	50 - 55	45 - 50
66	52 - 56	47 - 51
110	53 - 57	48 - 52

* Catalysed only by sulphuric acid CrO_3: H_2SO_4 = 100:1 (Table reproduced from M.O.D. Specification DEF160 - Chromium Plating for Engineering Purposes HMSO 1967)

4.3 Titanium Nitride

Titanium nitride has long been known as a hard material with a golden yellow colour whether produced via chemical vapour deposition (C.V.D.) or by a reactive physical vapour deposition process (P.V.D.)

The synthesis of titanium nitride by P.V.D. at temperatures below 500°C allows high speed steels to be coated after the final machining operation. Hence the coating is carried out as the ultimate step in an otherwise unchanged fabrication process.

The coatings prepared by an ion plating P.V.D. process are fully dense with a smooth surface[29]. Films containing less than 15at.%N are single-phase h.c.p.α-Ti with nitrogen dissolved in the lattice. Both the -Ti and the tetragonal Ti_2N phase are present in films containing between 15 and 33at.%N. With 35at.%N the Film consists of both the Ti_2N and the cubic TiN phases, and with above 35at.% the films are single phase TiN.

The microhardness as a function of the nitrogen content increases monotonically up to a composition containing 49at.%N and then decreases rapidly. The film density reaches a maximum and the electrical resistivity reaches a minimum also at 49at.%N, whereas the film density reaches minimum and the electrical resistivity reaches a maximum at 25at.%N[30].

In contrast, titanium nitride coating prepared by C.V.D. on cemented carbide cutting tools to improve their cutting performance, and sometimes as a double coating with titanium carbide, have not been applied to high speed steel. The economics of the C.V.D.

process necessitate temperatures within the range in which phase changes or dimensional changes of the steel will occur. The advantages of such a coating applied to high speed steel would be negated by the additional deformation arising from a subsidiary hardening heat-treatment because the treated tools cannot be reground without removing the coating[29].

Titanium nitrides and carbides produced by C.V.D. are at present well established and suitable for mass production. The components for coating are heated in a retort furnace at 1000°C.

$$TiCl_4 + 2H_2 \longrightarrow Ti + 4HCl$$

$$Ti + N \longrightarrow TiN$$

Methane is introduced to the system to produce titanium carbide.

$$TiCl_4 + CH_4 \longrightarrow TiC + 4HCl$$

These layers are very hard: titanium nitride approximately 2500Hv and titanium carbide approximately 3300Hv.

The C.V.D. process can be carried out at atmospheric or reduced pressure with a layer thickness of 5 - 10μm.

After processing the component must be hardened and tempered using a vacuum furnace, otherwise the coating would break down because titanium is highly reactive in air at temperatures above 500°C.

Ion Plating Equipment (PVD)

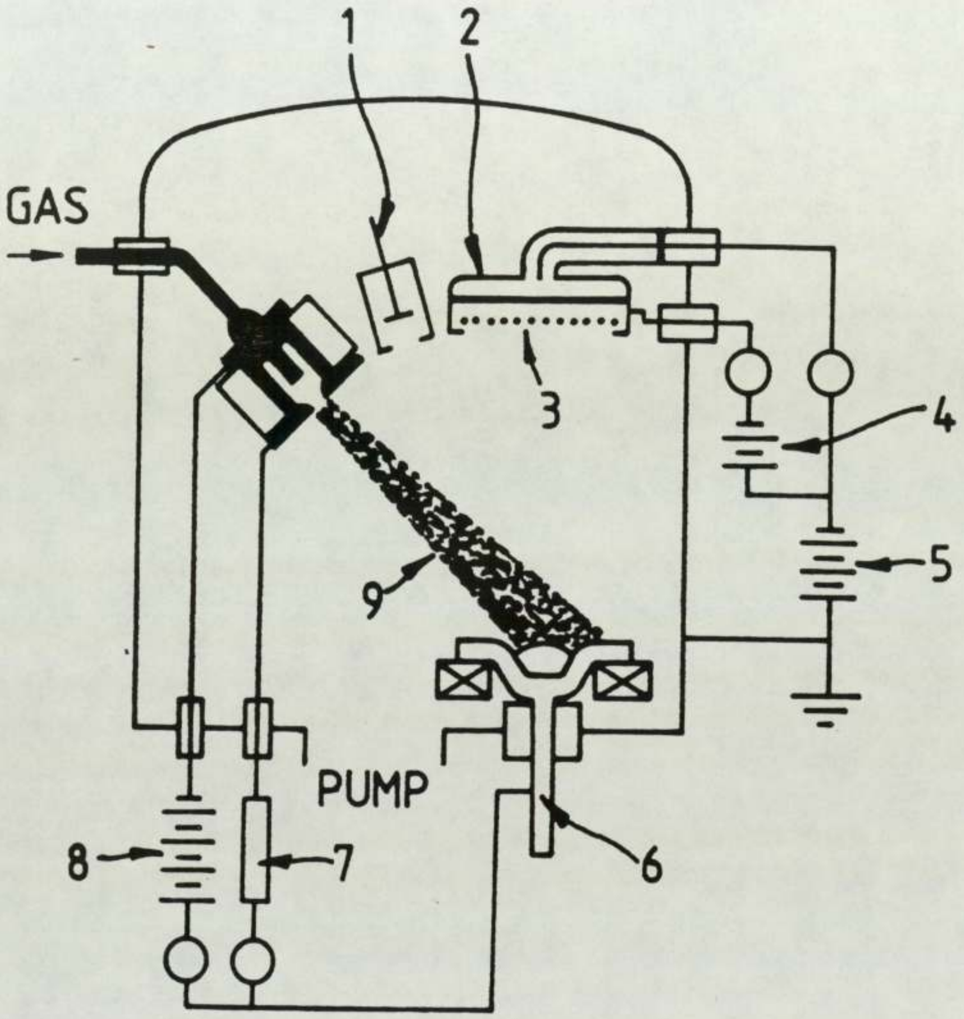

1 Thickness monitor
2 Collector 50 cm^2
3 Grid
4 Suppressor 25V
5 Collector bias 0–1000V
6 Water cooled copper hearth
7 Resistor 400Ω
8 Voltage source
9 Plasma electron beam

Fig. 8

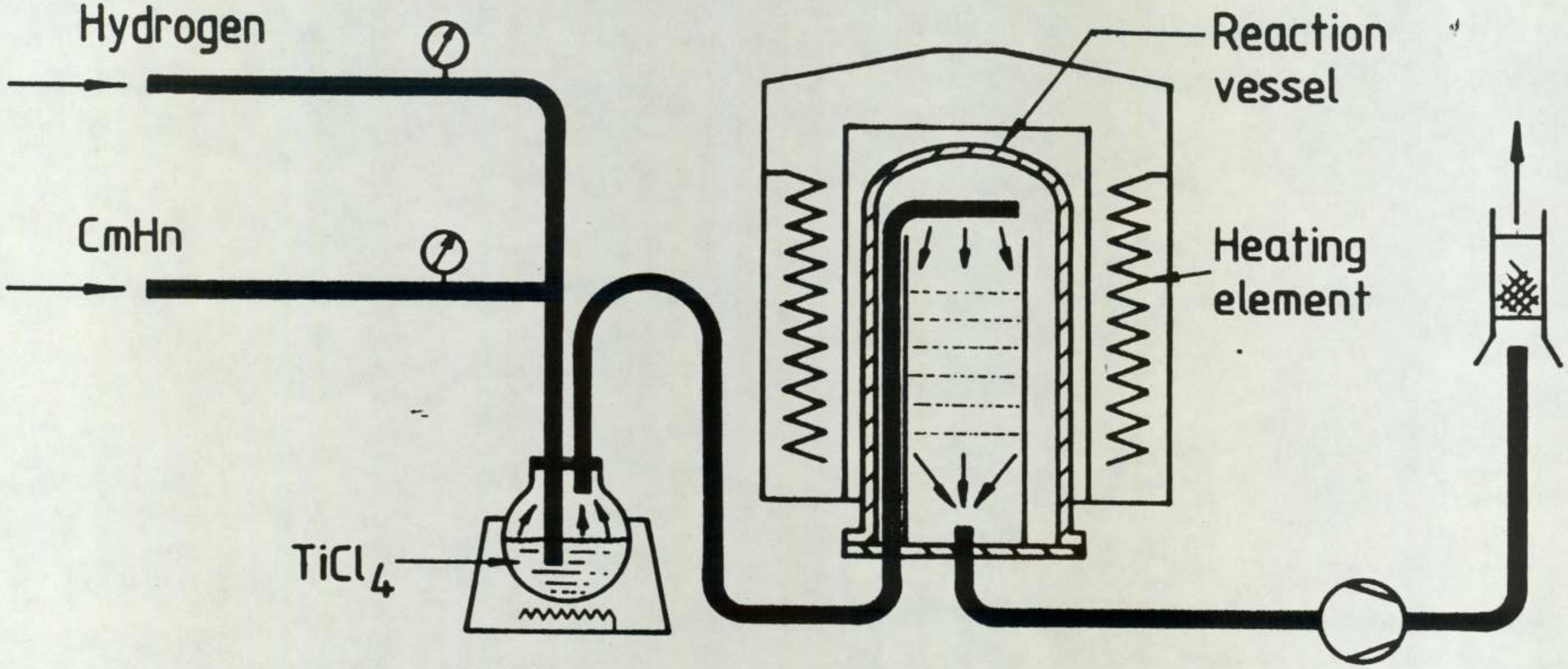

C V D Furnace

Fig. 9

Table 2

Comparison of Titanium Nitride Coatings by CVD and PVD

Items	C V D	P V D
Kind of formed coatings	TiC, TiN	TiC, TiN
Substrate materials usually used	High carbon steels such as high speed steel, cold working die steel, ball bearing steel, Cemented carbide	High speed steels, Cemented carbide
Procedure ( ) sometimes necessary [ ] almost necessary	Rough machining → (hardening) → finish grinding → CVD → [re-heating hardening]	Rough machining → hardening → finish grinding → PVD
Furnace temperature (°C)	900 ~ 1050	500 ~ 600
Cooling method	Gas cooling in the reaction vessel either fixed in hot CVD furnace or taken out of furnace during cooling operations	Furnace cooling
Substrate hardening	Simultaneously made only for extremely deep hardenability steels. Re-heating hardening should be done for most steels by use of vacuum furnace.	Should be done before PVD

Table 3

Comparison of Titanium Nitride Coatings by CVD and PVD

Items	C V D	P V D
Selective area coating	impossible	possible
Mass production	There may be some limitations due to poor flexibility in charging and discharging	There may be some limitations
Limitation of size of articles	Large articles are very difficult to commercially treated, because of enormous expense for the equipment and extension in time for heating up to the coating temperature.	There may be some limitations. Large articles are very difficult to be commercially practiced, because of enormous expense for the equipment and extension in time for heating up to the coating temperature.
Distortion problem	Improper coating procedure may cause problem	None
Working environment	Good	Good
Pollution problem	Emission problem can be resolved by use of effluent gas neutralizing equipment	None

Table 4

Comparison of Titanium Nitride Coatings by CVD and PVD

Items	C V D	P V D
Charging of articles to be coated	Charging into cold furnace or cold vessel, followed by heating furnace or vessel, including articles, to coating temperature	Charging into cold equipment, followed by heating articles to coating temperature
Discharging of articles	Discharging from furnace or vessel cooled down to near room temperature	Discharging after articles are cooled down to near room temperature
Controlling factors for layer thickness	Gas composition, Gas flow rate, Treating temperature, Treating time, Substrate material	Gas composition, Gas flow rate, Treating time, Position and size of both electrodes
Controlling factors for layer composition and structure	Gas composition, Gas flow rate, Substrate material, Treating temperature	Gas composition, Gas flow rate, Treating temperature, Substrate material, Position and size of both electrodes
Flexibility in charging and discharging	Charging of articles made of different substrate materials is highly limited. Variation of substrate material causes the difference in layer thickness, layer structure and substrate hardness, since gas composition, coating time and cooling method can not be changed for each articles in a coating operation.	To realize uniform coating in thickness and composition of layer, shape and number of articles are extremely limited.

4.4 Tin-Nickel

The electrodeposited tin-nickel alloy is a single-phase meta-stable compound, corresponding to the formula NiSn. The compound is quite stable at ordinary temperatures, but starts to recrystallise at elevated temperatures. For this reason the maximum safe working temperature of the deposit may be taken as 500°C[34].

The Tin Research Institute[34] claims that:-

(1) The hardness of electrodeposited tin-nickel alloy is about 700 H.V.

(2) The tin-nickel alloy is inherently somewhat brittle, and it is not practicable to carry out much fabrication after plating.

(3) The reflectivity of the deposit is approximately 50% in the visible region.

(4) Tin-nickel deposits can readily be soldered using activated resin fluxes.

In terms of corrosion resistance in the atmosphere, pore-free deposits of tin-nickel remain permanently bright and perform as well as or better than chromium on nickel of the same thickness

Tin-nickel resists many kinds of corrosive material better than either tin or nickel. It is uncorroded by cold nitric acid of all concentrations, by other acid solutions with a pH greater than 1.2, by neutral solutions and by alkalis; it is not discoloured by foodstuffs, by handling or by exposure to atmospheres grossly polluted with sulphur dioxide and hydrogen sulphide.

It may be tarnished by prolonged immersion in water, especially hot water, or by exposure to hot steam for some hours, but is unaffected by hot dry air up to 320°C, or by normal wetting or exposure to condensation involved in domestic use.

The tin-nickel alloy electroplate is used for industrial electrical fittings, electronic components, TV cable connectors, refrigerator equipment, drawing instruments, scientific and optical apparatus, aluminium coffee percolators, tea kettles, heavy gauge copper frying pans and saucepans, industrial drying equipment, and a wide range of other equipment that must be strongly resistant to corrosive chemicals. A tin-nickel coating has good frictional and oil retention properties and is also used for certain watch parts, pistons for brake mechanisms and frictional parts of musical instruments[34].

P.M.D. Chemicals[35] point out that their "Nistan" tin-nickel electroplating solution yields a deposit of 65% tin:35% nickel by wt., a composition which seldom varies unless the plating conditions or the electrolyte are grossly out of balance. "Nistan" is recommended for certain technical applications, as an alternative to tin-lead plating to provide a more corrosion resistant deposit, and also as an alternative to bright chromium in the bright nickel and chromium process. When electroplated onto a polished surface, the deposit is instantly mirror bright. "Nistan" can be used for barrel rack and reel-to-reel applications.

"Nistan" may be deposited directly onto copper and copper-based alloys. Steel and aluminium or zinc-based alloys must first be flash-plated with copper (minimum thickness 0.75 microns) before being electroplated with "Nistan". Thus the pins were copper electroplated after being conventionally cleaned. The solution used for copper plating was an alkaline cyanide type.

Operating Conditions:

Cathode Current Density	3-4 A.dm^{-2}
Temperature	50°C
Plating Time	1-2 minutes

After copper electroplating, the pins were water swilled, dilute acid dipped (10% by volume hydrochloric acid) and finally water swilled before electroplating in a working P.M.D. "Nistan" tin-nickel plating solution.

Operating Conditions:

Cathode Current Density	0.1-2.0 A.dm^{-2} (optimum 1.0 A.dm^{-2})
Temperature	68-75°C (optimum 70°C)
pH	5.0-5.8 (optimum 5.5)
Stannous Tin	15-27 g/l^{-3} (optimum 25 g/l^{-3})
Nickel	36-65 g/l^{-3} (optimum 60 g/l^{-3})
Deposition Rate	1 micron in 2 minutes at 1.5 A.dm^{-2}

P.M.D. Chemicals[36] claim the following properties of the as-deposited tin-nickel from the "Nistan" solution:

(1) Tin 65% : 35% nickel

(2) Density, 8.4 $g.cm^{-3}$

(3) Hardness, 680 - 720 HV

(4) Specific Resistance, $1 \times 10^{-4} \Omega$ cm

4.5 Tin-Cobalt

The tin-cobalt system has received much less study than that of tin-nickel. Three intermetallic compounds of tin and colbalt exist at low temperatures.

$CoSn_2$ (19.8% Co) tetragonal, a = 6.348 Å
c = 5.441 Å

CoSn (33.3% Co) hexagonal, a = 5.268 Å
c = 4.249 Å

Co_3Sn_2 (40.7 - 41.7% Co) a = 16.356 Å
hexagonal, c = 4.249 Å

Clarke, Elbourne and Mackay[37] aimed to produce an intermetallic phase like the commercial tin-nickel by substituting the nickel chloride for cobalt chloride in the electrolyte.

Cobalt Chloride	250 g/l
Ammonium Bifluoride	40 g/l
Stannous Chloride	50 g/l
Ammonium Hydroxide (0.88)	35 ml/l

This electrolyte was tested by means of Hull cell experiments (267 ml cell, 1 A, 5 minutes). The electrolyte gave an unattractive dull grey deposit except at very low current densities. At higher current density the deposit was largely tin, which tended to discharge as a coarse powdery coating.

Development of this cobalt-tin electroplating solution eventually gave a bright fine-grained coating over the whole Hull cell plate, and which seemed to have many of the characteristics of tin-nickel electrodeposits.

Cobalt Chloride	250 g/l
Ammonium Bifluoride	100 g/l
Stannous Chloride	50 g/l
Ammonium Hydroxide (0.88)	35 ml/l
Hydrochloric Acid (ION)	100 ml/l
Temperature	75°C
Current Density	2.5 $A.dm^{-2}$

Clarke, Elbourne and Mackay[37] claimed a deposit from this electroplating solution to contain 67% tin, which is very close to the composition CoSn (66.7% Sn).

Close similarities were observed between electrodeposited CoSn and the better known tin-nickel. Both electroplating solutions deposit close to the equiatomic composition, though while CoSn appears on the phase diagram NiSn does not. However, CoSn deposits crystallise in a different structure (cubic) from that of the diagram phase (hexagonal). Both electrodeposits CoSn and NiSn were hard and bright as-plated and can be obtained from similar fluoride electrolytes, though that for the cobalt alloy required greater suppression of the tin discharge. Both electrodeposits decomposed on heating, though the nickel alloy required higher temperatures and longer times. One hour at 200°C decomposed CoSn whereas 700°C was needed to decompose NiSn in the same time, although the tin-nickel electrodeposit decomposed at 300°C given longer time. The CoSn had a passive stability which was similar to that of NiSn, with a passivation potential well below that of the hydrogen electrode in the same solution. The film remained insoluble and protective over pH ranging from -1 - 14, so apart from special reagents which dissolved the film the electrodeposit would be expected to resist corrosion in any normal media, whether or not dissolved oxygen is present. A cast alloy with about 50% cobalt is resistant to attack by acids (including agua regia), but is so brittle as to render fabrication impossible.

Work carried out by Tyutina, Luk'yanova and Selivanova[38] aimed to produce tin-cobalt coatings containing less than 1% cobalt for ease of soldering for printed circuit applications.

The authors claim that silvery-white finely crystalline coatings of cobalt-tin alloy containing 0.003 - 0.5% cobalt were obtained from a sulphate based electrolyte.

Cobalt Sulphate	35 g/l
Stannous Sulphate	65 g/l
Ammonium Bifluoride	50 g/l
Sulphuric Acid (1.84)	10 ml/l
pH	4.0 - 4.5
Current Density	0.5 - 1.5 $A.dm^{-2}$

The tin-cobalt alloy from this solution exhibited good soldering characteristics even after twelve months storage. The only exception to this was tin-cobalt alloy electrodeposited onto brass. The reason for the deterioration in the solderability of the tin alloy coatings on brass is diffusion of zinc from the substrate to the outer layer of the coating. In order to avoid this the authors point out that a 3μ thick layer of copper or nickel can be used on the brass prior to tin alloy electroplating.

The electrolyte used for the production of the cobalt-tin coated pins during this study was a chloride based solution which was under development by P.M.D. Chemicals.

Sodium Gluconate	15 g/l
Cobalt Chloride	7 g/l
Stannous Chloride	3 g/l
Sodium Chloride	20 g/l
pH	8.0
Current Density	1 $A.dm^{-2}$

X-Ray microanalysis revealed that the electrodeposit consisted of 94% cobalt, 6% tin.

5.0 RESULTS

5.1 The Sursulf Layer

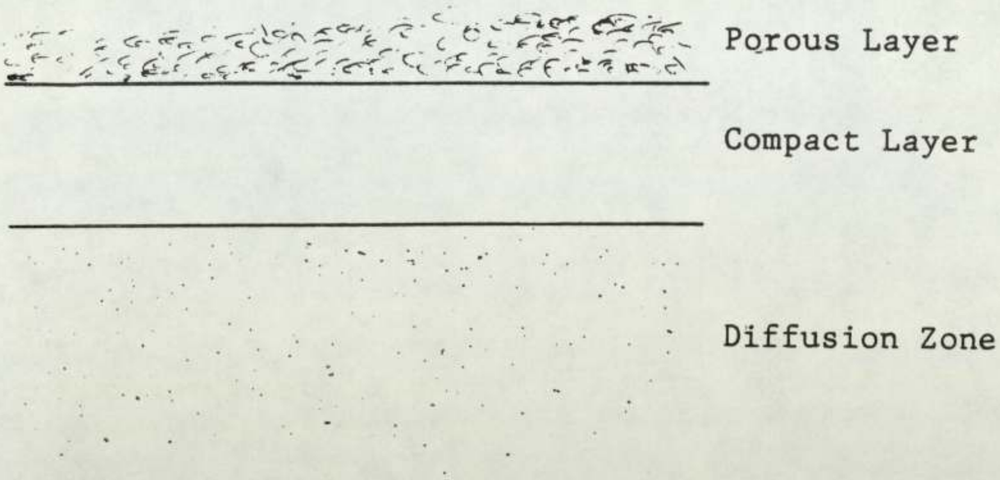

The porous layer contains salt from the bath and sulphur compounds in fine dispersion - dependent on bath concentration.

The compact layer consists of epsilon iron nitride Fe_3N and iron sulphide FeS.

The diffusion zone consists of a nitrogen concentration reducing with increased depth below the surface, the nitrogen being held in solid solution.

Table 5

Hardness Plot across Diffusion Zone

Depth Below Surface μm	Hardness HK.F = 0.245N
72	517
136	513
198	487
265	478
325	472
385	457
447	439
470	436
510	424
577	427

Hardness Compact layer 1120 HK, F = 0.245N

Fig. 10

Hardness Vs Depth across Sursulf Layer

Treatment time 90 minutes

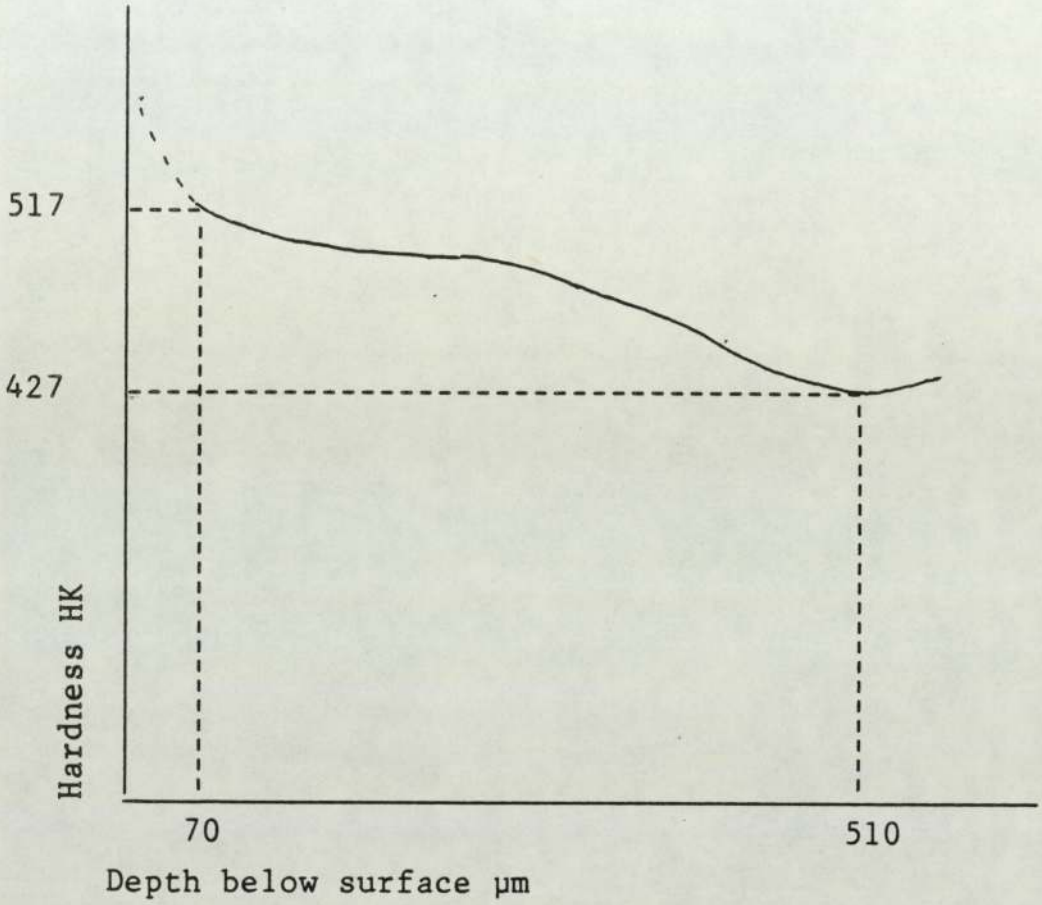

Depth Compact layer 12 µm hardness 1120 HK. Porous Zone 1-3 µm (the majority removed during lapping).

Disc hardness 427 HK at core.

5.2 Coating Thickness and Microhardness of Surface Coatings (Knoop Hardness F = 0.2452N)

The hardness of the as-plated electroless nickel PTFE composite (310-384 HK pins 1-4, 396-449 pins 52-57) was lower than that for conventional as-plated electroless nickel (528-560 HK). Heat treatment of the electroless nickel PTFE composite at 300°C for 4 hours increased the hardness 552-595 HK pins 5-9, 605-660 HK pins 52-57. Heat treatment of the conventional electroless nickel at 400°C for one hour increased the hardness to 893-910 HK. Heat treatment of an electroless nickel deposit at 400°C for one hour should result in the maximum hardness, and an electroless nickel deposit containing 9% phosphorus should increase in hardness to a maximum of 1000 HV 100g after heat treatment.
Semi-quantitative X-ray microanalysis suggested that the phosphorus content of the electroless nickel deposit was much higher than 9%, approximately 17% was recorded.

The hardness of the hard chromium electrodeposit was approximately 100 HK higher than that recorded for the heat treated conventional electroless nickel (1000-1087 HK and 893-910 HK respectively). The hard chromium deposit tended to be somewhat porous probably due to hydrogen gas evolution during electroplating. The hard chromium deposit also contained some fine cracks which may have been the result of the build-up of tensile stress in the growing electrodeposit.

The hardness of electrodeposited tin-nickel alloy was comparable to that of conventional electroless nickel as-plated (463-543 HK and 528-560 HK respectively). X-ray microanalysis of the tin-nickel alloy indicated a composition of 72% tin, 28% nickel.

The electrodeposited tin-cobalt alloy was marginally harder (559-630 HK) than the tin-nickel alloy. The tin cobalt alloy contained a high percentage of cobalt, X-ray microanalysis indicated a composition of 6% tin and 94% cobalt. Some microcracks were evident in both electrodeposited tin-nickel and tin-cobalt alloys. This is probably due to the residual tensile stress in the electrodeposit.

Titanium nitride coatings by chemical vapour deposition (C.V.D.) were in reality a triple coating.

(a) Titanium carbide deposited first
(b) Titanium carbide/nitride (very thin)
(c) Titanium nitride deposited last.

The titanium carbide/nitride layer is thought to increase the adhesion between TiC and TiN. The total layer thickness for CVD coatings on pins 10-15 was 7-12 μm (pin material 605A36 EN16).

The titanium nitride coating itself was approximately 50% of the total layer thickness and as a consequence it was difficult to test the hardness across the coating. However, on pins 12, 13, 14 the titanium nitride coating was just thick enough to obtain hardness values of 1513-1615 HK, (the titanium carbide was encroached in some cases during hardness testing). The hardness of the titanium nitride coating on pins 34-39 (pin material D2) was 1617-1815 HK. The titanium nitride layer varied in thickness from 11-13 μm. The mean hardness of the titanium carbide layer was measured at 2566 HK.

Titanium nitride coating by physical vapour deposition (PVD) were very thin (1-2.5 µm) and as a consequence it was impossible to test the hardness across the coating. Hardness values taken on the shank of the pin approximated to 1500-1800 HK. The layer appeared to be a homogeneous layer of TiN, gold in colour.

Table 6

Electroless Nickel PTFE As plated

Pin No.	Thickness μm	Microhardness HK
1	12	347
2	12	307
3	25	386
4	50	310
52	19	429
53	18	415
54	18	449
55	20	395
56	21	408
57	22	396

Table 7

Electroless Nickel PTFE (Heat treated at 300°C for 4 hours)

Pin No.	Thickness μm	Microhardness HK
5	12	570
6	12	552
7	25	581
8	50	564
9	50	595
58	18	605
59	21	627
60	18	660
61	19	608
62	19	648
63	19	635

Table 8

Electroless Nickel As plated

Pin No.	Thickness μm	Microhardness HK
22	20	528
23	19	557
24	19	550
25	18	537
26	19	560
27	20	547

Table 9

Electroless Nickel Heat Treated at 400°C for 1 hour

Pin No.	Thickness μm	Microhardness HK
28	15	893
29	14	901
30	15	903
31	12	910
32	12	902
33	13	909

Table 10

Hard Chromium

Pin No.	Thickness* μm	Microhardness HK
16	40	1062
17	64	1062
18	87	1058
19	38	1000
20	62	1087
21	82	1062

* Deposit Thickness after grinding

Table 11

Electrodeposited Tin/Nickel

Pin No.	Thickness μm	Microhardness HK
40	17	504
41	15	463
42	16	520
43	12	502
44	10	543
45	13	468

Table 12

Electrodeposited Tin/Cobalt

Pin No.	Thickness μm	Microhardness HK
46	10	590
47	10	630
48	12	612
49	10	570
50	9	559
51	12	616

Table 13

Titanium Nitride CVD (Pin material 605A36 (EN16))

Pin No.	Thickness* μm	Microhardness**HK
10	7 - 11	-
11	7 - 11	-
12	8 - 11	1615
13	9 - 12	1513
14	8 - 11	1575
15	7 - 11	-

* Total Layer Thickness TiN + TiC,
TiN Layer 3-5 μm

** Hardness of TiN only

Core hardness of pin 190 HV, subcutaneous layer of ferrite 210 HK.

Table 14

Titanium Nitride CVD (Pin material D2)

Pin No.	Thickness* µm	Microhardness**HK
34	20 - 22	1815
35	19 - 20	1655
36	18 - 25	1617
37	20 - 25	1706
38	17 - 21	1670
39	20 - 25	1790

* Total Layer Thickness TiN + TiC, TiC Layer 11-13 µm

** Hardness of TiN only, mean hardness of TiC layer 2566 HK.

Table 15

Titanium Nitride PVD (Pin material D2)

Pin No.	Thickness µm	Microhardness* HK
64	1 - 2	-
65	1 - 2	-
66	1 - 2	-
67	1 - 2.5	-
68	1 - 2	-
69	1 - 2	-

* Coating too thin to obtain hardness on microsection. Hardness values taken on shank of pin approximated to 1500 - 1800 HK.

5.3 Weight Loss and Wear Rates of Coatings

The wear of surface coatings on pins were analysed by:

(a) Wear or displacement transducer

The movement of the wear trace on the chart recorder for left to right implies wear and can be expressed as $mm.cm^{-1}$. Analysis of wear by this method was difficult because of the tendency for the pin and disc to thermally expand due to frictional forces encountered during rubbing which was detected by the wear transducer. The coatings examined in most cases were less than 25 μm, and the wear test period 30 minutes or less. This short test period was unlikely to allow thermal equilibrium of the pin and disc, thus rendering this method of expressing wear rate ineffectual in most cases.

(b) Total weight loss

The pins were weighed five times before and after wear testing, the mean value recorded and the wear rate expressed at total weight loss/total distance travelled by pin, $g.cm^{-1}$. The major disadvantage is that the weight loss must correspond to the removal of the coating material and not substrate. Scanning electron microscopy of representative samples after wear testing suggested that in a large number of cases the substrate had been encroached during testing, but there was always some coating remaining for examination.

Careful examination of the torque trace on the chart recorder during wear testing was a useful guide in ascertaining whether the coating had been worn away. In many cases there was a <u>marked</u> change in friction at the coating/substrate interface indicating wear of substrate material.

Table 16

Electroless Nickel PTFE As plated

Pin No.	Wear Disc Type	Weight Loss (g)
1	Sursulf treated	0.0053
2	" "	0.0027
3	" "	0.0115
4	" "	0.0030
55	" "	0.00285
56	" "	0.00258
57	" "	0.00159
52	534 A99	0.03162
53	"	0.01016
54	"	0.01194

Table 17

Electroless Nickel PTFE* Heat treated

Pin No.	Wear Disc Type	Weight Loss (g)
5	Sursulf treated	0.0050
6	" "	0.0108
7	" "	0.0098
8	" "	0.0066
9	" "	0.0151
58	" "	0.0099
59	" "	0.00247
60	" "	0.00205
61	534 A99	0.00352
62	"	0.00339
63	"	0.00253

* Electroless Deposit heat treated at 300^{o}C for 4 hours.

Table 18

Electroless Nickel As plated

Pin No.	Wear Disc Type	Weight Loss (g)
22	Sursulf treated	0.0097
23	" "	0.0050
24	" "	0.0073
25	534 A99	0.0052
26	"	0.0056
27	"	0.0047

Table 19

Electroless Nickel* Heat treated

Pin No.	Wear Disc Type	Weight Loss (g)
28	534 A99	0.0016
29	"	0.0019
30	"	0.0005
31	Sursulf treated	0.010
32	" "	0.0078
33	" "	0.0134

* Electroless Deposit heat treated at 400°C for 1 hour.

Table 20

Hard Chromium

Pin No.	Wear Disc Type	Weight Loss (g)
16	Sursulf treated	0.0014
17	" "	0.0011
18	" "	0.0012
19	534 A99	0.001
20	"	0.001
21	"	0.0009

Table 21

Electrodeposited Tin Nickel

Pin No.	Wear Disc Type	Weight Loss (g)
40	534 A99	0.0012
41	"	0.0017
42	"	0.0012
43	Sursulf treated	0.0066
44	" "	0.0055
45	" "	0.0099

Table 22

Electrodeposited Tin Cobalt

Pin No.	Wear Disc Type	Weight Loss (g)
46	534 A99	0.00072
47	"	0.0043
48	"	0.00177
49	Sursulf treated	0.00152
50	" "	0.00174
51	" "	0.00156

Table 23

Titanium Nitride CVD (Pin material 605A36 EN16)

Pin No.	Wear Disc Type	Weight Loss (g)
10	Sursulf treated	0.0002
11	" "	0.0005
12	534 A99	0.001
13	"	0.0190
14	Carbide	0.0087
15	"	0.0115

Table 24

Titanium Nitride CVD (Pin material D2)

Pin No.	Wear Disc Type	Weight Loss (g)
34	534 A99	+0.0006
35	"	+0.0001
36	"	+0.0005
37	Sursulf treated	+0.00086
38	" "	+0.00051
39	" "	+0.00026

Table 25

Titanium Nitride PVD (Pin material D2)

Pin No.	Wear Disc Type	Weight Loss (g)
64	534 A99	0.00181
65	"	0.00388
66	"	0.00016
67	Sursulf treated	+0.00066
68	" "	+0.00057
69	" "	+0.00072

5.3.1. Wear Test Results

Sliding Speed $S = \frac{\text{r.p.m. } D}{60}$

r.p.m. $= \frac{S \times 60}{D}$

Sliding Speed for all wear tests = 100cm S^{-1}

Load 2 Kg = 4Kg on Pin

Table 26

Electroless Nickel PTFE As plated

Pin No.	Disc Type	Wear Rate	
		From weight gcm ($\times 10^{-8}$)	Via Wear Transducer mm.cm ($\times 10^{-7}$)
1	Sursulf Treated	1.963 } 2.875	1.097
2	" "	1.500	1.132
3	" "	6.380	1.249
4	" "	1.660	0.946
55	" "	4.75 } 3.9	
56	" "	4.3	
57	" "	2.65	
52	534 A99	17.56*	
53	"	5.644 } 6.138	
54	"	6.633	

Pins 55-57 wear test terminated after 10 minutes

* Coating completely removed after wear test

Table 27

Electroless Nickel PTFE Heat Treated

Pin No.	Disc Type	Wear Rate		
		From weight gcm (x10^{-8})		Via Wear Transducer mm.cm (x10^{-7})
5	Sursulf Treated	2.700	5.236	5.984
6	" "	6.000		2.916
7	" "	5.44		2.502
8	" "	3.66		0.585
9	" "	8.38		1.999
58	" "	5.50	2.67	
59	" "	1.372		
60	" "	1.138		
61	534 A99	1.955	1.747	
62	"	1.883		
63	"	1.405		

Table 28

Electroless Nickel As plated

Pin No.	Disc Type	Wear Rate		
		From weight gcm (x10^{-8})		Via Wear Transducer mm.cm (x10^{-7})
22	Sursulf Treated	5.380	4.069	
23	" "	2.777		
24	" "	4.050		0.743
25	534 A99	2.888	2.87	0.184
26	"	3.111		
27	"	2.611		

Table 29

Electroless Nickel Heat Treated

Pin No.	Disc Type	Wear Rate	
		From weight gcm (x10^{-8})	Via Wear Transducer mm.cm (x10^{-7})
28	534 A99	0.888	7.77
29	"	1.055 } 0.879	
30	"	0.694	
31	Sursulf Treated	5.55	
32	" "	4.33 } 5.773	
33	" "	7.44	

Pin 30 wear test terminated after 12 minutes

Table 30

Hard Chromium

Pin No.	Disc Type	Wear Rate	
		From weight gcm (x10^{-8})	Via Wear Transducer mm.cm (x10^{-7})
16	Sursulf Treated	0.777	
17	" "	0.611 } 0.684	
18	" "	0.666	
19	534 A99	0.555	
20	"	0.555 } 0.536	
21	"	0.500	

Table 31

Electrodeposited Tin Nickel

Pin No.	Disc Type	Wear Rate	
		From weight gcm (x10^{-8})	Via Wear Transducer mm.cm (x10^{-7})
40	534 A99	0.666)	2.87
41	"	0.944) 0.758	
42	"	0.666)	
43	Sursulf Treated	3.666)	1.735
44	" "	3.055) 4.073	
45	" "	5.50)	

Table 32

Electrodeposited Tin Cobalt

Pin No.	Disc Type	Wear Rate	
		From weight gcm (x10^{-8})	Via Wear Transducer mm.cm (x10^{-7})
46	534 A99	0.80)	
47	"	4.77) 2.513	2.971
48	"	1.97)	
49	Sursulf Treated	2.53)	
50	" "	2.90) 2.676	
51	" "	2.60)	

Pins 46-48 wear test terminated after 15 minutes

Pins 49-51 wear test terminated after 10 minutes

Table 33

Titanium Nitride CVD (Pin material 605A36 EN 16)

Pin No.	Disc Type	Wear Rate	
		From weight gcm ($x10^{-8}$)	Via Wear Transducer mm.cm ($x10^{-7}$)
10	Sursulf Treated	0.111	
11	" "	0.277	1.950
12	534 A99	0.555	
13	"	10.55	0.877
14	Carbide	4.83	0.894
15	"	6.38	1.749

Pins 34-39 Titanium Nitride CVD on D2, which had been vacuum heat-treated and tempered after processing, exhibited no wear after 30 minutes when rubbed against either 534A99 or Sursulf treated discs. There had been some metallic pick-up on each pin Ref. Table 24.

Table 34

Titanium Nitride PVD (Pin material D2)

Pin No.	Disc Type	Wear Rate	
		From weight gcm ($x10^{-8}$)	Via Wear Transducer mm.cm ($x10^{-7}$)
64	534A99	1.005)	
65	"	2.155) 1.082	
66	"	0.088)	

Pins 67-69 Titanium Nitride PVD on D2, which had been hardened and tempered, exhibited no wear after 30 minutes when rubbed against Sursulf treated discs. There had been some metallic pick-up Ref. Table 25.

5.4 Coefficients of Friction

The static, dynamic (mean) and final (dynamic) friction values were calculated for all coated pin and disc combinations. For Pins 31 to 66 the change in coefficient of friction with time was calculated. The mean coefficient of friction for each series of wear tests was then plotted against time, Figs. 11 to 23.

Table 35

Electroless Nickel PTFE As plated/
Sursulf Treated Discs

Pin No.	Coefficient of Friction		
	Static	Dynamic (mean)	Final
1	0.30	0.59	0.5
2	0.30	0.18	0.3
3	0.22	0.49	0.43
4	0.20	0.19	0.1
55	0.2	0.62	0.8
56	0.16	0.49	0.73
57	0.16	0.5	0.64

Pins 1-4 test period 30 minutes
Pins 55-57 test period 10 minutes

Table 36

Change in Coefficient of Friction with Time
For Pins 55-57

Time (mins)	Coefficient of Friction			
	Pin 55	Pin 56	Pin 57	$\bar{x}$
0	0.2	0.16	0.17	0.17
2.5	0.5	0.32	0.43	0.42
5.0	0.7	0.52	0.64	0.62
7.5	0.88	0.73	0.64	0.75
10.0	0.8	0.73	0.64	0.72

Change in Coefficient of Friction with Time

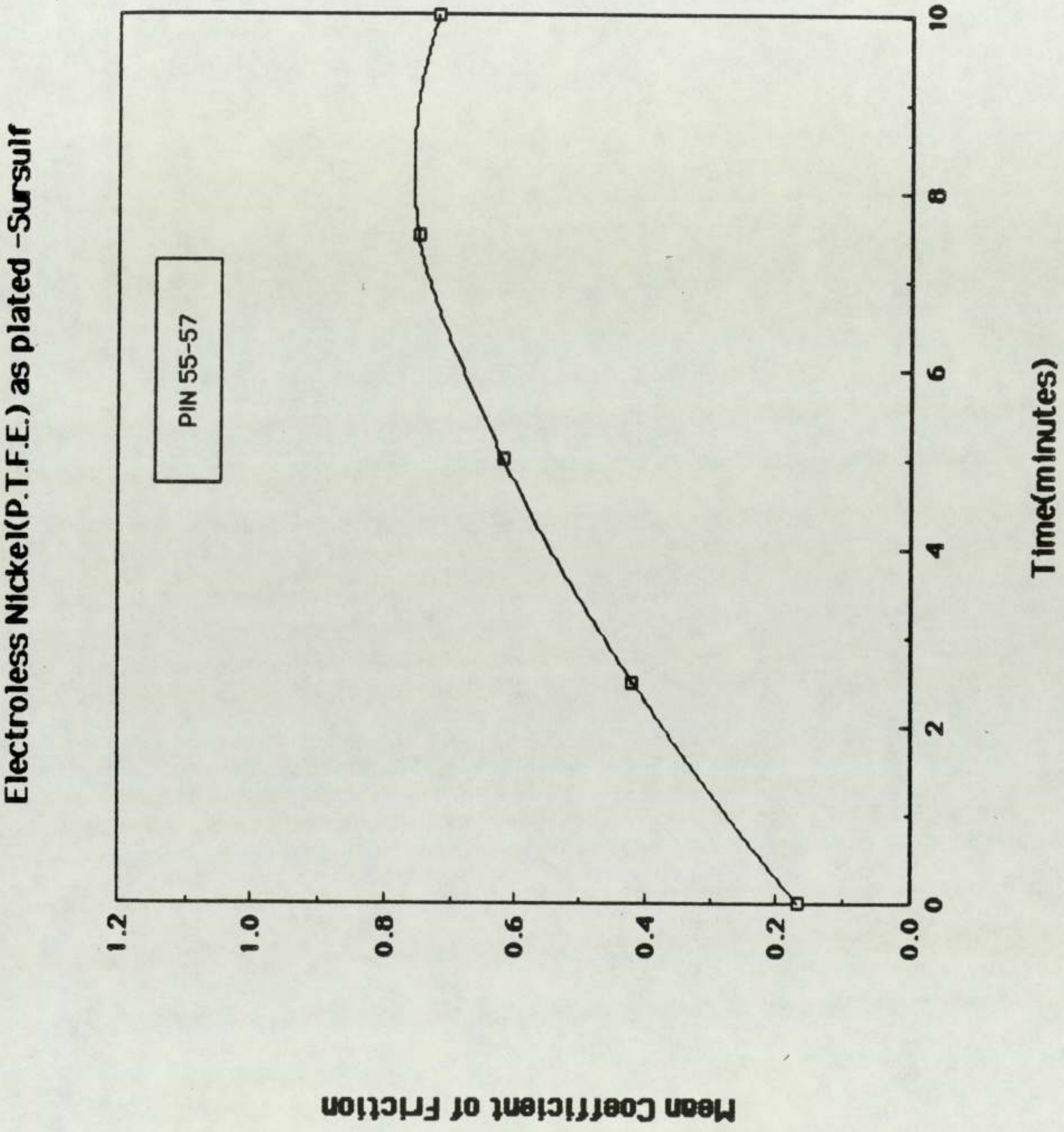

Fig. 11

Table 37

Electroless Nickel PTFE (Heat treated) /Sursulf Treated Disc

Pin No.	Coefficient of Friction		
	Static	Dynamic (mean)	Final
5	0.3	0.31	0.3
6	0.6	1.03	0.9
7	0.3	0.55	0.7
8	0.5	0.83	0.7
9	0.5	0.85	0.6
58	0.20	0.46	0.3
59	0.21	0.53	0.62
60	0.32	0.47	0.48

Table 38

Change in Coefficient of Friction with time For Pins 58-60

Time (mins)	Coefficient of Friction			
	Pin 58	Pin 59	Pin 60	$\bar{x}$
0	0.2	0.21	0.32	0.24
5	0.43	0.54	0.53	0.5
10	0.45	0.49	0.53	0.49
15	0.68	0.62	0.48	0.59
20	0.63	0.62	0.48	0.58
25	0.53	0.62	0.48	0.54
30	0.3	0.62	0.48	0.47

Change in Coefficient of Friction with Time

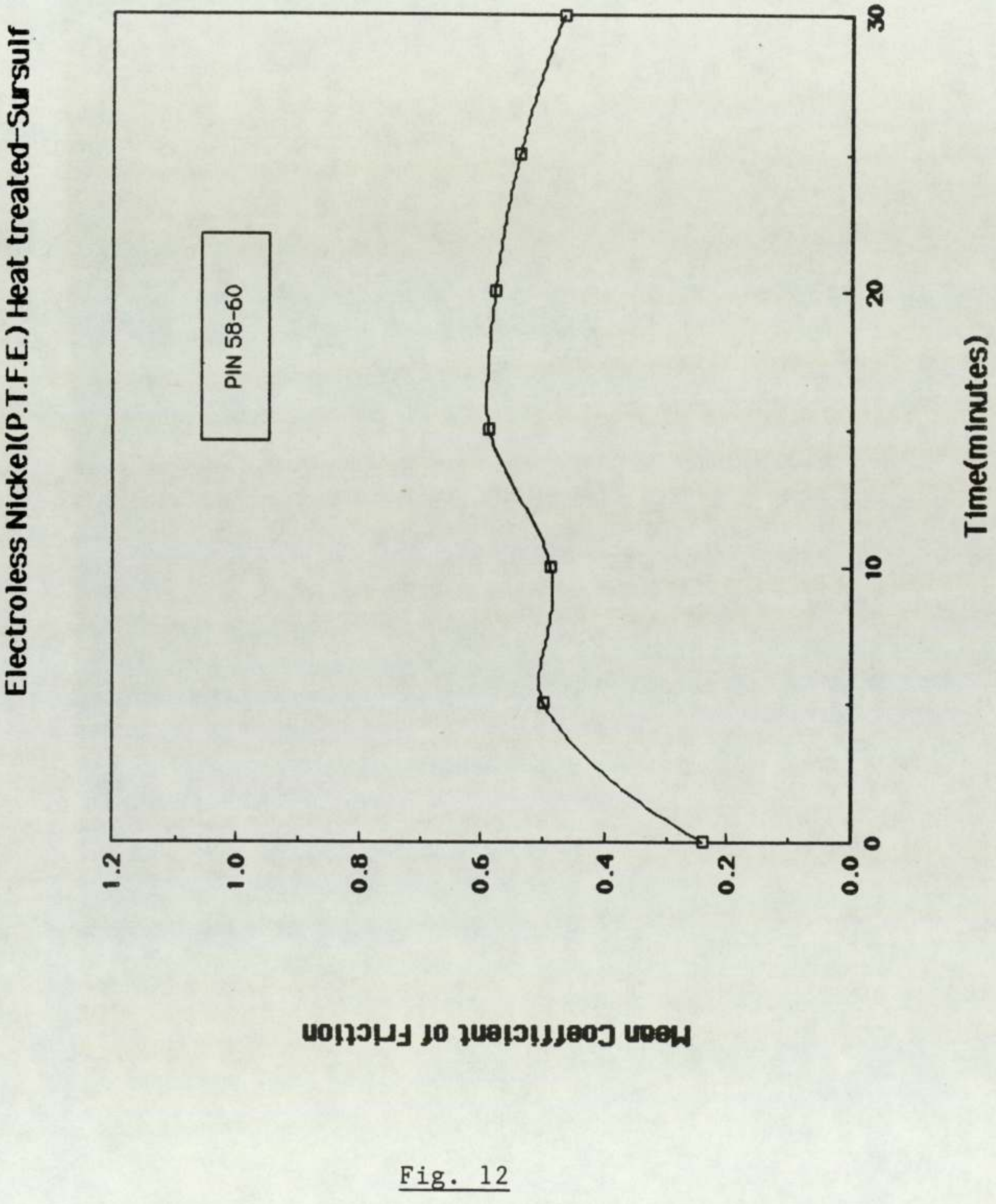

Fig. 12

Table 39

Electroless Nickel PTFE As plated/
534A99 (EN 31) Discs

Pin No.	Coefficient of Friction		
	Static	Dynamic (mean)	Final
52	0.15	0.61	0.65
53	0.26	0.62	0.60
54	0.21	0.45	0.48

Table 40

Change in Coefficient of Friction with Time
For Pins 52-54

Time (mins)	Coefficient of Friction			
	Pin 52	Pin 53	Pin 54	$\bar{x}$
0	0.15	0.26	0.21	0.2
2.5	0.30	0.59	0.37	0.42
5	0.92	0.70	0.56	0.72
10	0.95	0.78	0.51	0.74
15	0.65	0.78	0.48	0.63
20	0.65	0.65	0.48	0.59
25	0.65	0.60	0.53	0.59
30	0.65	0.60	0.48	0.57

Change in Coefficient of Friction with Time

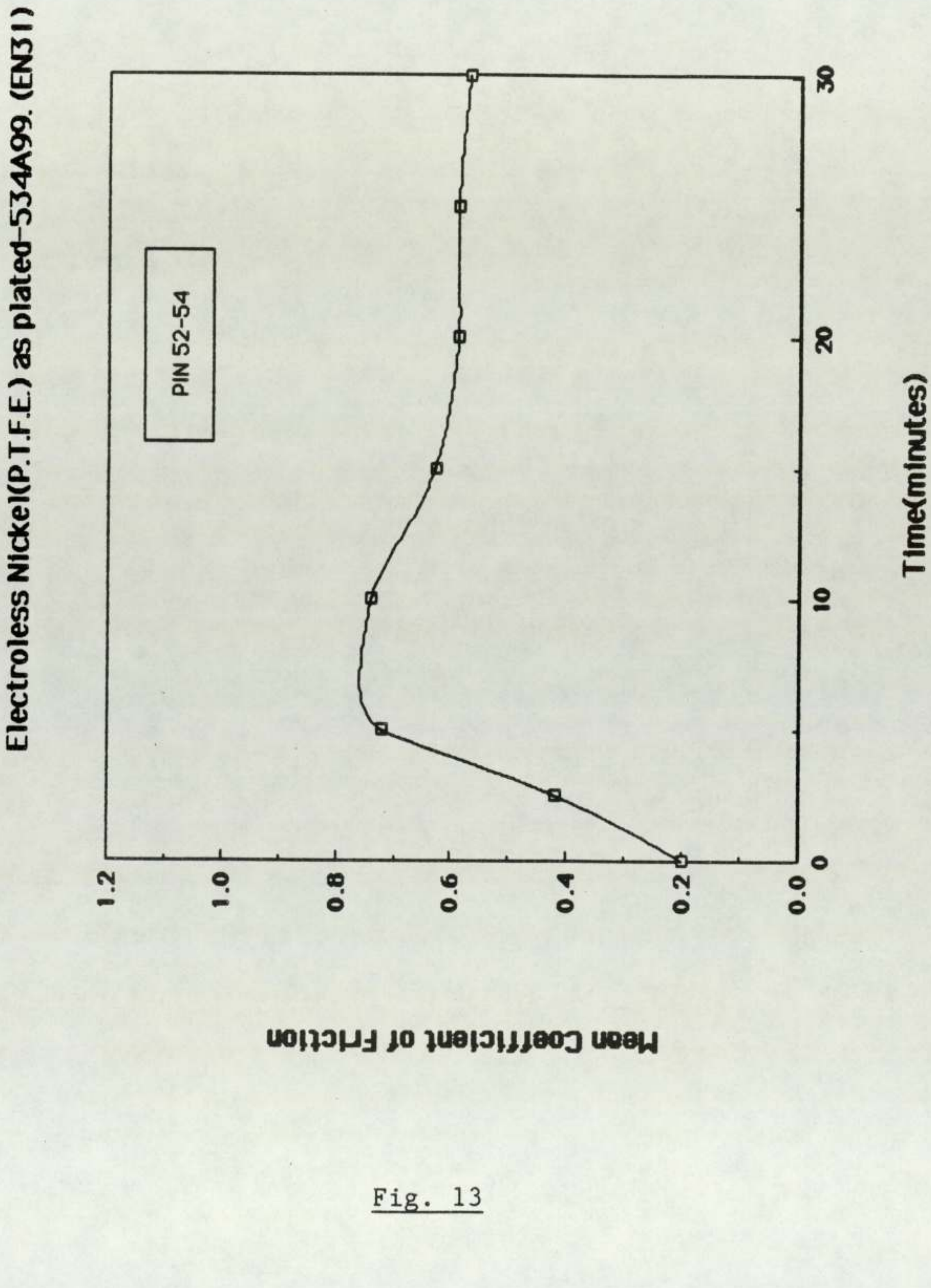

Fig. 13

Table 41

Electroless Nickel PTFE Heat Treated/
534A99 (EN 31) Discs

Pin No.	Coefficient of Friction		
	Static	Dynamic (mean)	Final
61	0.2	0.54	0.45
62	0.21	0.65	0.83
63	0.21	0.45	0.48

Table 42

Change in Coefficient of Friction with Time
For Pins 61-63

Time (mins)	Coefficient of Friction			
	Pin 61	Pin 62	Pin 63	$\bar{x}$
0	0.2	0.21	0.21	0.206
5	0.65	0.54	0.53	0.57
10	0.65	0.62	0.48	0.58
15	0.73	0.73	0.48	0.64
20	0.6	0.83	0.48	0.63
25	0.48	0.83	0.48	0.60
30	0.45	0.83	0.48	0.59

Change in Coefficient of Friction with Time

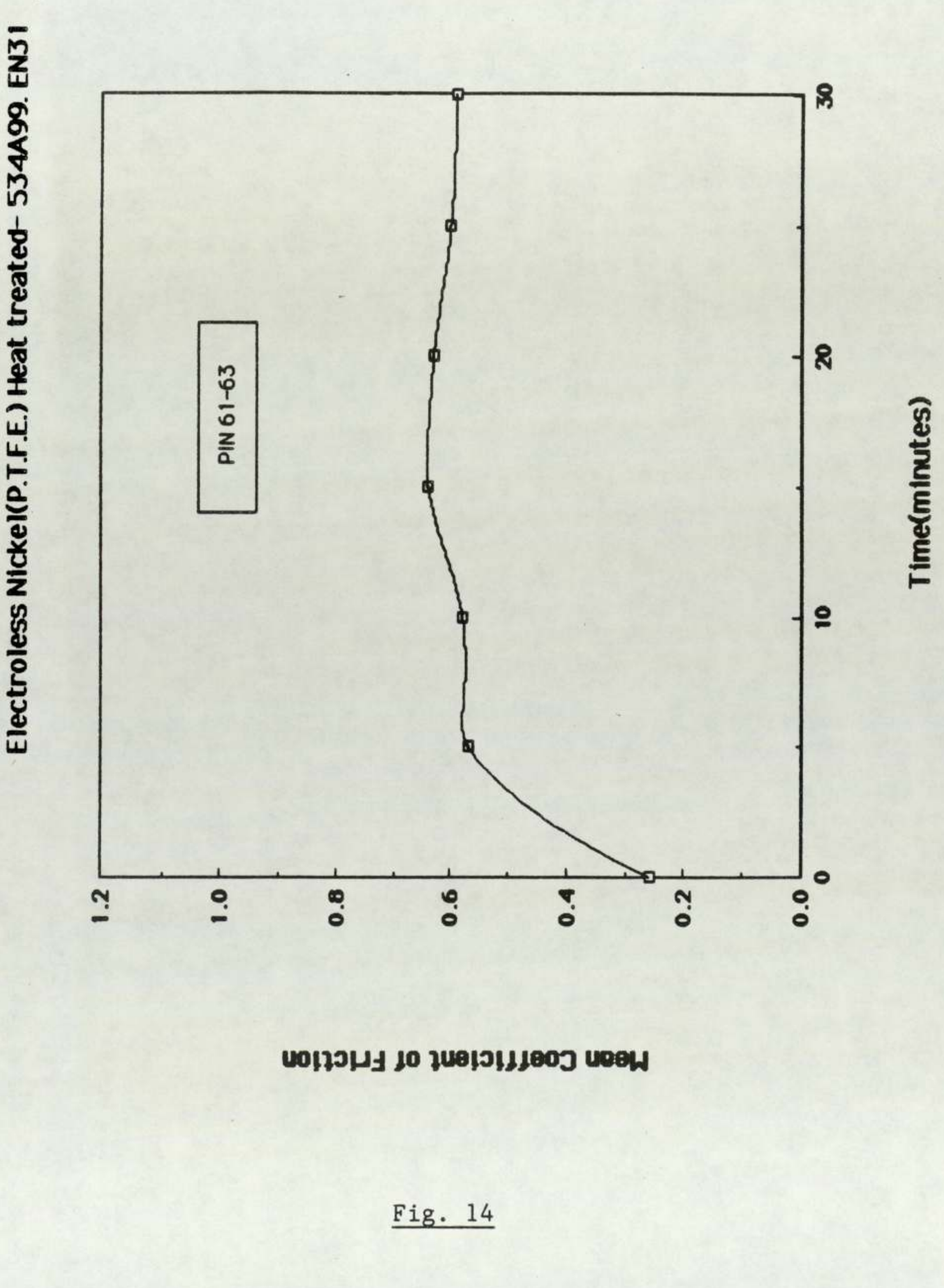

Fig. 14

Table 43

Electroless Nickel (Heat Treated) /Sursulf Treated Discs

Pin No.	Coefficient of Friction		
	Static	Dynamic (mean)	Final
31	0.45	0.49	0.35
32	0.73	0.94	1.1
33	0.69	0.78	0.69

Table 44

Change in Coefficient of Friction with Time For Pins 31-33

Time (mins)	Coefficient of Friction			
	Pin 31	Pin 32	Pin 33	$\bar{x}$
0	0.45	0.73	0.69	0.62
5	0.4	0.93	0.77	0.70
10	0.65	0.68	1.06	0.79
15	0.7	0.83	0.91	0.81
20	0.57	1.24	0.64	0.81
25	0.35	1.24	0.69	0.76
30	0.35	1.1	0.69	0.71

Change in Coefficient of Friction with Time

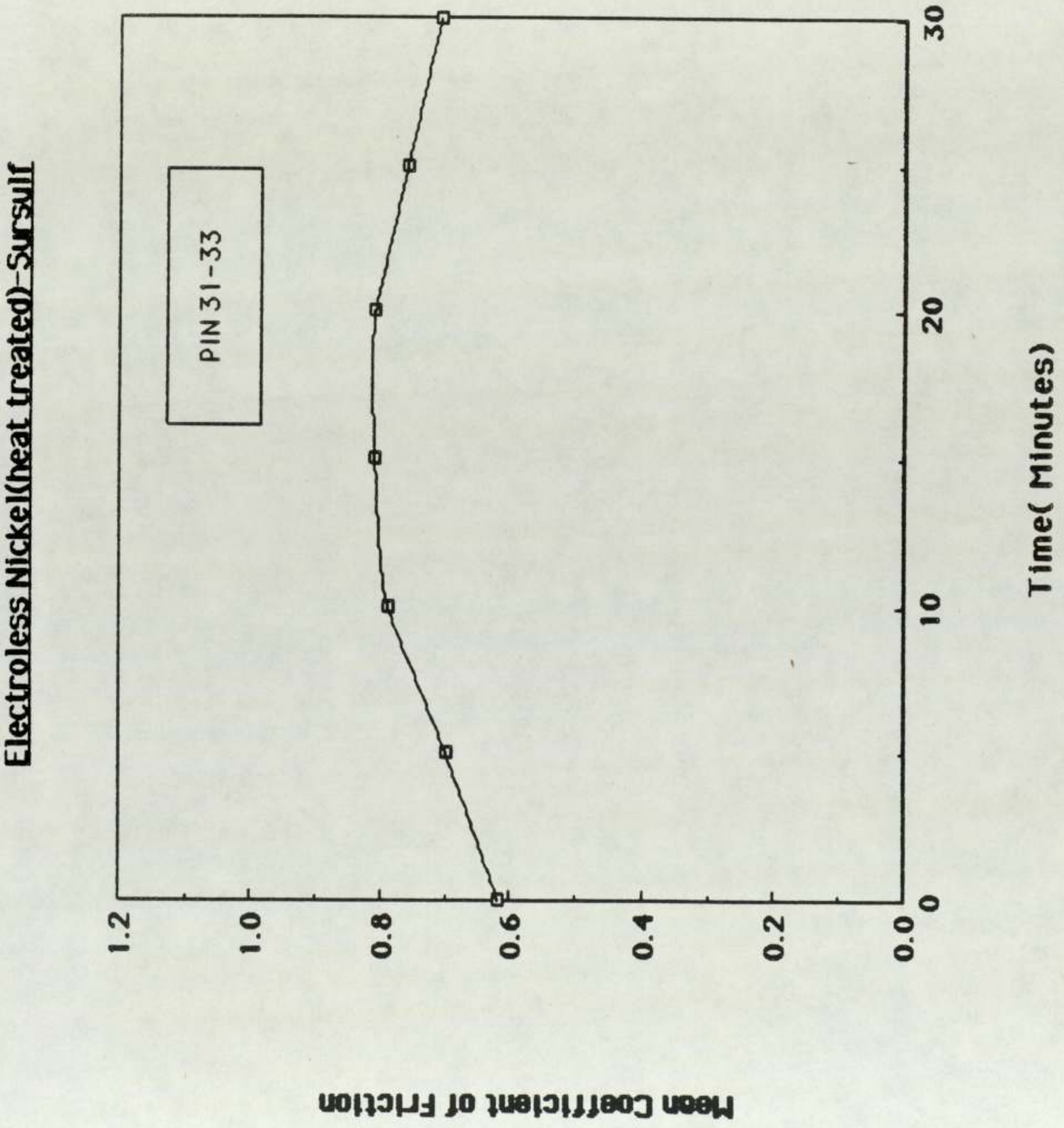

Fig. 15

Table 45

Electroless Nickel (As plated)
/Sursulf Treated Discs

Pin No.	Coefficient of Friction		
	Static	Dynamic (mean)	Final
22	--	--	--
23	0.5	0.58	0.4
24	0.5	0.43	0.4

Table 46

Electroless Nickel (As plated)
/534A99 (EN 31) Discs

Pin No.	Coefficient of Friction		
	Static	Dynamic (mean)	Final
25	0.24	0.5	0.6
26	0.2	0.33	0.4
27	0.3	0.42	0.5

Table 47

Electroless Nickel (Heat Treated)
/534A99 (EN 31) Discs

Pin No.	Coefficient of Friction		
	Static	Dynamic (mean)	Final
28	0.2	0.49	0.55
29	0.3	0.58	0.66
30	0.6	0.47	0.50

Table 48

Hard Chromium/Sursulf Treated Discs

Pin No.	Coefficient of Friction		
	Static	Dynamic (mean)	Final
16	0.48	0.39	0.5
17	0.52	0.35	0.4
18	0.34	0.26	0.35

Table 49

Hard Chromium/534A99 (EN 31) Discs

Pin No.	Coefficient of Friction		
	Static	Dynamic (mean)	Final
19	0.4	0.83	0.7
20	0.2	1.04	1.2
21	0.4	1.06	0.6

Table 50

Electrodeposited Tin Nickel/ Sursulf Treated Discs

Pin No.	Coefficient of Friction		
	Static	Dynamic (mean)	Final
43	0.3	0.53	0.7
44	0.41	0.57	0.52
45	0.32	0.54	0.75

Table 51

Change in Coefficient of Friction with Time For Pins 43-45

Time (mins)	Coefficient of Friction			
	Pin 43	Pin 44	Pin 45	$\bar{x}$
0	0.3	0.41	0.32	0.34
5	0.5	0.41	0.48	0.46
10	0.25	0.52	0.53	0.43
15	0.5	0.62	0.53	0.55
20	0.7	0.83	0.53	0.68
25	0.75	0.72	0.64	0.70
30	0.7	0.52	0.75	0.65

Change in Coefficient of Friction with Time

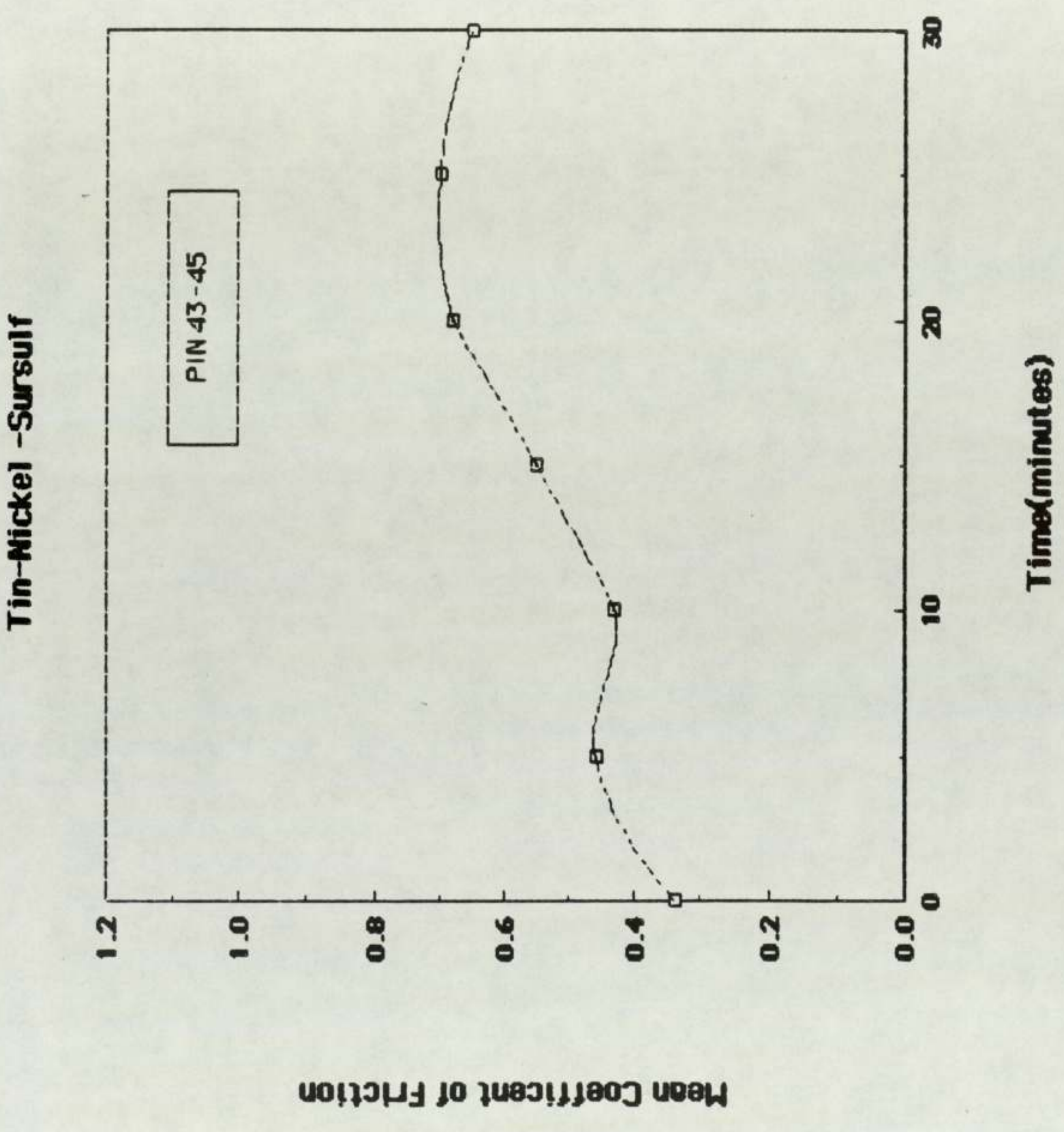

Fig. 16

Table 52

Electrodeposited Tin Nickel/
534A99 (EN31) Discs

Pin No.	Coefficient of Friction		
	Static	Dynamic (mean)	Final
40	0.45	0.44	0.4
41	0.31	0.3	0.26
42	0.37	0.49	0.53

Table 53

Change in Coefficient of Friction with Time
For Pins 40-42

Time (mins)	Coefficient of Friction			
	Pin 40	Pin 41	Pin 42	$\bar{x}$
0	0.45	0.31	0.37	0.37
5	0.5	0.31	0.48	0.48
10	0.4	0.36	0.43	0.39
15	0.48	0.21	0.48	0.39
20	0.48	0.36	0.59	0.47
25	0.4	0.31	0.59	0.43
30	0.4	0.26	0.53	0.39

Change in Coefficient of Friction with Time

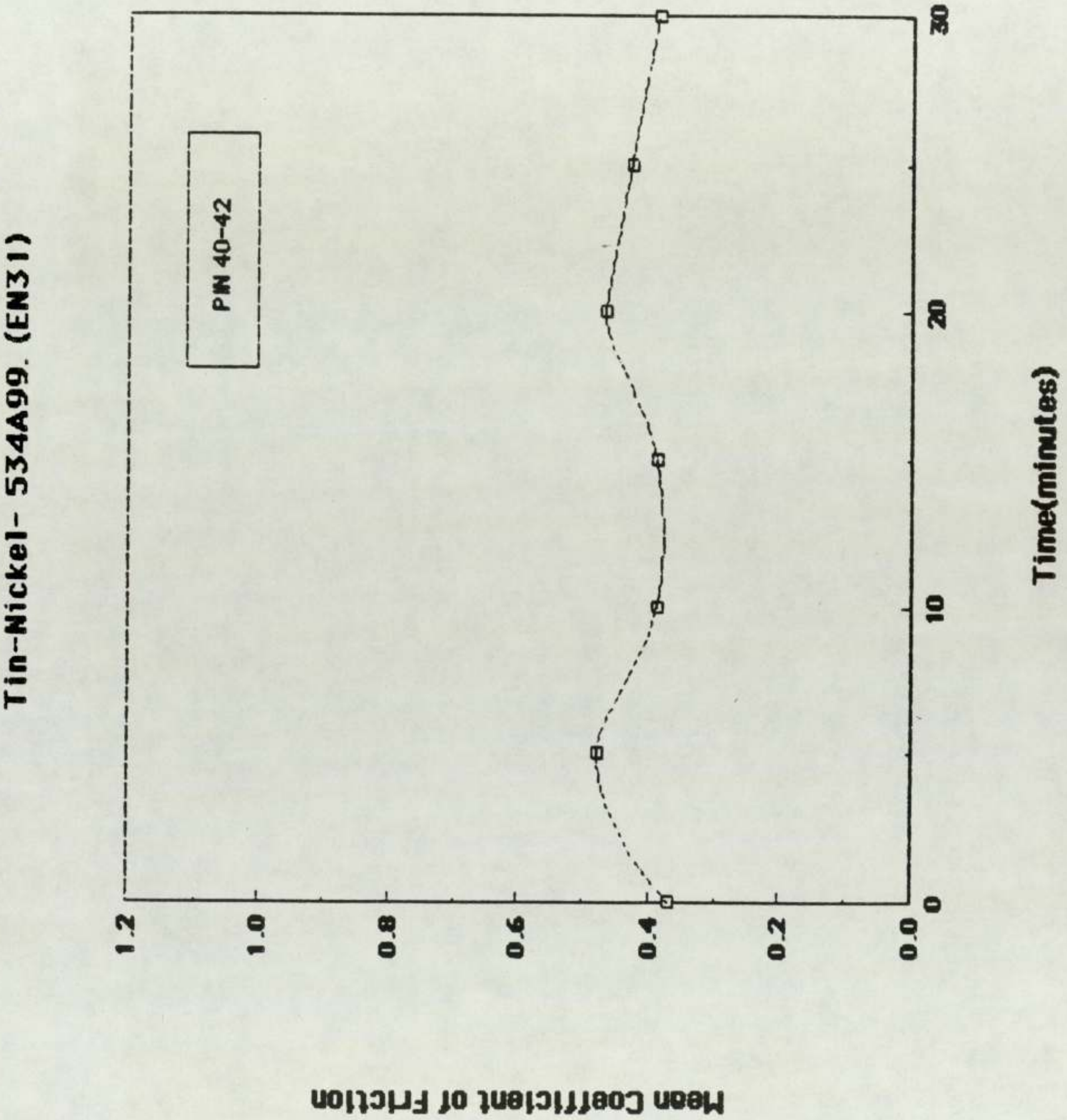

Fig. 17

Table 54

Electrodeposited Tin Cobalt/ Sursulf Treated Discs

Pin No.	Coefficient of Friction		
	Static	Dynamic (mean)	Final
49	0.35	0.45	0.5
50	0.41	0.43	0.46
51	0.37	0.49	0.37

Wear Test terminated after 10 minutes.

Table 55

Change in Coefficient of Friction with Time For Pins 49-51

Time (mins)	Coefficient of Friction			
	Pin 49	Pin 50	Pin 51	$\bar{x}$
0	0.35	0.41	0.37	0.37
2.5	0.4	0.42	0.64	0.48
5	0.5	0.44	0.53	0.49
7.5	0.5	0.44	0.53	0.49
10	0.5	0.46	0.37	0.44

Change in Coefficient of Friction with Time

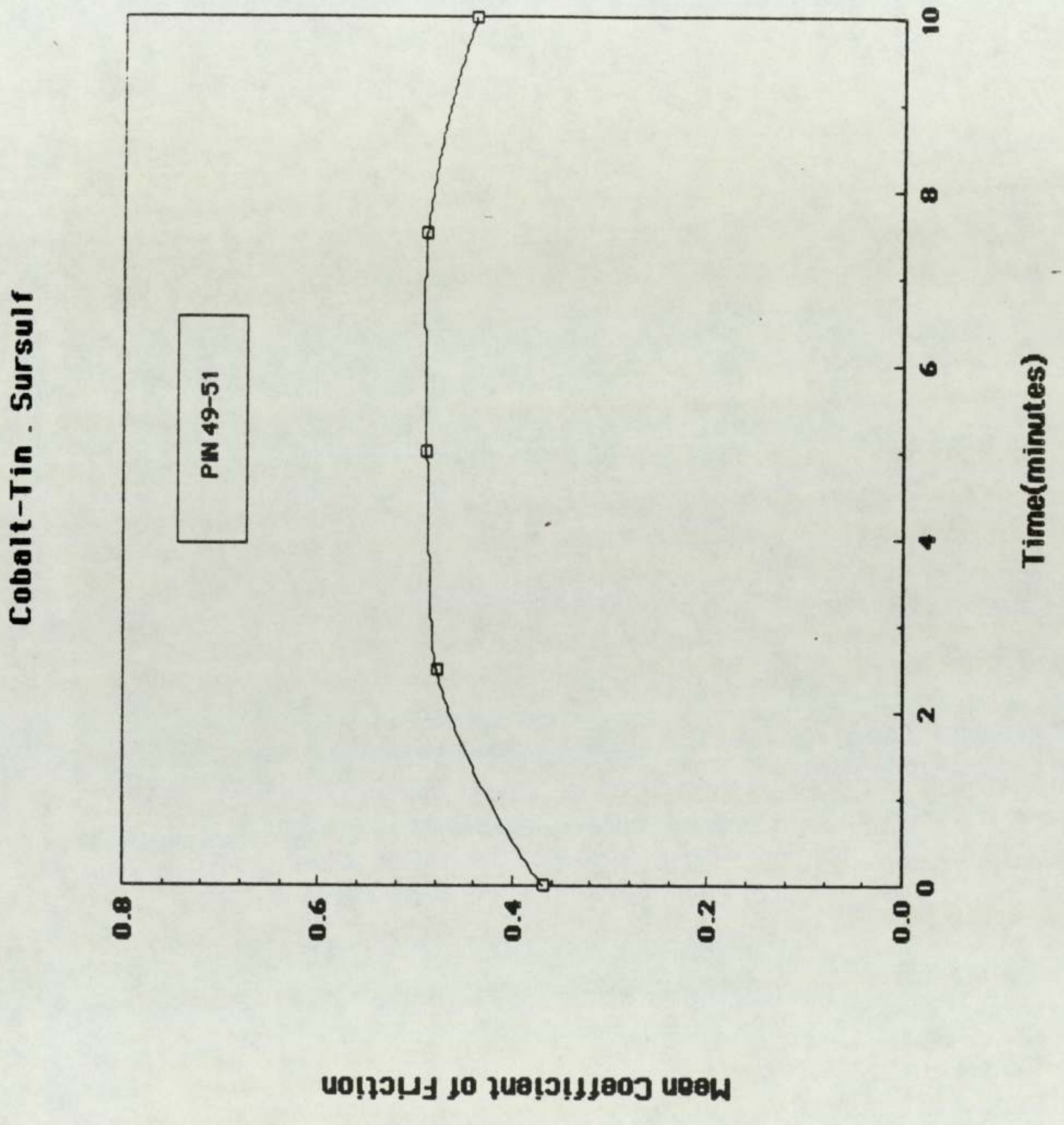

Fig. 18

Table 56

Electrodeposited Tin Cobalt/
534A99 (EN 31) Discs

Pin No.	Coefficient of Friction		
	Static	Dynamic (mean)	Final
46	0.15	0.32	0.45
47	0.15	0.31	0.46
48	0.16	0.22	0.21

Wear Test terminated after 15 minutes.

Table 57

Change in Coefficient of Friction with Time
For Pins 46-48

Time (mins)	Coefficient of Friction			
	Pin 46	Pin 47	Pin 48	$\bar{x}$
0	0.15	0.15	0.16	0.153
5	0.31	0.41	0.32	0.34
10	0.37	0.21	0.21	0.26
15	0.45	0.46	0.21	0.37

Change in Coefficient of Friction with Time

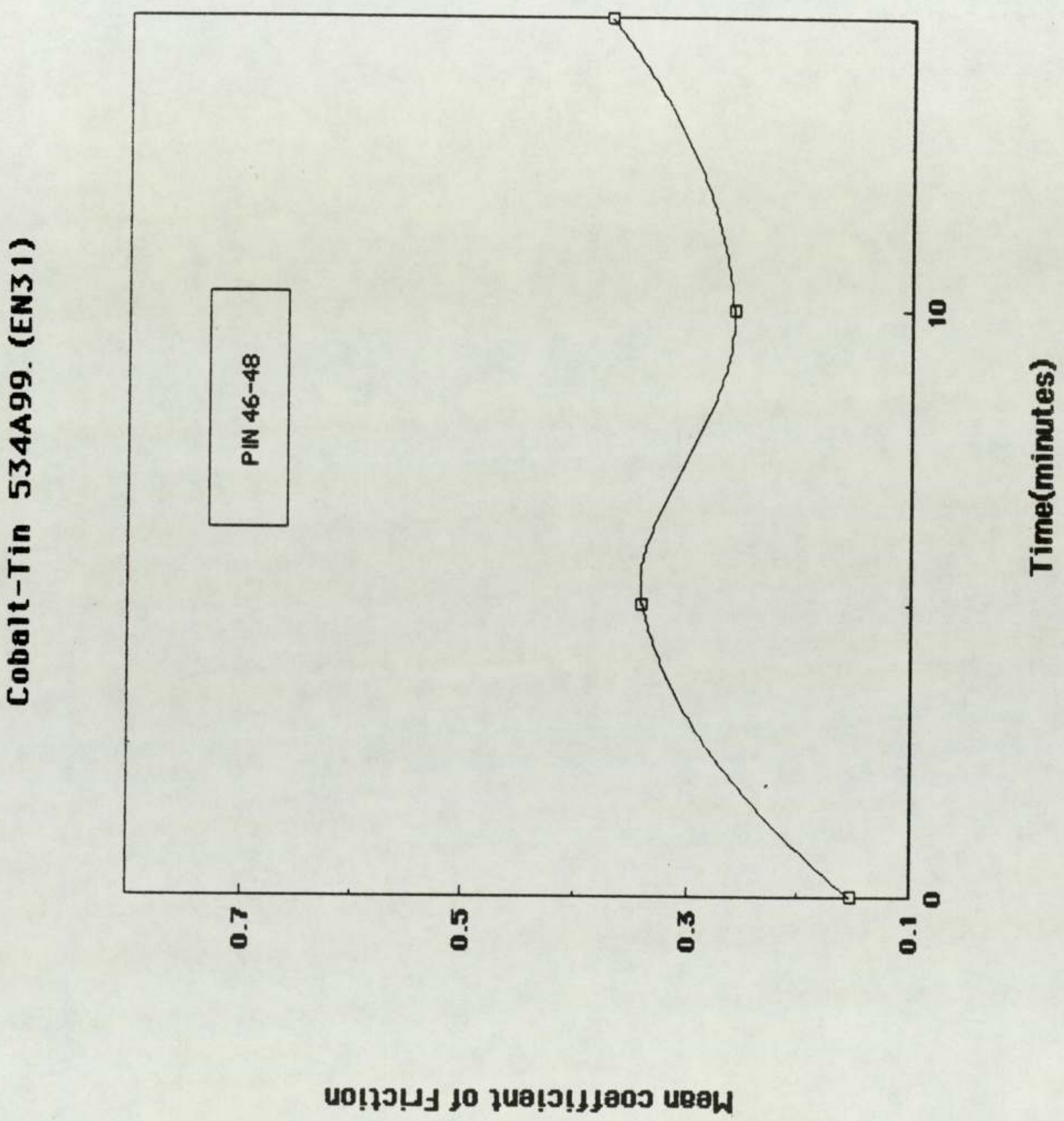

Fig. 19

Table 58

Titanium Nitride (CVD)/Sursulf Treated Discs
(Pin material 605A36, EN 16)

Pin No.	Coefficient of Friction		
	Static	Dynamic (mean)	Final
10	--	--	--
11	0.5	0.93	0.7

Table 59

Titanium Nitride (CVD)/534A99 (EN 31)Discs
(Pin material 605A36, EN 16)

Pin No.	Coefficient of Friction		
	Static	Dynamic (mean)	Final
12	0.3	0.26	0.3
13	0.5	0.31	0.2

Table 60

Titanium Nitride (CVD)/Carbide Discs
(Pin material 605A36, EN 16)

Pin No.	Coefficient of Friction		
	Static	Dynamic (mean)	Final
14	0.59	0.2	0.2
15	0.3	0.26	0.3

Table 61

Titanium Nitride (CVD)/Sursulf Treated Discs (D2 pins)

Pin No.	Coefficient of Friction		
	Static	Dynamic (mean)	Final
37	0.3	1.17	1.35
38	0.31	0.83	0.78
39	0.37	0.42	0.4

Table 62

Change in Coefficient of Friction with Time For Pins 37-39

Time (mins)	Coefficient of Friction			
	Pin 37	Pin 38	Pin 39	$\bar{x}$
0	0.3	0.31	0.37	0.33
5	1.1	0.96	0.4	0.82
10	1.45	0.98	0.43	0.95
15	1.5	0.93	0.45	0.96
20	1.25	0.93	0.45	0.87
25	1.25	0.96	0.48	0.89
30	1.35	0.78	0.4	0.84

Change in Coefficient of Friction with Time

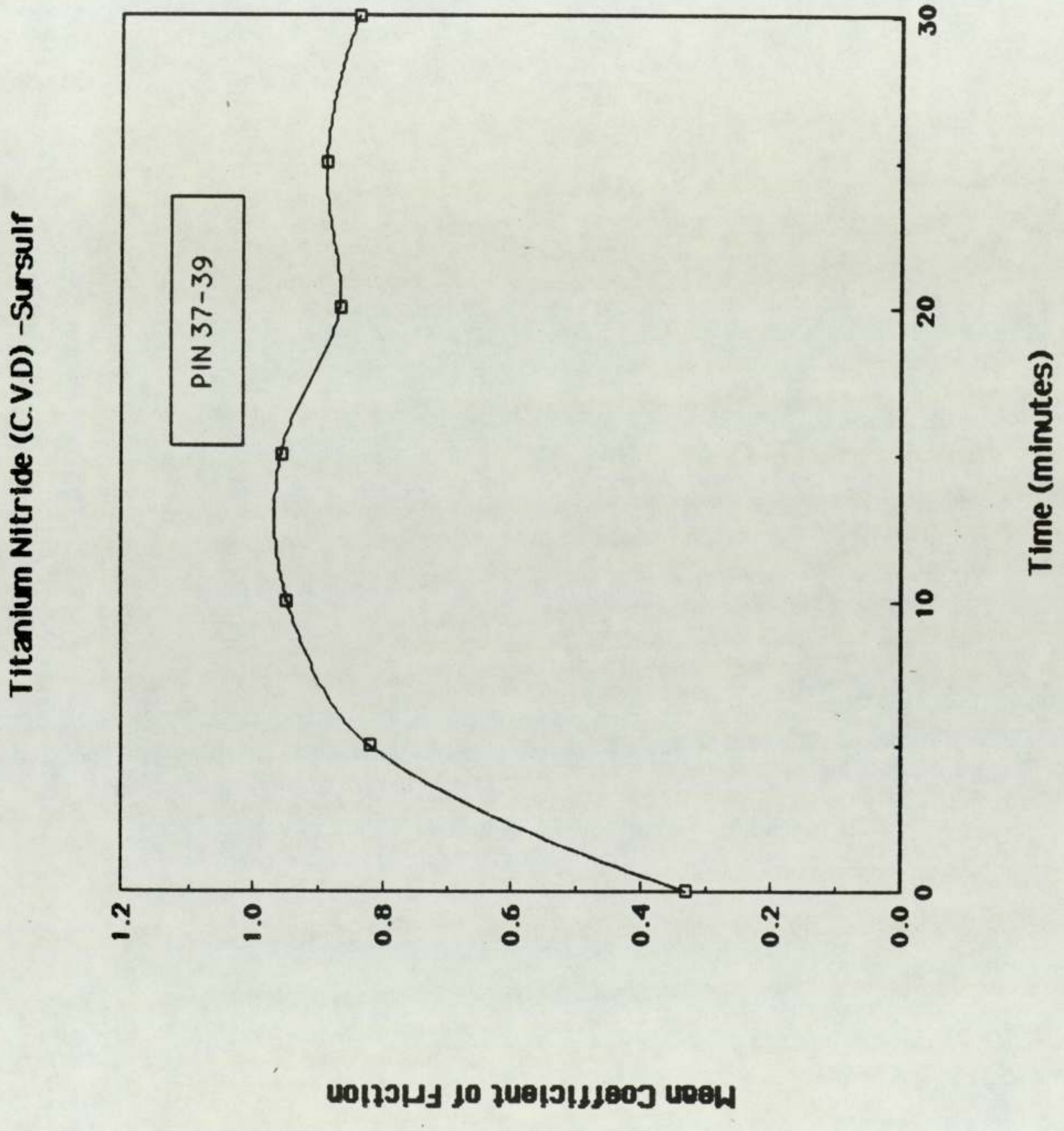

Fig. 20

Table 63

Titanium Nitride (CVD)/534A99 (EN 31) Discs (D2 pins)

Pin No.	Coefficient of Friction		
	Static	Dynamic (mean)	Final
34	0.25	0.36	0.4
35	0.26	0.47	0.62
36	0.16	0.27	0.32

Table 64

Change in Coefficient of Friction with Time For Pins 34-36

Time (mins)	Coefficient of Friction			
	Pin 34	Pin 35	Pin 36	$\bar{x}$
0	0.25	0.26	0.16	0.22
5	0.30	0.31	0.21	0.27
10	0.40	0.33	0.24	0.32
15	0.38	0.52	0.27	0.39
20	0.40	0.62	0.32	0.44
25	0.40	0.62	0.37	0.46
30	0.40	0.62	0.32	0.44

Change in Coefficient of Friction with Time

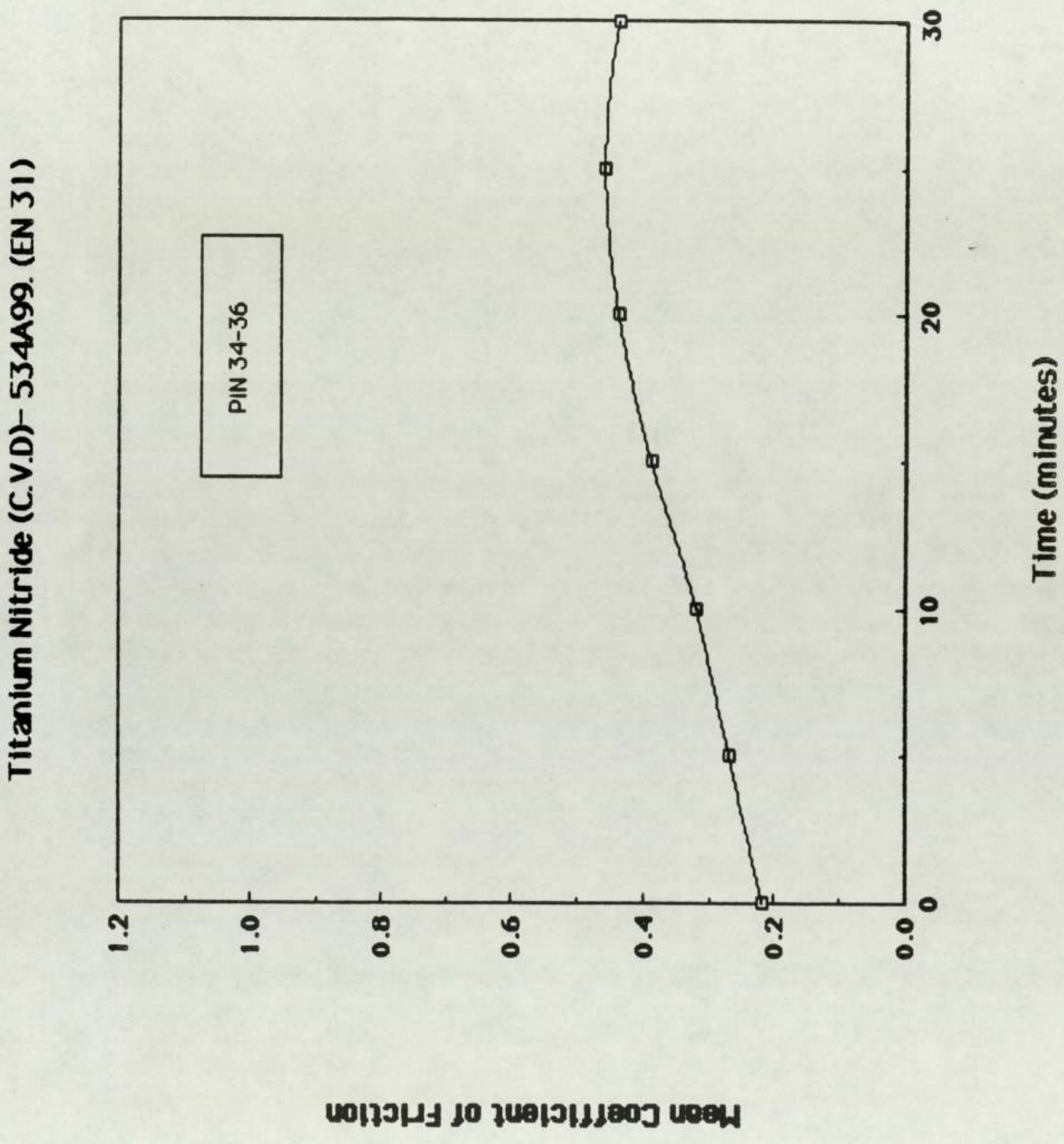

Fig. 21

Table 65

Titanium Nitride (PVD)/Sursulf Treated Disc (D2 pins)

Pin No.	Coefficient of Friction		
	Static	Dynamic (mean)	Final
67	0.3	0.46	0.45
68	0.31	0.41	0.41
69	0.32	0.44	0.53

Table 66

Change in Coefficient of Friction with Time For Pins 67-69

Time (mins)	Coefficient of Friction			
	Pin 67	Pin 68	Pin 69	$\bar{x}$
0	0.3	0.31	0.32	0.31
5	0.5	0.47	0.4	0.46
10	0.5	0.47	0.37	0.45
15	0.45	0.41	0.37	0.41
20	0.5	0.41	0.53	0.48
25	0.5	0.41	0.53	0.48
30	0.45	0.41	0.53	0.48

Change in Coefficient of Friction with Time

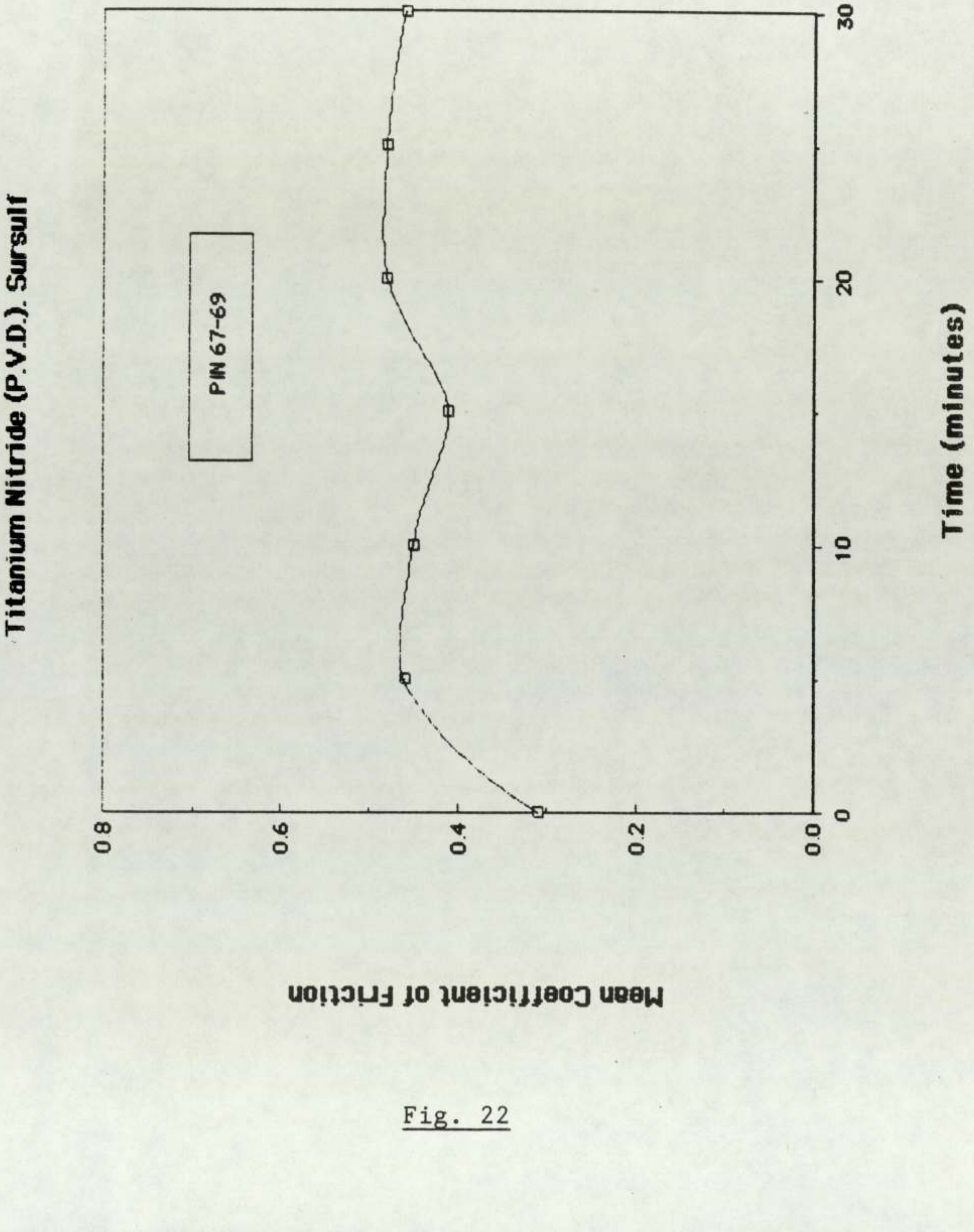

Fig. 22

Table 67

Titanium Nitride (PVD)/534A99 (EN 31) Discs (D2 pins)

Pin No.	Coefficient of Friction		
	Static	Dynamic (mean)	Final
64	0.3	0.39	0.4
65	0.31	0.66	0.62
66	0.27	0.54	0.59

Table 68

Change in Coefficient of Friction with Time For Pins 67-69

Time (mins)	Coefficient of Friction			
	Pin 64	Pin 65	Pin 66	$\bar{x}$
0	0.3	0.31	0.32	0.31
5	0.45	0.47	0.4	0.46
10	0.4	0.47	0.37	0.45
15	0.4	0.41	0.37	0.41
20	0.4	0.41	0.53	0.48
25	0.4	0.41	0.53	0.48
30	0.4	0.41	0.53	0.46

Change in Coefficient of Friction with Time

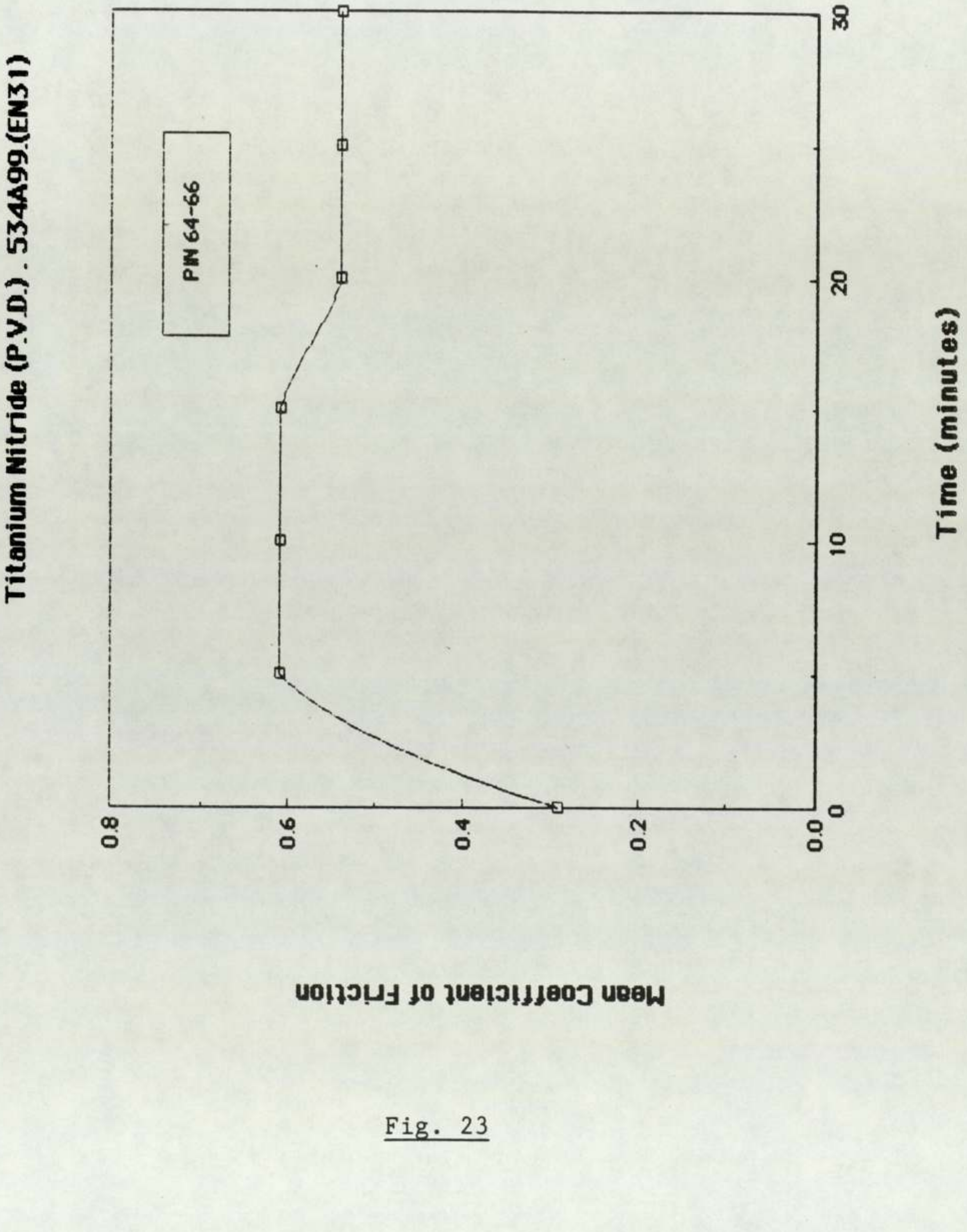

Fig. 23

5.5 Surface Roughness

The roughness average Ra values for each pin and disc combination was measured using the Rank Taylor Hobson Talysurf 10 Surface Texture measuring instrument. The surface roughness values were assessed as mean results of several sample lengths taken consecutively across the surface of the pin or in four separate areas on the surface of the disc.

Table 69

Electroless Nickel PTFE As Plated

Pin No.	Ra pin μm	Ra disc μm	Disc Type
1	0.84	0.12	Sursulf
2	0.76	0.12	"
3	0.86	0.12	"
4	0.99	0.18	"
52	1.90	0.10	534A99
53	1.60	0.10	"
54	2.03	0.10	"
55	2.03	0.17	Sursulf
56	2.16	0.17	"
57	1.52	0.17	"

Table 70

Electroless Nickel PTFE
(Heat treated at 300°C for 4 hours)

Pin No.	Ra pin μm	Ra disc μm	Disc Type
5	0.85	0.18	Sursulf
6	2.02	0.18	"
7	2.29	0.10	"
8	2.03	0.10	"
9	2.16	0.10	"
58	0.76	0.12	"
59	0.86	0.12	"
60	1.02	0.12	"
61	1.65	0.11	534A99
62	2.03	0.11	"
63	1.60	0.11	"

Table 71

Electroless Nickel As plated

Pin No.	Ra pin µm	Ra disc µm	Disc Type
22	0.76	0.79	Sursulf
23	0.76	0.79	"
24	0.63	0.79	"
25	0.76	0.63	534A99
26	0.76	0.63	"
27	0.81	0.63	"

Table 72

Electroless Nickel Heat Treated at 400°C for 1 hour

Pin No.	Ra pin µm	Ra disc µm	Disc Type
28	0.20	0.33	534A99
29	0.20	0.33	"
30	0.20	0.33	"
31	0.48	0.22	Sursulf
32	0.33	0.22	"
33	0.30	0.22	"

Table 73

Hard Chromium

Pin No.	Ra pin µm	Ra disc µm	Disc Type
16	0.28	0.15	Sursulf
17	0.28	0.15	"
18	0.30	0.15	"
19	0.28	0.84	534A99
20	0.28	0.84	"
21	0.30	0.84	"

Table 74

Electrodeposited Tin/Nickel

Pin No.	Ra pin µm	Ra disc µm	Disc Type
40	0.58	0.12	534A99
41	0.42	0.12	"
42	0.71	0.12	"
43	0.38	0.15	Sursulf
44	0.56	0.15	"
45	0.48	0.15	"

Table 75

Electrodeposited Tin/Cobalt

Pin No.	Ra pin µm	Ra disc µm	Disc Type
46	0.62	0.12	534A99
47	0.56	0.12	"
48	0.66	0.12	"
49	0.81	0.35	Sursulf
50	0.71	0.35	"
51	0.62	0.35	"

Table 76

Titanium Nitride CVD
(Pin material 605A36 (EN 16))

Pin No.	Ra pin µm	Ra disc µm	Disc Type
10	1.14	0.15	Sursulf
11	1.22	0.15	"
12	1.40	0.68	534A99
13	1.17	0.68	"
14	1.17	0.81	Carbide
15	1.15	0.81	"

Table 77

Titanium Nitride CVD
(Pin material D2)

Pin No.	Ra pin μm	Ra disc μm	Disc Type
34	1.22	0.11	534A99
35	1.22	0.11	"
36	1.10	0.11	"
37	1.10	1.13	Sursulf
38	1.10	1.13	"
39	1.22	1.13	"

Table 78

Titanium Nitride PVD
(Pin material D2)

Pin No.	Ra pin μm	Ra disc μm	Disc Type
64	0.46	0.13	534A99
65	0.50	0.13	"
66	0.41	0.13	"
67	0.46	0.13	Sursulf
68	0.51	0.13	"
69	0.51	0.13	"

5.6 Photomicroscopy

Representative samples of each coated pin were examined before and after wear testing, using scanning electron microscopy, together with X-ray microanalysis (energy dispersive technique).

5.6.1 Electroless Nickel/PTFE

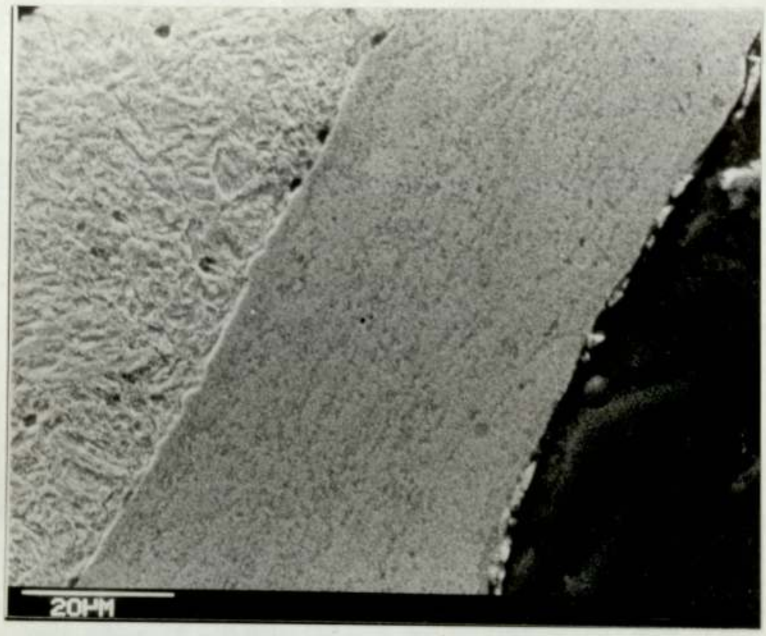

Photomicrograph 1: Transverse section of unworn Electroless nickel/PTFE. Pin No. 9 x 1000 magnification.

Photomicrograph 2: Transverse section of worn Electroless nickel/PTFE showing some delamination of the deposit. Pin No. 5 x 1000 magnification.

Photomicrograph 3: As photomicrograph 2, x 5000 magnification.

Photomicrograph 4: Surface of unworn Electroless nickel/PTFE Pin no. 53, showing some porosity in the coating, x 1000 magnification.

Photomicrograph 5: Surface of worn Electroless nickel/PTFE, pin no. 53, showing the majority of the coating worn away, x 1000 magnification.

5.6.2 Electroless Nickel

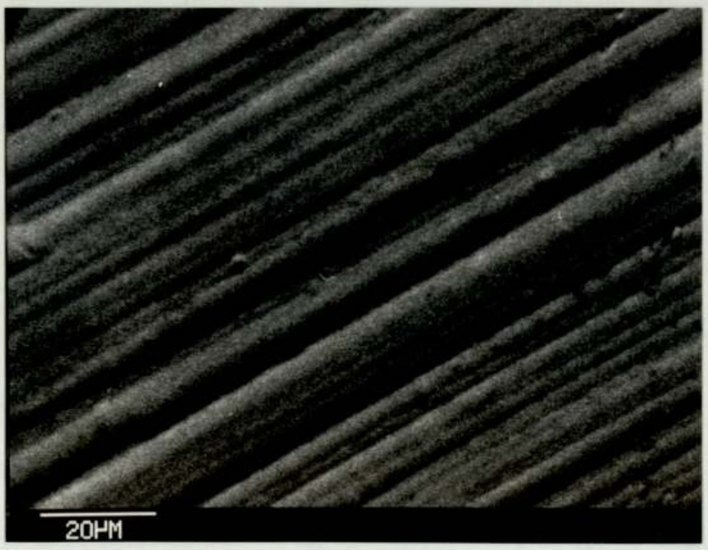

Photomicrograph 6: Surface of unworn Electroless nickel, pin no. 31, showing the electroless deposit following the grinding marks of the substrate, x 1000 magnification.

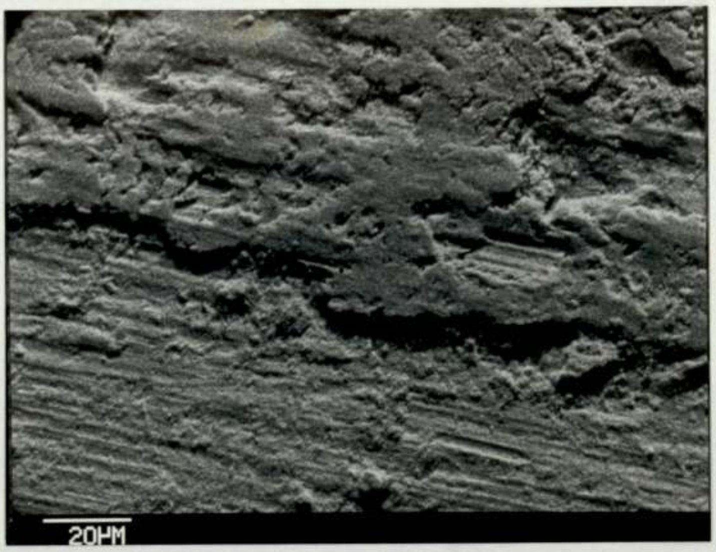

Photomicrograph 7: Surface of worn electroless nickel, pin no. 31, showing both wear of coating and substrate, x 1000 magnification.

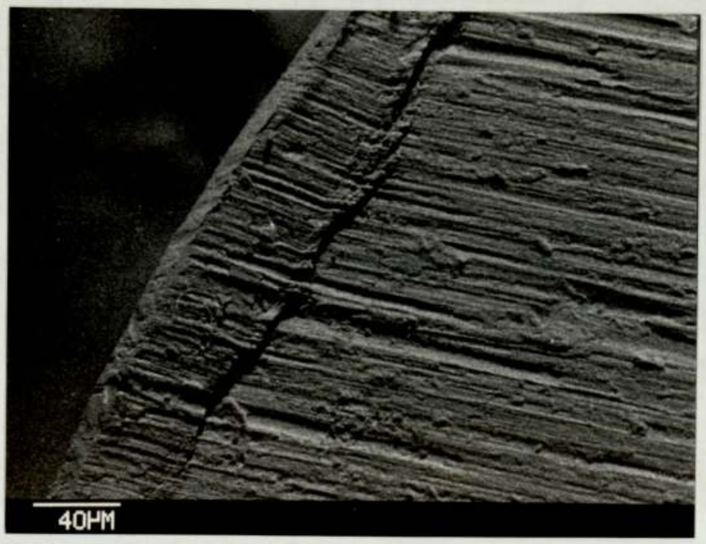

Photomicrograph 8: Surface and edge of worn electroless nickel, pin no. 31, showing coating remaining on the shank of the pin and some mechanical damage on the edge of the substrate, x 500 magnification.

5.6.3 Hard Chromium

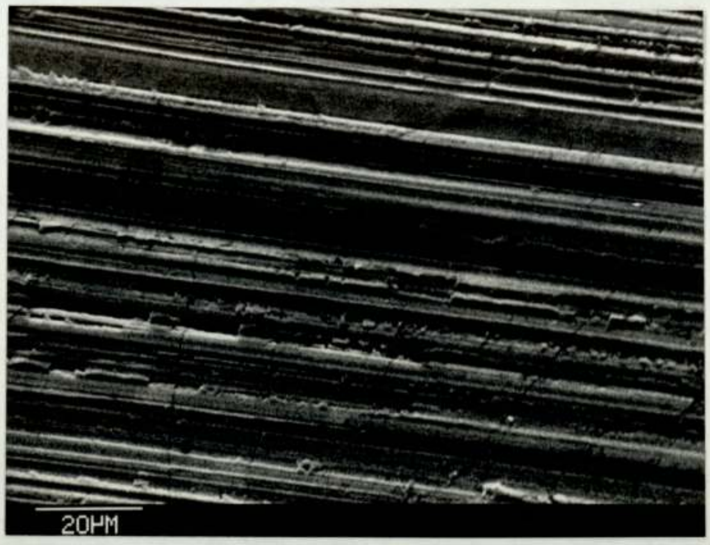

Photomicrograph 9: Surface of unworn hard chromium deposit, pin no. 19, showing grinding marks and grinding cracks. Grinding cracks running normal to the grinding direction. x 1000 magnification.

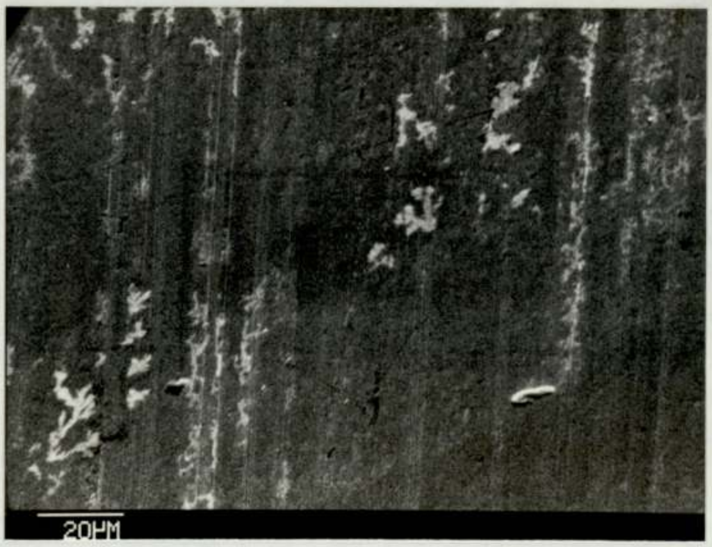

Photomicrograph 10: Surface of worn hard chromium deposit, pin no. 19, showing that the coating was still intact, but the majority of the grinding marks had worn away. The bright areas visible suggest the generation of wear particles, x 1000 magnification.

5.6.4 Tin/Nickel

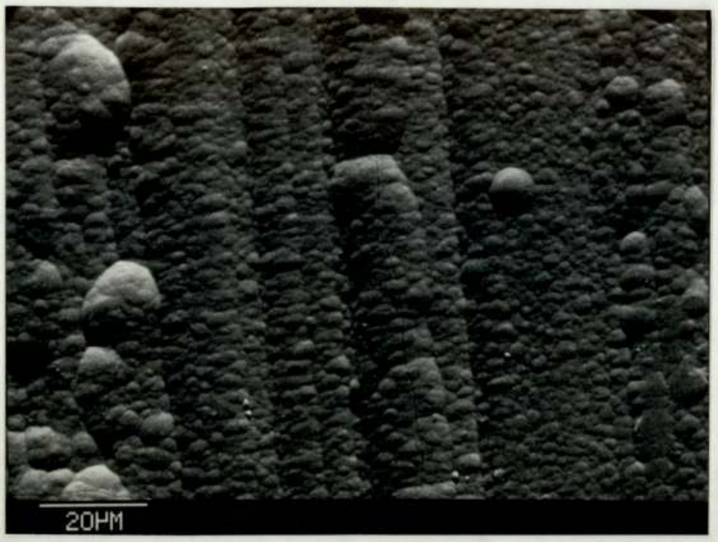

Photomicrograph 11: Surface of unworn electrodeposited tin/nickel, pin no. 43, showing the electrodeposit following the grinding marks of the substrate, x 1000 magnification.

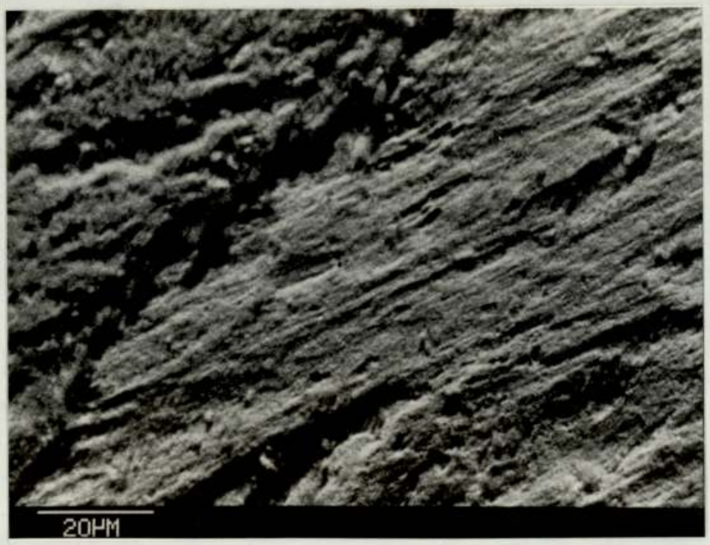

Photomicrograph 12: Surface of worn electrodeposited tin/nickel, pin no. 43, showing both wear of the coating and substrate, x 1000 magnification.

5.6.5 Tin/Cobalt

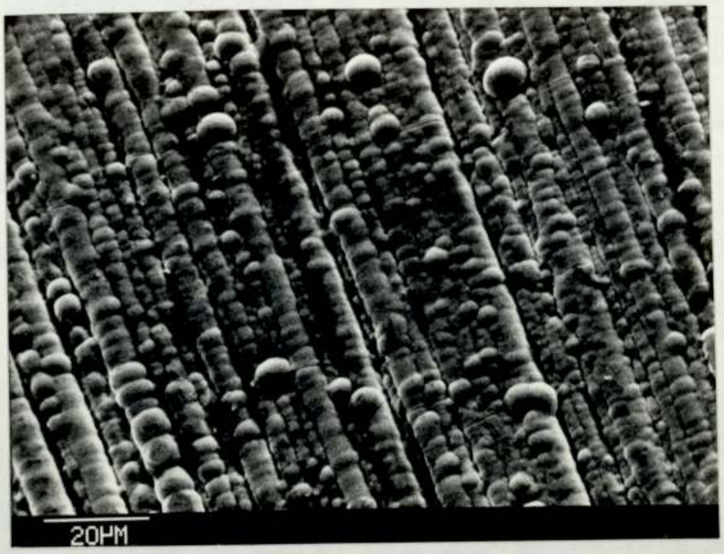

Photomicrograph 13: Surface of unworn electrodeposited tin/cobalt, pin no. 46, showing the electrodeposit following grinding marks of the substrate, x 1000 magnification.

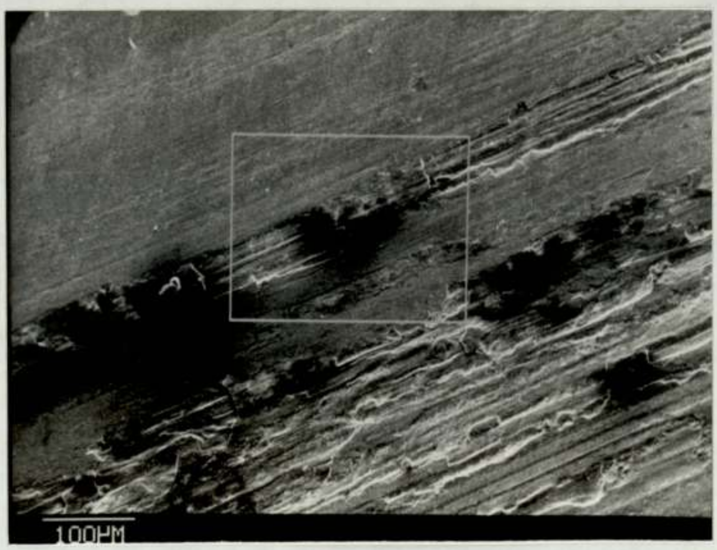

Photomicrograph 14: Surface of worn electrodeposited tin/cobalt, pin no. 46, showing the electrodeposit still intact and highlighting the generation of a wear particle, x 200 magnification.

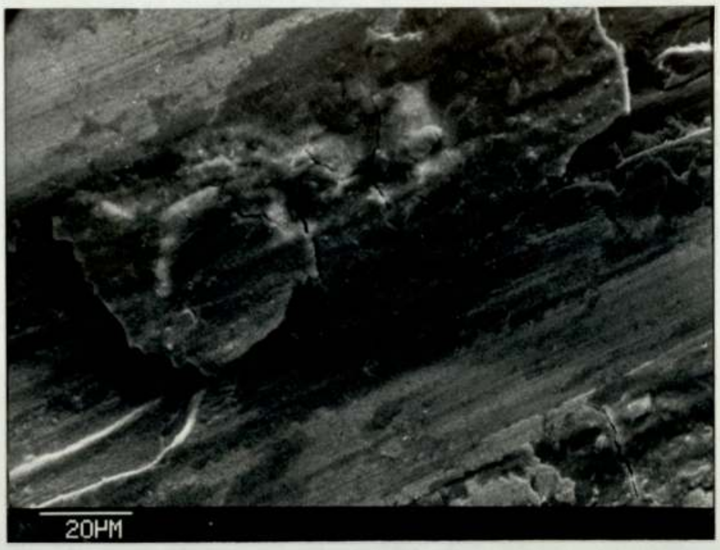

Photomicrograph 15: As photomicrograph 14, x 1000 magnification.

5.6.6 Titanium Nitride (CVD)

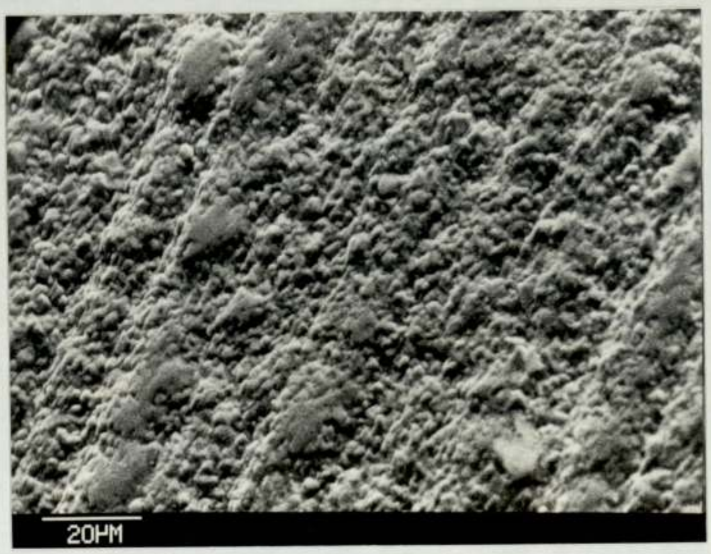

Photomicrograph 16: Unworn titanium nitride coating, pin no. 34, x 1000 magnification.

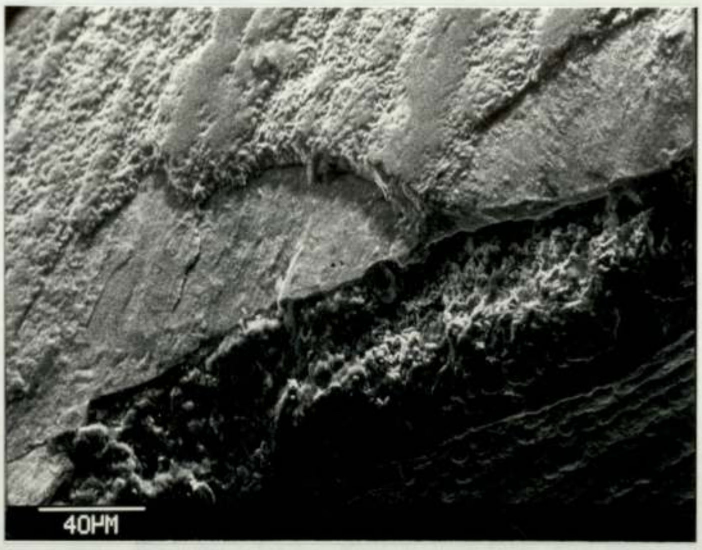

Photomicrograph 17: Surface of titanium nitride, pin no. 34, after wear testing, showing some edged deterioration with possible delamination of the titanium nitride coating, x 500 magnification.

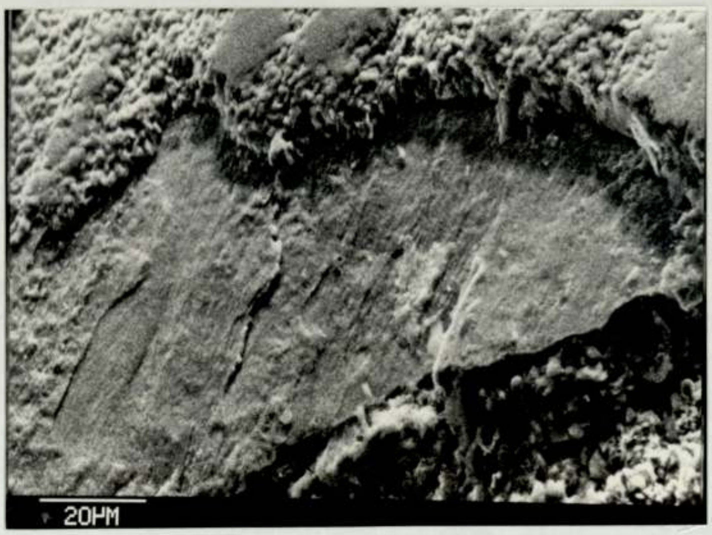

Photomicrograph 18: As photomicrograph 17, x 1000 magnification.

Photomicrograph 19: Surface of titanium nitride coating, pin no. 34, after wear testing showing metallic transfer of disc material smearing the surface of the pin, x 200 magnification.

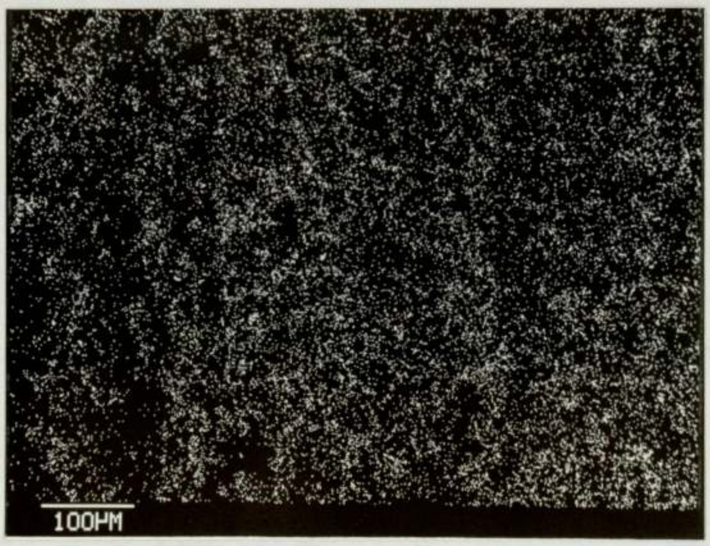

Photomicrograph 20: "X-ray" map of photomicrograph 19, showing metallic transfer from disc approximately 20% of surface area contaminated with iron, x 1000 magnification.

6.0 DISCUSSION

To evaluate the wear and friction characteristics of surface coatings the pin on disc method was used. By using a flat pin rubbing against a flat disc, this type of contact has the advantage of ensuring uniform wear over a relatively large area of surface.

To ensure flat surface/flat surface contact both the pin and disc must be accurately machined. If the pin is not flat against the disc preferential wear on one side of the pin can take place. This in turn can lead to rapid encroachment of the substrate during the wear test, which can give spurious wear rates.

The original research was carried out using Sursulf treated BS 970 708A37 (EN 19) discs, hardened and tempered to "T" condition (pins 1-9). Sursulf treatment converts the steel surface into three distinct layers. A porous layer which was removed prior to wear testing. A compact layer consisting of epsilon iron nitride and iron sulphide, and below that a diffusion zone where nitrogen is held in solid solution. Thus the Sursulf compact layer which was in direct contact with the pin coating is not a true metallic surface and the normal conditions for adhesive wear may not apply. For a direct comparison with a true metallic surface discs of BS 970 534A99 (EN 31) were used. The 534A99 discs were hardened and tempered to give a macrohardness of 840-860HV. The Sursulf compact layer hardness was approximately 1100HK.

The static and dynamic frictional components were analysed without difficulty from the torque measurements, however the analysis of wear proved more difficult. Analysis of wear by the wear transducer method was unreliable because of the tendency for the pin and disc to expand, the reason for this was due to the frictional forces encountered during wear testing. Analysis of wear by weight loss is more intelligible but care must be taken that the weight loss corresponds to the removal of the coating only and not some of the substrate. In addition to the problems associated with possible encroachment of the substrate during wear testing, the weight loss method can only assume a uniform wear rate of coatings, and thus cannot take into account any possible change from one wear regime to another during the wear test period. Only a limited number of results were obtained using the wear transducer method, therefore the discussion of the results is based on the weight loss method. The wear rate for each pin/disc combination was individually calculated and the results expressed as gcm^{-1} (tables 26-34).

The coating that exhibited the best wear resistance was titanium nitrided (CVD) on D2 pin material (pins 34-39). No wear of the coating was indicated by the weight loss method after wear testing for 30 minutes on either the Sursulf treated or 534A99 discs. There had been a weight gain on each pin indicating some metallic "pick up" from the disc during wear testing. This metallic "pick up" was substantiated using an "X"ray mapping technique on the scanning electron microscope.

Titanium nitride (CVD) coatings were originally deposited onto 605M36T pin material but gave poor results (pins 10-15). The CVD process temperatures are high at 1000°C. After coating the pins were furnace cooled resulting in a coarse ferrite/pearlite microstructure with a core hardness of only 190HV. In addition there was a subcutaneous layer of ferrite adjacent to the coating. The low bulk hardness of the recrystallised microstructure may not be sufficient to support the coating. Unlike the D2 pins that were processed at the same temperature, the processed 605M36T pins were unable to be hardened in vacuum because the critical cooling velocity required for the production of martensite could not be attained by forced inert gas quenching.

Titanium nitride coating produced by Physical Vapour deposition on D2 pin material gave varying results. Titanium nitride (PVD) when tested against Sursulf treated discs revealed no wear by the weight loss method after testing for 30 minutes. There had been a weight gain on each pin indicating some metallic "pick up" similar to the results obtained from titanium nitride by CVD. With an equivalent set of titanium nitride (PVD) coated pins when wear tested against 534A99 discs the results obtained indicated a wear rate that varied from 0.088-2.155 gcm^{-1}. The very wide range for the wear rate of titanium nitride produced by physical vapour deposition may be due to the thin nature of this particular coating, i.e. 1-2.5μm, and possible lack of adhesion with some of the wear being attributed to the substrate.

Of the more conventional aqueous methods of producing wear resistant coatings, hard chromium showed the lowest wear rates. However, for a number of years heat treated electroless nickel has rivalled hard chromium for a number of engineering applications where hardness and general wear resistance is required. From the results obtained the as-plated microhardness of the chromium deposit was approximately 150HK greater than the heat treated electroless nickel deposit.

The higher microhardness of the chromium deposit may in part be responsible for the superior wear resistance of the hard chromium compared with heat treated electroless nickel when tested against 534A99 discs.The mean wear rate of the hard chromium and heat treated electroless nickel was $0.536gcm^{-1}$ and $0.879gcm^{-1}$. The hard chromium deposit did not perform so well when tested against Sursulf treated discs, and a mean wear rate of $0.684gcm^{-1}$ was recorded.

When considering the wear characteristics of electroless nickel the deposit's response to heat treatment should first be established. Examination of the microhardness values (tables 8-9) reveals that the electroless nickel had responded to heat treatment and the hardness of the deposit had increased from 528-560HK to 893-910HK. Therefore it may be expected that the heat treated electroless nickel should exhibit superior wear resistance. This was found to be the case when tested against 534A99 discs. The reason for the very high wear rate of the heat treated electroless nickel when tested against Sursulf treated discs (pins 31-33) was due to preferential wear on one side of the pin, thus the majority of the weight loss was from the substrate material giving spurious wear rates for this particular pin and disc combination. Scanning electron microscopy of the worn end (pin 31) revealed that in the area of preferential wear electroless nickel was evident on the edge of the pin only.

The wear characteristics of electroless nickel/PTFE composite coatings both in the as-plated and the heat treated condition were originally evaluated using Sursulf treated discs only (pins 1-9). The electroless nickel/PTFE composite in the as-plated condition exhibited better wear resistance than heat treated electroless nickel/PTFE composite. Examination of the microhardness values (tables 6-7) revealed that the composite coating had responded to the heat treatment process and the hardness had increased from 307-347HK to 552-595HK. Therefore it may be expected that the heat treated composite coating should exhibit better wear resistance. A possible reason for the reduced wear resistance of the heat treated pins is heat treatment at 300°C for four hours has caused thermal degradation of the PTFE. The wear tests were repeated using both Sursulf treated and 534A99 discs (pins 52-57 electroless nickel/PTFE as-plated, pins 58-63 electroless nickel/PTFE heat treated). The same conditions of load and sliding speed were used but gave contradictory results when tested against Sursulf treated discs. The wear test results obtained for pins 1-9 would suggest that thermal treatment of the composite coating reduced the wear resistance, whereas for pins 55-60 the opposite was found.

(i) Electroless nickel/PTFE as-plated

Pins 1-4	$\bar{x}$ 2.875 g.cm^{-1}
Pins 55-57	$\bar{x}$ 3.9 g.cm^{-1}

(ii) Electroless nickel/PTFE heat treated

Pins 5-9	$\bar{x}$ 5.23 g.cm^{-1}
Pins 58-66	$\bar{x}$ 2.67 g.cm^{-1}

The reason for the contradictory results was not known but it was not considered to be associated with the hardness of the composite after heat treatment or any change in the characteristics of the Sursulf layer. A more likely cause may have been associated with the phosphorous content of the composite or a change in the volume fraction of the PTFE entrapped in the electroless nickel deposit. It must, however, be pointed out that the wear test period for pins 55-57 was only 10 minutes. The reason for this was to ensure that the substrate would not be encroached during wear testing and all the wear associated with the deposit. The lowest wear rate for the composite coating was in the heat treated condition when tested against 534A99 discs giving a mean wear rate of 1.747 g.cm^{-1}. When tested against Sursulf treated discs a mean wear rate of 2.67 g.cm^{-1} was recorded. In the as-plated condition the composite did not perform so well against 534A99 discs. The mean wear rate recorded was 6.14 g.cm^{-1} and 3.9 g.cm^{-1} for 534A99 discs and Sursulf treated discs respectively.

Scanning electron microscopy of the worn ends of the composite pin 1 as-plated and pin 5 heat treated showed the presence of fine cracks. The electroless nickel layer builds up with a uniform thickness with a growth front parallel to the substrate interface, it would appear that during plating the PTFE particles settle on the growth front and appear to be incorporated in layers. Composite growth in this form may weaken the coating and the fine soft particles of PTFE may act as a path for crack propagation. This would appear to be the case as no cracks normal to the coating/substrate interface were observed. Since the maximum Hertzian Shear Stress is below the surface, it is probable that a fatigue crack would nucleate there and propagate along the layering on to the surface to produce wear debris. Hence the coating probably delaminates rather than being worn uniformly.

Electrodeposited tin/nickel and cobalt/tin, although not commonly used for wear applications, have an as-plated microhardness similar to that of as-plated electroless nickel.

(i)	Tin/nickel	463-543 HK
(ii)	Cobalt/tin	559-630 HK
(iii)	Electroless nickel	528-560 HK

The tin/nickel electrodeposit is basically a high tin alloy containing 71% tin whereas the cobalt/tin electrodeposit contained only 6% tin. The electroless nickel deposit contained approximately 17% phosphorus.

The electroless nickel and tin/nickel gave very similar wear rates when tested against Sursulf treated discs with a mean wear rate of 4.069 and 4.073 $g.cm^{-1}$ respectively. When the wear tests were repeated using a 534A99 disc the wear rate was much lower for the tin/nickel electrodeposit with a mean wear rate value of only 0.753 $g.cm^{-1}$. The electroless nickel did not perform so well as the tin/nickel and a mean wear rate of 2.87 $g.cm^{-1}$ was recorded.

Scanning electron microscopy of the tin/nickel coating after wear testing against Sursulf treated discs revealed that in certain areas the substrate had been encroached thus a very small proportion of the wear must have been from the substrate. With the knowledge of this the wear test period was reduced to 10 minutes for the cobalt/tin, Sursulf pin/disc combination and 15 minutes for the cobalt/tin, 534A99 pin/disc combination. The cobalt/tin electrodeposit gave very similar mean wear rates when tested against both Sursulf treated and 534A99 discs. The mean wear rate value recorded was 2.676 and 2.515 $g.cm^{-1}$ respectively. Scanning electron microscopy revealed that the coating was still intact after wear testing. At a magnification of 2000x there was evidence of microcracking which leads to the formation of wear platelets. At lower magnification wear platelets were in evidence with platelets about to become detached.

For the majority of coatings examined the wear resistance of the coating was impaired when tested against a Sursulf treated disc. The fact that the presence of traces of sulphur allows stabilization of the epsilon phase at normal operating temperature of the Sursulf bath (560/565^{o}) results in the production of monophased and homogeneous compound layers which in turn leads to good wear resistance.

In general the hardness of the surface coatings may be taken as an indicator of wear resistance, but other factors such as adhesion to the substrate, brittleness, coating morphology, solubility and crystal structure are also important. On considering hardness alone as the sole criterion for wear resistance, titanium nitride coatings by PVD should have exhibited good wear resistance. However, the coating failed by lack of adhesion when tested against 534A99 discs.

The coating morphology can influence how cracks develop and propagate. It is known that the tendency to crack formation in hard chromium electrodeposits is more predominant in the immediate vicinity of the channel cracks[39]. Interactions on the atomic scale in wear situations are promoted by the crystal structure and the mutual solubility of the mating surfaces. The solubility rule states that the tendency towards adhesion is lowest for pairs of metals with almost zero mutual solubility. However, strong forces between two metals frequently lead to the formation of intermetallic compounds. Thus the strong adhesive bonds generated between mating surfaces, the possibility of surface contaminants and the formation of oxide films can all influence the wear and frictional characteristic of materials and coatings.

The static, dynamic (mean) and final coefficient of friction was calculated for all pin and disc conbinations. In addition for pins 31-69 the mean coefficient for each series of wear tests was plotted against time. This was to establish any frictional trends during the wear test period, i.e. the possible formation of thermally generated tribo-oxidational products.

Considering the static coefficient of friction, the coating that gave the lowest mean value of 0.15 was the cobalt/tin electrodeposit when tested against a 534A99 disc. A similar set of pins when tested against a Sursulf treated disc gave a mean value of 0.37.

The electroless nickel PTFE composite in the as-plated condition gave a mean value of 0.17, when tested against a Sursulf treated disc and 0.2 for 534A99 discs. In the heat treated condition the mean value increased to 0.24 when tested against Sursulf treated discs and 0.206 for 534A99 discs.

The relatively low value for the mean static coefficient of friction was thought to be due to the thin film of PTFE which may exist on the pin after it was removed from the electroless nickel bath. This film would therefore initially reduce the contact between the pin and disc and consequently reduce the static frictional component. The marginal increase in the mean static coefficient of friction for the composite in the heat treated condition may be due to volatilisation of this film during the heat treatment process.

Considering the dynamic coefficient of friction, with the exception of hard chromium plated pins tested against Sursulf treated discs (pins 16-18) the frictional value increased during the wear test period. This increase in the coefficient of friction was either a steady increase up to a maximum value, or an increase up to a maximum value with a subsequent decrease in the coefficient of friction resulting in a steady-state condition of dynamic friction. The frictional change during the wear test period was thought to be related either to the presence of contamination or the formation of tribo-oxidational products with a possible change from one wear regime to another.

CONCLUSIONS

From the results obtained in this thesis, the following conclusions can be drawn.

(1) Titanium nitride (CVD) coating on D2 pin material did not exhibit any wear when tested against Sursulf treated or 534A99 discs.

(2) Titanium nitride (CVD) coating on 605M36T pin material incurred catastrophic failure, due to the inability to harden the substrate and the presence of a subcutaneous layer of ferrite.

(3) Titanium nitride (PVD) coating on D2 pin material did not exhibit any wear when tested against Sursulf treated discs. An equivalent set of pins when tested against 534A99 discs exhibited a wear rate which varied from 0.085-2.155 $g.cm^{-1}$.

(4) Hard Chromium exhibited the lowest mean wear rate of the other coatings examined when tested against Sursulf treated or 534A99 discs; followed by tin/nickel and heat treated conventional electroless nickel when tested against 534A99 discs.

The mean wear rate increased by a factor of 5.4 and 6.5 when an equivalent set of tin/nickel and heat treated electroless nickel was tested against Sursulf treated discs.

(5) Electroless nickel PTFE composite coated pins gave conflicting wear test results depending upon which series of test results were examined. Thus no definitive data could be extracted from the results.

(6) The coating which exhibited the lowest value for static coefficient of friction was tin/cobalt, with a value of 0.15 being recorded. An equivalent set of pins when tested against Sursulf treated discs gave a value of 0.37.

(7) From the limited number of results obtained there appeared to be no direct relationship between either surface roughness and wear rate or coefficient of friction, however, to obtain any meaningful data regarding this relationship a larger sample size would be required and statistical analysis adopted.

SUGGESTIONS FOR FURTHER WORK

(1) Due to the conflicting wear test results of electroless nickel PTFE composite, and the fact that the second series of pins coated with the composite revealed some porosity on the coating, an additional series of wear tests should be performed.

(2) The pin on disc wear testing apparatus tended to be somewhat inflexible owing to the fact that the test cannot be rapidly stopped, the specimen visually examined and the test restarted. Thus other wear testing methods should be used especially when testing "thin" softer coatings.

(3) It would be advantageous to find suitable methods for the removal of wear debris. The inability to remove the wear debris allows rapid transition from adhesive to adhesive/abrasive wear.

REFERENCES

(1) Eyre, T.S. "The Mechanisms of Wear" Tribology, 91-97, (1976)

(2) Archard, J.F. "Contact and Rubbing of Flat Surfaces", J. Appl. Phys., 24, 981-988, (1953)

(3) Bhansali, K.J. "Adhesive Wear of Nickel and Cobalt Alloys" Wear 60, 95-110, (1980)

(4) Rabinowinz, E. "An Adhesive Wear Model Based on Variations in Strength Values" Wear 63, 175-181, (1980)

(5) Clemow, A.J. and Daniell, B.L. "The Influence of Microstructure on the Adhesive Wear Resistance of a Co-Cr-Mo Alloy" Wear 61, 219-231, (1980)

(6) Moore, M.A. "Abrasive Wear Resistance of Ferritic Materials" Wear 28, 59, (1974)

(7) Lipson, C. "Wear Considerations in Design" 10th Edition 1967, Prentice-Hall, Inc.N.Y.

(8) Welsh, N.C. "The Dry Wear of Steels", Phil. Trans. Roy. Soc., 257, 31-70, (1965)

(9) Quinn, T.F.J. "The Application of Modern Physical Techniques to Tribology" (1971) Newnes-Butterworths (London)

(10) Archard, J.F. "The Wear of Metals" New Scientist, 5 (1959)

(11) Archard, J.F. and Hirst, W. "The Wear of Metals under Unlubricated Conditions" Proc. Roy. Soc. A236, 397, (1956)

(12) Bell, T. "Ferritic Nitrocarburising" Heat Treatment of Metals 2, (1975)

(13) Bell, T. "Ferritic Nitrocarburising" Metals Engineering Quarterly, May 1976

(14) Gregory, J.C. "Sursulf - Improving the Resistance of Ferrous Materials to Scuffing, Wear, Fretting and Fatigue by Treatment in a Non-Tox Salt Bath"
Heat Treatment of Metals 2, 55-64, (1975)

(15) Gregory, J.C. "Chemical Conversion Coating of Metals to Resist Scuffing and Wear"
Tribology International, 105-112, April 1978

(16) Hydromécanique et Frottement, "The Role of Sulphur Compounds in a Non-Polluting Nitrocarburising Salt Bath"
Heat Treatment of Metals 3, 71-74, (1980)

(17) Hydromécanique et Frottement, Journal du Frottement Industriel, 7, (1980)

(18) Hydromécanique et Frottement, Journal Industriel, 8, (1980)

(19) Hydromécanique et Frottement, The Sursulf Process Licencees Manual

(20) Dennis, J.K. and Such, T.E. "Nickel and Chromium Plating" 2nd Ed (1986) Newnes-Butterworths London IS BN 0-408-01124-6

(21) Parker, K., "Hardness and Wear Resistance Tests of Electroless Nickel Deposits", Plating, 61, 834-840, (1974)

(22) Sadeghi, M., Longfield, P.D., Beer, C.F. "Effects of Heat Treatment on the Structure, Corrosion Resistance and Stripping of Electroless Nickel Coating"
Trans. I.M.F. 61, 141-146, (1983)

(23) Ma, U., Gawne, D.T. "Wear of Electroless Nickel-Phosphorus Coating"
Trans. I.M.F. 63, 64-69, (1985)

(24) Randin, J.P., Hinterman, H.E., "Electroless Nickel Deposited at Controlled pH; Its Mechanical Properties as a function of the Phosphorus Content", Plating, 54, 523, (1967)

(25) Tulsi, S.S. "Composite PTFE-Nickel Coatings for Low Friction Applications",
Trans. I.M.F., 61, 147-150, (1983)

(26) Brown, L. "Electroless Nickel Composites"
Trans. I.M.F. 62, 139-141, (1985)

(27) W. Canning Materials Limited,
Instruction Sheet No. 1653D

(28) The Canning Handbook on Electroplating
22nd Edition (1978), E. & F.N. Spon Limited,
London IS BN 0-419-10950

(29) Buhl, R., Pulker, H.K., Moll, E. "Tin Coatings on Steel" Thin Solid Films 80, 265-270, (1981)

(30) Hibbs, M.K., Sundgren, J.E., Jacobson, B.E., Johansson, B.O. "Microstructure of Reactively Sputtered Tin Films" Thin Solid Films 107, 149-157, (1983)

(31) Gutzeit, G. "An Outline of the Chemistry Involved in the Process of Catalytic Nickel Deposition from Aqueous Solution" Plating 46, (10) 1158-64, (11) 1257-8, (12) 1377-8, (1959)

(32) Gutzeit, G. "An Outline of the Chemistry Involved in the Process of Catalytic Nickel Deposition from Aqueous Solution" Plating 47, (1) 63-70, (1960)

(33) Ma, U., Gawne, D.T. "Effect of Counterface Material on the Wear of Electroless Nickel-Phosphorus Coating"
Trans. I.M.F. 64, 129-133, (1986)

(34) Tin Research Institute, "Electroplated Tin-Nickel Alloy" 4th Edition April 1968

(35) P.M.D. Chemicals, Nistan - Tin-Nickel Plating Solution Process Instructions

(36) P.M.D. Chemicals, "Evaluation of some of the Plating Parameters of Nistan" July 1981

(37) Clarke, M., Elbourne, R.G., Mackay, C.A. "Electrodeposited Bright Tin-Cobalt Intermetallic Compound CoSn"
Trans. I.M.F. 50, 160-163, (1972)

(38) Tyutina, K.M., Lukyanova, L.G., Selivanova, G.A.
"Electrodeposition of Tin-Cobalt Alloy"
Translated from Zashehita Metallov 20, (1984)

(39) Bowden, F.P., Tabor, D. "Friction - An Introduction to Tribology"
Heineman Educational Books Ltd., London